Performance Amelioration of Fingerprint Recognition

by

Li Wang
B.Eng Software Engineering
Master of Computer Science

Thesis
Submitted for fulfillment of the requirements for the degree of
Doctor of Philosophy (0190)
Faculty of Information Technology
Monash University
Oct, 2014

Declaration

I hereby declare that this thesis contains no material which has been accepted for the award of any other degree or diploma at any university or equivalent institution and that, to the best of my knowledge and belief, this thesis contains no material previously published or written by another person, except where due reference is made in the text of the thesis.

Li Wang

31 Oct,2014

Dedicated to my parents

To my wife

Acknowledgements

I would like to express my deepest appreciation and thanks to my supervisors Dr. Nandita Bhattacharjee and Dr Maria Indrawan. Their advice on my research, my life as well as on my career have been priceless. Without their guidance and persistent help this thesis would not have been possible.

I would particularly like to thank Professor Bala Srinivasan and Professor Gopal Gupta who have given me precious assistance and suggestions on my research. Professor Bala Srinivasa is my informal supervisor, and has done a lot of reversion work of my thesis and given amount of invaluable feedbacks. I also appreciate the valuable feedbacks offered by Dr. Peter Tischer who attended my confirmation, mid-candidature review and pre-submission seminars.

In addition, I would like to thank all faculty staff who have helped me in my research career at Monash University. I would like to offer my special thanks to Leeanne Evans who helped me process various applications.

Specially, I would to thank Dr. Noriake Sato for helping me improve my language skills. I would also than Dr. Jan Miller who did the proofreading work for me.

Furthermore, I would like to thank my friends and colleagues: Parman, Nitin, Nevo, Anwar who have helped me a lot during my PhD career.

Finally, I would like to thank all my family members. I owe my deepest gratitude to my parents for their unconditional support throughout my degree. My father passed away during my last year of candidature, I wish him a happy life in heaven. I also wish my mom a happy and healthy life. Words cannot express how grateful I am to my mother-in law, father-in-law and my wife. My wife has been extraordinarily tolerant and supportive to

both my life and research.

List of Publications

[1] Wang, L., Bhattacharjee, N., Gupta, G., Srinivasan, B., 2010. Adaptive Approach to Fingerprint Image Enhancement. 8th International Conference on Advances in Mobile Computing and Multimedia,42-49, Paris, France.

[2] Wang, L., Bhattacharjee, N., Srinivasan, B., 2011, A novel technique for singular point detection based on Poincaré Index, Proceedings of the 9th International Conference on Advances in Mobile Computing and Multimedia, 12-18, Ho Chi Minh City, Vietnam.

[3] Wang, L., Bhattacharjee, N., Srinivasan, B., 2012, Fingerprint Reference Point Detection Based on Local Ridge Orientation Patterns of Fingerprints, 2012 International Joint Conference on Neural Networks, 1-8, Brisbane, Australia.

[4] Wang, L., Bhattacharjee, N., Srinivasan, B., 2012, A Method for Fingerprint Alignment and Matching, Proceedings of the 10th International Conference on Advances in Mobile Computing and Multimedia, 297–301, Bali, Indonesia.

[5] Wang, L., Srinivasan, B., Bhattacharjee, N., 2011. Security Analysis and Improvements on WLANs. Journal Of Networks, 6(3), 470-481.

Abstract

Fingerprints have been used for personal identification for centuries because of their uniqueness and consistency over time. Fingerprint recognition is one of the most popular methods for personal identification due to its high accuracy, cost efficiency and ease of acquisition. Automated fingerprint recognition has the advantages of fast processing and high accuracy, however its performance deeply depends on the quality of the collected fingerprint images. The matching accuracy of current automatic fingerprint recognition systems decreases dramatically when the quality of fingerprint images are poor. For example, a fingerprint image may contain massive noise, cleaves or inks. In these cases, manual fingerprint recognition achieves better matching results than automatic systems. One of the major challenges in fingerprint recognition is how to improve the performance of an automatic fingerprint recognition system in terms of reliability and accuracy especially for low quality images.

The motivation of this research is derived from the raised need for fingerprint recognition techniques with better matching accuracy and reliability. How to improve the accuracy and reliability of an automatic fingerprint recognition system when processing low quality fingerprint images is the major objective of this research work. Because feature extraction and feature matching are two main components in a fingerprint recognition system, the above objective could be restated as: (i), to design reliable and accurate feature extraction techniques suitable for low quality images and (ii), appropriate matching methods or matching metric with high tolerance for image noise and feature extraction errors.

In order to achieve the above objectives, much effort has been made to improve the matching accuracy of an automatic fingerprint recognition system by introducing the following methods: an fingerprint image pre-processing method in the spatial domain, two different singular point detection approaches, and a new matching metric named binarized minutiae block for fingerprint matching.

Firstly, we have investigated current fingerprint enhancement techniques. A typical fingerprint enhancement module is composed of an image pre-processing stage and a contextual filtering stage. Traditionally, image pre-processing (or named pixel-wise enhancement) techniques are used to improve the *contrast* of an image rather than removing noise. In this study, we found that removing noise and improving the image quality in this stage enables the subsequent contextual filtering stage to obtain a better clarity of ridge and valley structure especially for poor quality fingerprint images, particularly suitable for wet and smudged fingerprint images, based on experimental observation. Therefore, we proposed an image pre-processing approach using contrast stretching and power-law transformation techniques to improve the quality of fingerprint images. The metric goodness index (which is used to evaluate the image quality) is used to evaluate this method. The experimental results show that this approach is able to improve the clarity of ridge and valley structures especially for wet and smudged fingerprints. The average goodness index value obtained from the experiment is improved by 14% compared to other reported methods. In addition, it enables the subsequent contextual filtering (e.g. Gabor filtering) stage for better image enhancement results, and ultimately improve the reliability of feature extraction (e.g. minutiae extraction).

Secondly, we have investigated feature extraction techniques, especially singular point detection which is a global feature in a fingerprint. The performance of current singular point detection techniques is relatively low for poor quality images (mostly around 90% of correct detection rate, and much lower for Poincaré Index based approaches). As a consequence, it becomes the major bottle neck for fingerprint recognition techniques which rely on singular points, such as reference point based fingerprint global pre-alignment and fingerprint classification. In order to address this issue, we first investigated the popular Poincaré Index based approaches. The Poincaré Index technique highly depends on image quality, and it suffers from the problem of a large number of spurious singular points especially for low quality images. As a consequence, we designed a rule-based post-proccessing technique to validate and remove spurious singular points. The experimental results show that the correct detection rate on average is 89.48% on DB1a and DB2a of Fingerprint Verification Competition (FVC) 2002 datasets. These datasets contain fingerprint images with various quality levels, and are especially suitable for evaluation of fingerprint recognition algorithms. It is around 3% improvement over other reported Poincaré Index based approaches in terms of overall correct detection rate. However, one limitation of the Poincareé Index technique is that it processes data *locally* while singular points are *global* features, which are easily influenced by local noise and may cause a number of spurious singular points, especially for low quality images. Therefore, we have proposed a new singular point detection method globally over the whole image, based on the analysis of local ridge orientation maps. In addition, this method is also able to locate a reference point for arch type fingerprints which is useful for fingerprint

pre-alignment as a reference point as well as for fingerprint classification. The experimental results show that the correct detection rate on average is 94.05% on the datasets of FVC 2002 DB1a and DB2a. This experimental result is superior than any other reported methods in terms of correct detection rate of singular points.

Finally, we have investigated the current fingerprint matching methods, and proposed a new matching metric named binarized minutiae block for fingerprint matching. Current matching methods could be classified as: minutiae based, correlation based, and other non-minutiae based methods. Among these methods, correlation and other non-minutiae based methods have better tolerance to image noise and feature extraction errors than minutiae based methods. However, minutiae based methods have better tolerance to non-linear distortion and obtain better matching results on medium or high quality images. This new metric utilize the minutiae and its surrounding texture information. Thus, it has high tolerance to image noise and feature extraction errors as well as non-linear distortion. These binarized minutiae blocks are normalized to the same minutiae direction for easy comparison. Then, the local similarities are calculated by the dissimilarities between each pair of binarized minutiae blocks. In addition, four global similarity calculation methods are designed and implemented using this matching metric. The experimental results show that this method achieves overall matching accuracy of 98.24%, 97.87% and 98.19% on the datasets FVC2002 DB1a, DB2a and FVC2006 DB2a. As a consequence, the results suggest that using binarized minutiae blocks is an alternative way to obtain accurate and reliable matching results other than correlation based (grey scale texture information), minutiae based and other non-minutiae

based methods. Compared to other state-of-the-art matching methods, this metric achieves better experimental results in terms of matching accuracy than most reported matching methods on the same testing databases.

In conclusion, this thesis focuses on the research of how to improve the overall matching accuracy of a fingerprint recognition system even for low quality images. Several methods have been developed to achieve this research objective. The experimental results show that these proposed fingerprint recognition techniques are able to improve the recognition accuracy significantly.

Contents

List of Figures

List of Tables

Chapter 1

Introduction

1.1 Overview

Fingerprints have been used for personal identification since ancient times. The earliest history records show that fingerprints were used as signatures in ancient Babylon in the second millennium BC [Ast07]. Even the ancients had realized the uniqueness of fingerprints. But the discussion of using fingerprints for personal identification was started by Dr. Henry Faulds in 1880 [Bar13], about 3000 years later, after the first use of fingerprints in human history. In the modern era, the first computer data based automated fingerprint identification system was developed by Federal Bureau of Investigation (FBI) in 1980 [Bar13]. For now, fingerprint recognition systems have become one of the most popular biometric systems used in both government and civilian applications, including law enforcement, border control, forensics, security facility access and employment background checks.

Unlike traditional authentication and identification systems, fingerprint and other biometric recognition techniques rely on physiological characteristics (who you are) instead of smart card, photo ID (what you have) and/or passwords (what you know). Using fingerprints or other biometrics as supplements to traditional authentication and identification systems is one of the solutions to identity fraud. Identity fraud has become a serious social problem in the last ten years. The Australian Bureau of Statistics reported that personal identity fraud cost Australia AUD$1.4 billion from 2007 to October, 2010 [Sta12].

With the increasing demand of fingerprint recognition systems, fingerprint recognition techniques have been developed rapidly since the first introduction of commercial fingerprint recognition systems in the 1990s [LL03]. Although current fingerprint techniques are mature and can satisfy people's ordinary needs of personal identification, the accuracy of this technique still needs to be improved to a higher level. That is because the quality of scanned fingerprint images may be influenced by many factors such as displacement, distortion, and the conditions of fingers. For example, wet fingers may produce merging of ridges while dry ones may produce discontinuities of ridges. These inevitable high variations of intra-class fingerprints (refers to fingerprints from the same finger) cause difficulties in achieving high accuracy of automatic fingerprint recognition systems. In the Fingerprint Verification Competition 2002 (FVC2002), Maio et al. [MMC+02] reported that typically, 20% of the database is responsible for about 80% of the matching errors of intra-class fingerprint matchings in the FVC2002 database. Another example is the 2004 Madrid train bombings. In this case, Brandon Mayfield, an American attorney, was wrongfully

identified via fingerprints by FBI. However, these fingerprints actually belonged to an Algerian national, Ouhnane Daoud. The FBI stated that "this identification was based on an image of substandard quality, which was particularly problematic" and caused the false identification [Ley04]. This wrong identification costs the FBI US$2 millions as compensation for the loss of reputation to Brandon Mayfield [SF06]. Therefore, accurate and reliable fingerprint recognition techniques are important to avoid or reduce such matching errors.

To sum up, how to improve the overall performance of fingerprint recognition systems is still a challenging task. The next section introduces the issues and challenges to minimize the intra-class fingerprint variance and improve the performance of fingerprint recognition techniques.

1.2 Issues and Challenges

One of the biggest challenges of fingerprint recognition is the high variance found between intra-class fingerprints. This variance is caused by several factors, including: (a) displacement or rotation between different acquisitions; (b) partial overlap, especially in sensors of small area; (c) skin conditions, due to permanent or temporary factors (cuts, dirt, humidity, etc.); (d) noise in the sensor (for example, residues from previous acquisitions); and (e) nonlinear distortion due to skin plasticity and differences in pressure against the sensor [MMJP09]. Fingerprint matching remains as a challenging pattern recognition problem due to the difficulty in matching fingerprints affected by one or several of the above mentioned factors.

In the literature, much effort has been devoted to the challenge of developing fingerprint recognition techniques to minimize the intra-class variances and improve the overall performance. These techniques include: (i) image enhancement methods; (ii) reliable feature extraction methods, and (iii) reliable feature matching methods.

The image enhancement techniques could be classified into two subclasses, which are image pre-processing techniques and contextual filtering techniques. The purpose of the above two types of techniques are different. The image pre-processing techniques (also named pixel-wise enhancement) aim to improve the *contrast* of the image and uniformly distribute the intensity values into selected ranges. These techniques act as an initial processing stage before a more sophisticated image enhancement algorithm. There are many pixel-wise enhancement techniques which have been used in fingerprint recognition systems including histogram equalization [WCT98], Wiener filtering [GAKD00], normalization [HWJ98], adaptive normalization [KP02], and a method based on the analysis of finger skin profile [SG06]. An example of a normalization result is shown in Figure 1.1. On the other hand, the contextual filtering techniques aim to remove the noise and enhance the clarity of ridge and valley structures. These techniques include Gabor filter [HWJ98, LB09, GAKD00, JPLK06], log-Gabor filter [WLHF08], directional Fourier domain filter [SMM94], directional median filter [WSG04], curved Gabor filter [Got12b, Got12a] and oriented diffusion filtering techniques [GS12]. Current research focuses more on contextual filtering techniques, because they can significantly enhance the fingerprint images. However, in our study, we found that removing a certain amount of noise (e.g. Gaussian noise and other non-uniform noise) in the image pre-processing stage is

able to obtain a better processing result in the subsequent contextual filtering stage. *Therefore, designing a fingerprint image pre-processing method which enables successive sophisticated contextual filtering (e.g. Gabor filtering) to perform with improved results and enhanced feature (e.g. minutiae) extraction is a challenge in fingerprint recognition.*

(a) (b)

Figure 1.1: An example of normalization described in [HWJ98].

For feature extraction methods, the local ridge orientation, minutiae and singular points are three major features which are important to fingerprint recognition (see Figure 1.2). Local ridge orientation indicates the direction of ridge lines. Minutiae points are the local ridge characteristics including ridge ending and ridge bifurcation as shown in Figure 1.2. The singular points indicate the global structure of ridge and valley lines. There are two types which are core and delta points ('U' shape like and 'Y' shape like as shown in Figure 1.2). Among the above features, reliable singular point detection is a challenge in fingerprint recognition. The performance of current singular point detection techniques is relatively low with about a

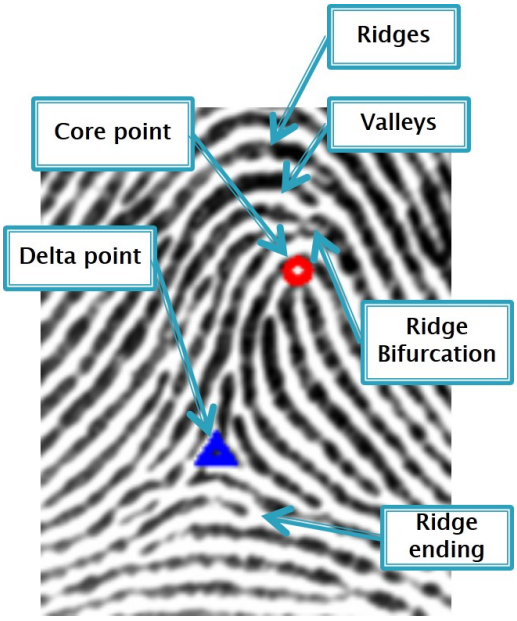

Figure 1.2: Features in a fingerprint. Core points and delta points are two types of singular point. Ridge bifurcation and ending are two important types of minutiae.

80 92% correct detection rate according to the experimental results reported in current research (e.g. [WYY11, OWT+08, LML13]). As a consequence, it becomes the major bottle neck for other fingerprint techniques which rely on singular points, such as fingerprint classification and reference points based fingerprint global pre-alignment. In order to improve the singular point detection accuracy, much research has been done. The most popular approach is based on the Poincaré Index which was first proposed by Kawagoe and Tojo [KT84]. It is a simple and effective approach to detect the singular points. However, it is well recognized that the accuracy of this approach highly depends on the quality of fingerprint images. For low quality fingerprint images, this approach can generate a large number of spurious singular points [MMJP09]. Several improved approaches have been proposed to overcome the problem of spurious singular points

in recent years [KJ96, WLN07, ZGZ07, BLE09]. Besides Poincaré Index based methods, some other approaches have been designed such as detecting singular points by reliability/coherence [CLMM99, KCH12], a zero-pole model [SM93][CEMM00] [FLW00] and complex filtering [NB05]. However, the correct detection rates of singular points is still low, the best result is 92.6% reported by Ravinde et al. [KCH12]. *Therefore, designing a reliable singular point detection method is a challenge in fingerprint recognition.*

For fingerprint matching techniques, they could be classified into minutiae based [BDNB06, LXL04, OR04, TB03, SHFD07, CMMS09, CFM10], correlation based [LELJSM07, KAN08, LTG07] and other non-minutiae based or hybrid methods [CCK11] in terms of features used for matching. Among these methods, correlation, ridge and other non-minutiae based methods have better tolerance to image noise than minutiae based methods. This is because these methods do not need to extract minutiae which is highly influenced by image quality levels. However, minutiae based methods obtain better matching results for medium or high quality images [MMJP09]. On the other hand, fingerprint matching techniques could also be classified into global pre-alignment and local alignment (also called alignment free in some papers) in terms of fingerprint alignment types. Global pre-alignment methods normally use the singular points, or/and some minutiae points as reference points. The thought of global pre-alignment is that if two fingerprints are pre-aligned before the matching, then the following matching stage becomes a simple feature (e.g. minutiae and texture information) comparison problem. These methods are mainly used in correlation and non-minutiae methods (e.g. [YA06]), but also used in some minutiae based or hybrid methods (e.g. [ZYZ05]). Local alignment or alignment

free methods are mostly used in minutiae based matching methods (e.g. [CFM10, FFCS06]). These methods exploit the local interrelations between minutiae points and match two fingerprints by the similarities of local interrelations. Moreover, hybrid alignment methods have been researched as well in order to improve the alignment accuracy (e.g. [JY00]). Regardless of which matching techniques used, the ultimate goal is to minimize the intra-class variance and inter-class similarity (fingerprints of different fingers may sometimes appear quite similar). Large intra-class variance in different acquisitions of the same finger (e.g. displacement, rotation, partial overlap, noise non-linear distortion) makes the fingerprint matching a difficult problem [MMJP09]. *Therefore, reliable fingerprint matching which is accurate and has a high tolerance to noise and feature extraction error is a challenging problem in fingerprint recognition.*

1.3 Motivations and Objectives

The motivation of our research is derived from the raised need of a better overall performance (matching accuracy) of fingerprint recognition systems. Cappelli et al. [CMM+06] reported that the average error rate in the 2006 Fingerprint Verification Competition is 4.74%. That means there are about one false match/non-match error in 20 comparisons. For an attacker (for example, Marvin), if he tries 20 times using brute force attacks, it is possible that he can fool the system once on an average. In a scenario of an airport with daily flow of 100,000 passengers, there are about 4740 passengers who would not be verified by current fingerprint verification systems. Additionally, in the case of an identification system, if the system database

contains 100,000 templates, and there are about 4740 users who are falsely identified as candidates for each identification. Therefore, the demand for an accurate fingerprint recognition system is urgent especially when the uses of fingerprint recognition systems are widely accepted nowadays.

The major objective of our research is to improve the overall performance of a fingerprint recognition system in terms of matching accuracy. More specifically, to address the three challenges described in the previous section are our objectives. These objectives are summarized as:

- Design a fingerprint image pre-processing method which facilitates the successive contextual filtering enhancement.
- Design a reliable singular point detection method which is able to obtain high correct detection rate of singular points even for low quality images.
- Design a reliable fingerprint matching method which is accurate and has a high tolerance to noise and feature extraction errors.

1.4 Contributions

Contributions address three problems in fingerprint recognition to improve the performance of feature extraction and matching, as well as the overall performance of a fingerprint recognition system. The major contributions of this research are listed as below:

Firstly, we have investigated current fingerprint enhancement techniques. A typical fingerprint enhancement module is composed of an image pre-processing stage and a contextual filtering stage. Traditionally, image pre-

processing (also named pixel-wise enhancement) techniques are used to improve the *contrast* of an image rather than removing noise. In this study, we found that removing certain amount of noise in this stage enables obtaining a better processing result in the subsequent contextual filtering stage. Therefore, we proposed an image pre-processing approach using contrast stretching and power-law transformation techniques with automatic parameter selections to facilitate the successive sophisticated contextual filtering (e.g. Gabor filtering) for better enhancement results and feature (e.g. minutiae) extraction. The experimental results suggest that this method is able to significantly remove noise and improve the ridge and valley structure especially for wet and smudged fingerprint images.

Secondly, we have focused on the studies of feature extraction techniques especially singular point detection. In order to address this issue, we initially investigated the popular Poincareé Index based approach. This technique highly depends on the image quality, and it suffers from the problem of a large number of spurious singular points. As a consequence, we designed a rule-based post-proccessing technique to validate and remove spurious singular points. However, one limitation of Poincareé Index technique is that it processes data *locally* while singular points are *global* features, which is easier to be influenced by local noise and may cause a number of spurious singular points. Therefore, we have designed a new singular point detection method globally over the whole image based on the analysis of local ridge orientation maps. In addition, this method is able to locate a reference point for arch type fingerprints. The experimental results show that the correct detection rate is 94.05% on DB1a and DB2a of Fingerprint Verification Competition 2002 datasets. The results are better than any other reported

methods on the same testing datasets.

Finally, we have investigated the state-of-the-art fingerprint matching methods, and proposed a new matching metric using minutiae points and their surrounding texture information. Four global similarity score calculation methods are developed and implemented to evaluate this matching metric. The experimental results suggest that using binarized minutiae blocks as a metric is an alternative way to obtain accurate and reliable matching results besides correlation based (grey scale texture information), minutiae based and other non-minutiae based methods. The experimental results show that this method achieves overall matching accuracy of 98.24%, 97.87% and 98.19% on the datasets FVC2002 DB1a, DB2a and FVC2006 DB2a. The experimental results also suggest that it is superior than most state-of-the-art matching methods (e.g. methods in [WSOA13, LN06, GYZZ11, WSOA13]) in terms of matching accuracy.

The research activities carried out during the Ph.D., led to publication of the following scientific papers: [WBGS10, WBS11, WBS12b, WBS12a].

1.5 Organization of Thesis

The rest of the thesis is organized as follows:

- Chapter 2: this chapter will introduce the background of the fingerprint recognition and the challenges to design an accurate fingerprint recognition system. A fingerprint recognition system consists of many parts. We will describe each stage of the fingerprint recognition system in detail. Besides, the evaluation metrics and fingerprint databases used in the experiments, are also introduced.

- Chapter 3: this chapter introduces our image pre-processing method. Image pre-processing is a stage in fingerprint recognition aiming to pre-process the image to obtain better clarity and remove noise for subsequent stages. The proposed method uses power-law transformation and contrast stretching techniques to process the original image. The experimental results are also discussed in this chapter.

- Chapter 4: this chapter introduces two methods of singular point detection. The first method is the Poincaré Index based singular point detection. A post-processing method is developed to validate singular points. Furthermore, in order to overcome the limitations of this method, another singular point detection method is developed which is based on the analysis of the local ridge orientation patterns.

- Chapter 5: this chapter will introduce a new metric for matching. This chapter first stresses on the fingerprint template generation, in which a new metric named binarized minutiae block is generated. Then four different global similarity calculation methods are designed to calculate the final matching score between two fingerprints. A comparison between the experimental result and other reported results and a discussion are also provided.

- Chapter 6: this chapter includes the conclusion of this thesis and future work.

Chapter 2

Background of Fingerprint Recognition

2.1 Fingerprints and Other Biometrics

Biometrics consists of methods for uniquely recognizing human based upon one or more intrinsic physical or behavioral traits [Wik14a]. Biometrics techniques include iris recognition, fingerprint recognition, face recognition and other recognition methods (e.g. voice and handwriting recognition). Figure 2.1 shows six biometrics used currently which are fingerprint, iris, voice, deoxyribonucleic acid (DNA), face and palmprint.

Among the biometrics used currently, fingerprint recognition is one of the most widely used personal identification technique for its efficiency, effectiveness and economy [MMJP09]. Face, voice and handwriting recognitions have the limitations of low accuracy compared to fingerprint and iris recognition. Both iris and fingerprint recognitions are favored biometrics because of their high accuracy, but iris is not as widely adopted as

fingerprint recognition in daily commercial systems due to the concerns of deployment difficulties and costs. That is because iris recognition systems cost much more than fingerprint recognition system in terms of data acquisition equipment prices.

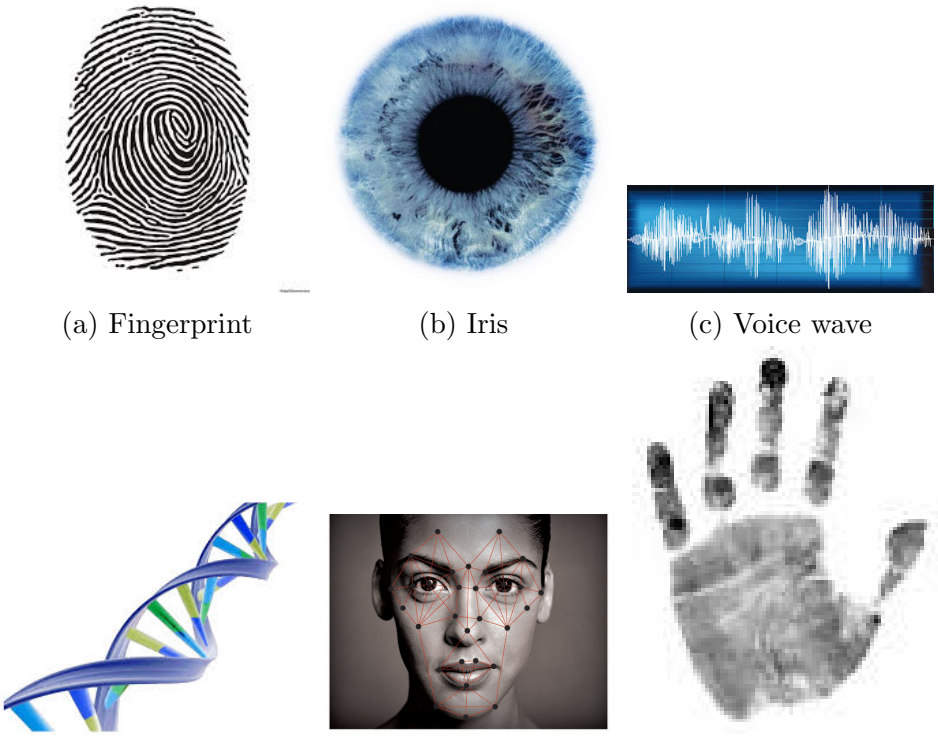

(a) Fingerprint (b) Iris (c) Voice wave

(d) DNA (e) Face geometry (f) Palmprint

Figure 2.1: Samples of different biometrics (images from internet).

Different biometrics techniques may be suitable to different information systems for security enhancement or/and authentication/identification purposes. However, all biometrics need to fulfill the common requirements to satisfy the above purposes. Prabhakar et al. [PPJ03] and Jain et al. [JRP04, MMJP09] have introduced seven biometric characteristics which a biometric system should satisfy:

- **Universality**: Every person or most people should have this biometric characteristic. Most biometric characteristics used currently fulfill this requirement. However, there is a very small chance that some people are not suitable for one or several types of biometric recognitions such as blind, dumb, people with no fingerprints, etc.

- **Distinctiveness**: This biometric characteristic should be unique for any two different individuals. In other words, any two fingerprints from two people should be different.

- **Permanence**: This biometric characteristic should be consistent throughout the life of an individual. Not all biometrics completely fulfill this requirement. For example, the voice of a person changes as one grows older. Besides, the voice also changes when a person suffers some kind of illnesses like cold and flu. Thus voice recognition requires people to update their voice data frequently to obtain an accurate matching result.

- **Collectability**: The biometric characteristic should be able to be easily collected quantitatively. The cost of collecting and processing biometric data of different types of biometrics varies. For example, the cost of using DNA recognition is much higher (reported about AUD$250-300 per test in Australia in [DNA14]) than using other recognized biometrics. The cost of fingerprint recognition is relatively lower compared to biometrics.

- **Performance**: The biometric system based on this characteristic should have satisfactory accuracy and running speed. The perfor-

mance mainly depends on the complexity and uniqueness of the biometric features.

- **Acceptability**: Individuals are willing to accept this biometric method (e.g. collecting fingerprint and iris)in daily life. This involves the problems of complexities of data acquisition and sensitiveness of the biometric data. For example, people may prefer fingerprint and face recognitions to DNA recognition for a computer authentication system.

- **Circumvention**: It refers to the potential of impersonation by other attackers. An impostor could use fake biometric data to attack biometrics recognition systems. For example, voice can be recorded by any device (mobile phones, computers, etc.) with a voice recorder. Besides, 2-D face images, fake fingerprints, fake iris contacts may be used by an impostor to impersonate other genuine users.

Table 2.1 summarizes the comparisons of different biometrics based on the characteristics introduced by Prabhakar et al. [PPJ03]. From the table, we can see that fingerprint satisfies most of the requirements of these characteristics. This is the fundamental reason why fingerprint is more popular than other biometrics. For example, iris recognition is also one of the widely used biometric techniques. But Iris implementations cost more than fingerprint implementations (mostly due to the iris image capture devices). Thus more applications adopt fingerprint recognition techniques. A vivid example is that fingerprint recognition has been used for authentications in laptops (e.g. Lenovo Thinkpad series) and mobile devices (e.g. Iphone 5s), but iris techniques have not been implemented in these or similar systems. Other

biometrics also suffer from some disadvantages in practice. Voices could be easily recorded, and they may change according to the health conditions. Taking photos of faces is a simple task, and these 2-D face photos could be used to impersonate genuine users. The cost of DNA identification is much higher than using other biometrics. Palmprints are good supplements to fingerprints in a biometric system, but capturing a whole palmprint means that the size of the capture devices has to be much larger than fingerprint capture devices. Thus palmprint techniques are not suitable to those biometric systems implemented in small devices. Above all, the fingerprint is most balanced biometric satisfying all the seven requirements among those biometrics listed on Table 2.1.

Table 2.1: Comparison of different biometric techniques [PPJ03, JRP04].

Biometric	Universality	Distinctiveness	Permanence	Performance	Acceptability	Circumvention	Collectability
Fingerprint	High	High	High	High	High	Low	Medium
Iris	High	High	High	High	High	Low	High
Voice	High	Low	Low	Low	High	Medium	High
DNA	High	High	High	High	Low	Low	High
Face	High	Low	Medium	Low	High	Medium	Medium
Palmprint	Medium	High	Medium	High	High	Low	Medium

2.2 Fingerprint Features

In section 1.2, we briefly listed several important fingerprint features which could be used for fingerprint matching including minutiae and singular points.

Specifically, the Committee to Define an Extended Fingerprint Feature Set (CDEFFS)[CDE09] defines three levels of fingerprint features:

- Level 1 features: friction ridge flow and general morphological information. Level 1 features include ridge flow, ridge orientation, core points and delta points. Level 1 features could be used for fingerprint classifications. In this thesis, level 1 features also refer to global features.

- Level 2 features: individual friction ridge paths and friction ridge events, e.g., bifurcations, ending. Level-2 features include minutiae and the interrelationships between minutiae.

- Level 3 features: friction ridge dimensional attributes, e.g., edge shapes, and pores.

Figure 2.2 shows the examples of level 1, 2 and 3 features. Table 2.2 lists fingerprint feature types and their descriptions. Traditionally, level 1 features could be used for fingerprint classification, and combining with level 2 features could be used for fingerprint matching. Level 3 features have gained researchers' interests recently. Normally, level 3 features are used for manual matching by experts in forensic cases. But now, level 3 features (e.g. pores) could be also used in automated recognition systems (e.g. in [JCD07, ZZZL10]) but high resolution images (>= 1000dpi (dot per inch))

are required in this case. Some researchers have reported that the average accuracy of using solely level 3 features for matching is lower than using level 1 and 2 features, which is about 15-20% lower by comparing the results in [JCD07, ZZZL09]. However, Jain [JCD07] reported that the accuracy could be improved by 20% if level 3 features are used as supplements to level 1 and 2 features for matching. But the image resolution requirement (at least 1000 dpi [JCD06]) for using level 3 features is a constraint condition, because most of the capture devices use 500 dpi as a standard such as FVC databases and NIST databases [MMC+02].

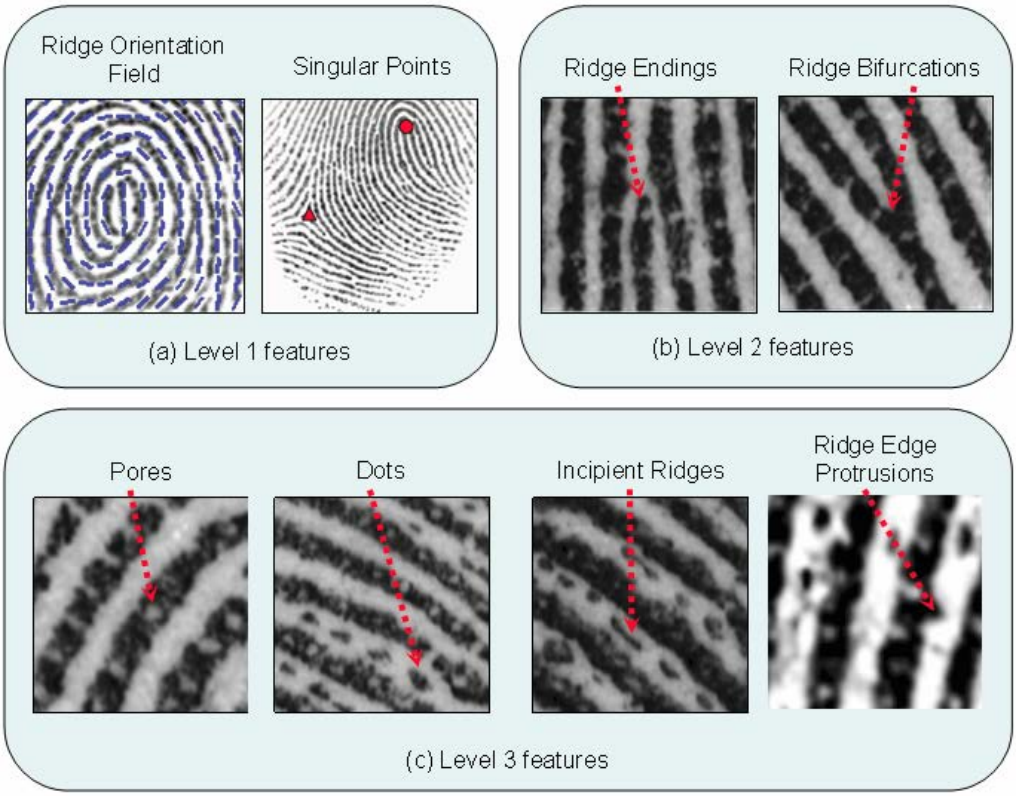

Figure 2.2: Three levels of fingerprint features. It shows the features extracted from level 1 to 3 respectively. The first one is the orientation map and singular points, the second one shows two types of minutiae, and the last one shows level 3 features.(from [Jai11])

Table 2.2: Fingerprint features and their description.

Features	Description
Local ridge orientation	The angle that the local ridges formed with horizontal axis. It is the unoriented direction of ridges lying in [0, 180) degrees [MMJP09].
Local ridge frequency	The number of ridges per unit length orthogonal to the local ridge orientation.
Core point	A core is located at the focus of the innermost recurving ridge line. It is a 'U' like pattern.
Delta point	It's the point on a friction ridge at or nearest to the point of divergence of two type ridge lines. It is a 'Y' like pattern
Minutiae	It refers to local ridge characteristics, Ridge ending and bifurcation are 2 most important minutiae types
Pore	Sweat pores in the ridges.
Dots, incipient ridges and ridge edge protrusions	Other level 3 features.

In this thesis, we concentrate on the use of level 1 and 2 features because of the limitation of resolution requirement of level 3 features. The fingerprint images in the FVC databases are obtained by using current commercial fingerprint capture devices, whose resolution standard is 500 dpi [MMC+02, MMC+04]. Besides, level 1 and 2 features are sufficient to achieve our research objectives, which aims to improve the overall performance of a fingerprint recognition system.

On the other hand, reliable and accurate feature extraction is difficult due to the fingerprint variations caused in the scanning stage, these variations are introduced in the next section.

2.2.1 Fingerprint image variations

The scanned fingerprint images from the same finger may contain variations (e.g. displacement and rotation) due to many factors. Feature extraction and matching errors may be caused due to the variations. There are various reasons causing the variations including the fingerprint conditions (e.g. impairment and humidity), system errors (limitations of fingerprint recognition techniques), inadequate fingerprint impression capturing (e.g. displacement, large rotation angle and partial fingerprint impression captured) and non-linear distortions (mapping 3-D fingers into 2-D images). Therefore, fingerprint recognition is a difficult task due to the variations of the impressions of the same finger. The main factors responsible for intra-class (refers to fingerprints from the same finger) variations are summarized below [MMJP09] and Figure 2.3 shows the examples of such variations:

- **Displacement**: The same finger may be placed in different locations on a touch sensor during different acquisitions resulting in a translation of the fingerprint area. A finger displacement of just 2 mm results in a translation of about 40 pixels in a fingerprint image scanned at a resolution of 500 dpi.

- **Rotation**: The same finger may be rotated at different angles with respect to the sensor surface during different acquisitions.

- **Partial overlap**: Finger displacement and rotation often cause part of the fingerprint area to fall outside the sensor, resulting in a smaller overlap between the foreground areas of the template and the input fingerprints. This problem is particularly serious for small-area touch sensors

- **Non-linear distortion**: The act of mapping of the three-dimensional shape of a finger onto the two-dimensional surface of the sensor results in a non-linear distortion in successive acquisitions from the same finger due to skin plasticity.

- **Pressure and skin condition**: The ridge structure of a finger would be accurately captured if ridges of the part of the finger being imaged were in uniform contact with the sensor surface. However, finger pressure, dryness of the skin, skin disease, sweat, dirt, grease, and humidity in the air all compound the situation, resulting in a non-uniform contact. As a consequence, the acquired fingerprint images are very noisy and the noise strongly varies in successive acquisitions of the same finger depending on the magnitude of the above causes.

- **Noise**: It is mainly introduced by the fingerprint sensing system. For example, residuals are left over on the glass plate from the previous fingerprint capture.

- **Feature extraction errors**: The feature extraction algorithms are imperfect and often introduce measurement errors. Errors may be made during any of the feature extraction stages (e.g., estimation of orientation and frequency images, detection of the number, type, and position of the singularities, segmentation of the fingerprint area from the background, etc.).

- **Feature matching errors**: The feature matching algorithms are imperfect and introduce measurement errors. These errors may be caused by the unreliable extracted features and/or unreliability of the matching algorithms.

In summary, there are three major fingerprint variations: displacement, rotation and non-linear distortion, which needs to be addressed in an automated fingerprint recognition system. When one or more of the above situations happen during the matching process, it may raise the difficulty of obtaining a satisfactory matching result. During the feature extraction and matching stages, the influence of the above factors should be minimized to obtain a reliable and accurate matching result. In the next section, we will introduce a typical fingerprint recognition system which illustrates how these fingerprint features are extracted and processed for matching.

Figure 2.3: Each row shows two fingerprint images from the same finger from FVC2002 database. Maio et al. [MMJP09] reported that these fingers were falsely non-matched by most of the algorithms submitted to FVC2002.

2.3 Fingerprint Recognition Systems

A fingerprint recognition system refers to a system which is able to verify whether a pair of fingerprints belongs to the same individual automatically [MMJP09, Wik14b] . Fingerprint recognition by human experts normally obtains better results than an automated fingerprint recognition system, because there are some situations that machines can not handle with (e.g. extremely poor quality fingerprints obtained from crime scene and some latent fingerprints) [MMJP09]. However, an automated fingerprint recognition system has the huge advantage of time and cost consumptions with adequate accuracies for fingerprint images with normal or above levels of qualities.

Fingerprint recognition systems could be classified into two sub-systems based on their purposes. These two sub-systems are called automated fingerprint identification system (AFIS) and fingerprint verification system (AFVS).

An AFIS is able to identify a person's identity based on the captured fingerprint(s). In this system, it searches the entire fingerprint database in order to find out a match. If there is a match, then this person is identified. Therefore, a fingerprint identification system is able to answer the question of "*Who is this person?*". But in an AFVS, a person provides his/her identity (e.g. ID and name) that he/she claims to be, then the system verifies that the captured fingerprint matches the registered fingerprint template stored in the database. If there is a match, then this person is recognized by the system. Therefore, a fingerprint verification system is used to solve the problem of "*Is this person the one claimed to be?*". Based on the above

description, we can see that the major difference between these two systems is that a fingerprint identification system contains a component for database searching for one-to-many matching (normally uses fingerprint classification techniques to speed up the searching time). But a fingerprint verification system uses one-to-one matching, which only needs to verify whether two fingerprints are a match or not.

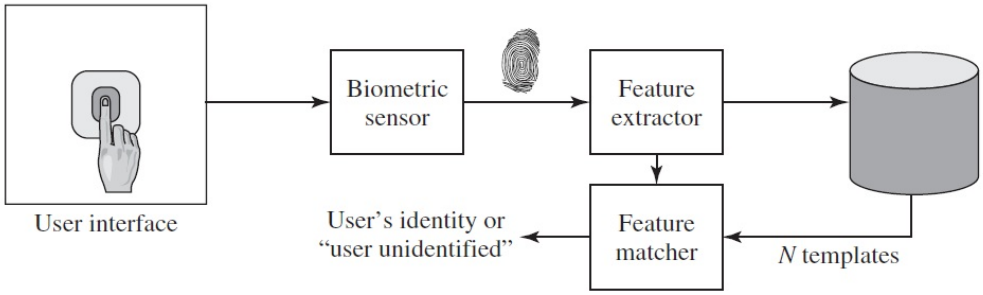

(a) Identification

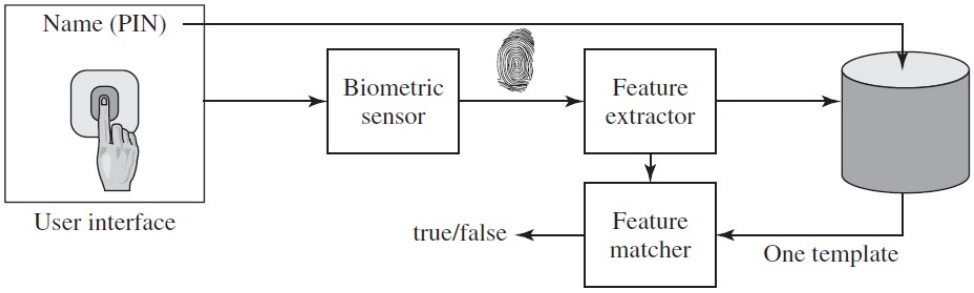

(b) Verification

Figure 2.4: The flowcharts of fingerprint identification and verification systems (from [SB11]).

Figure 2.4 illustrates the flowcharts of fingerprint identification and verification systems. From Figure 2.4a, we can see that the query fingerprint tries to match N templates in an identification system to find a match in order to identify the user's identity. And in Figure 2.4b, the user needs to input his/her name and pin along with the fingerprint to verify his/her identity. Fingerprint identification systems are normally used by law en-

forcement agencies for criminal identifications. But a fingerprint verification system can be integrated with any authentication systems to improve the security and reliability of these systems.

From the above figure, we can also see that both AFIS and AFVS have two components which are feature extraction and feature matching. Performance of these two parts may influence the overall performance of a fingerprint recognition system. The less feature extraction errors occur, the more reliable is the extracted features. Extracted features are inputs to the feature matcher, so that reliable features may reduce the matching errors of both matching algorithms and the whole system. Therefore, improving the accuracies of feature extraction and feature matching may improve the overall accuracy of either a fingerprint verification system or a fingerprint identification system. From the above analysis, we can see that focusing on the research of the feature extraction and matching techniques is able to improve the matching accuracy of a fingerprint identification or verification system.

Figure 2.5 illustrate a big picture of a fingerprint recognition system. From the figure, we can see that fingerprint identification systems have an additional component called fingerprint classification, which is able to determine the fingerprint types (refers to five types in Figure 2.6). In fingerprint classification, singular points (core and delta points) are used to determine the fingerprint types according to the number and location of core and delta points in a fingerprint image. Besides, the singular points are also used in fingerprint alignment (used to solve the rotation and displacement problem in fingerprint recognition) in both minutiae and correlation based (refer to matching methods using texture information) matching methods. In the

feature matching block, there are two major classes of matching techniques according to the selected features, one of which is minutiae based and the other is based on patterns other than minutiae (non-minutiae and correlation based). Most fingerprint recognition systems use minutiae based techniques for their high accuracy especially when reliable minutiae can be easily obtained [MMJP09]. However, the accuracy of minutiae extraction is heavily depended on the quality of fingerprint images, and noise in a fingerprint image may introduce spurious minutiae points. Therefore, non-minutiae based fingerprint recognition techniques are popular when the quality of fingerprint images are low and it is hard to extract accurate minutiae. No matter which features are used for matching, accurate feature extraction is essential to a fingerprint recognition system.

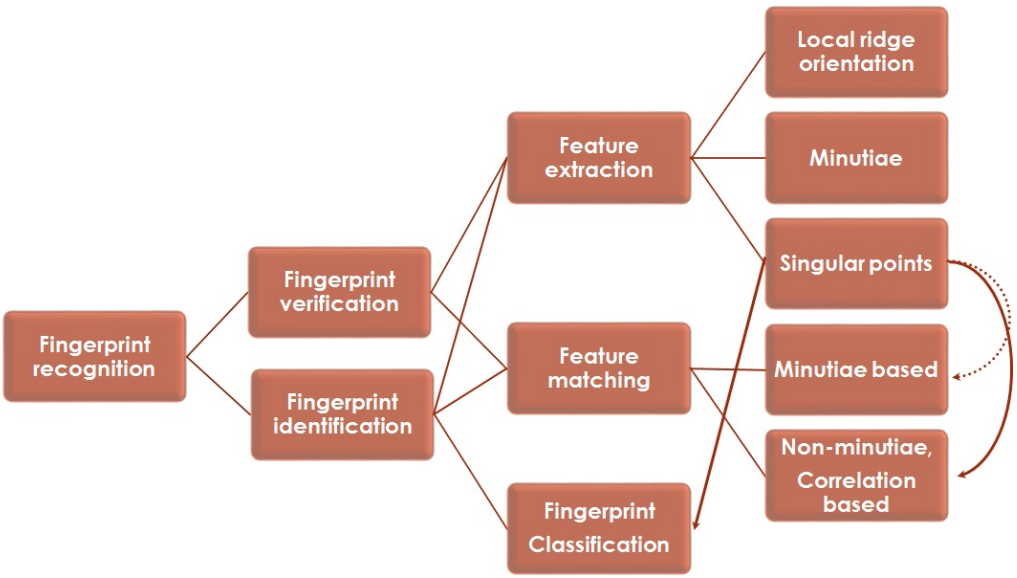

Figure 2.5: A big picture of a fingerprint recognition system.

Both feature extraction and feature matching have great impact on the final matching scores. The purpose of feature extraction is to extract reliable features as the input to the matching algorithms. The feature matching

section has the function of computing the overall similarity between two enrolled fingerprint images. If the similarity between two fingerprints is high, then these two fingerprints have a high probability of belonging to the same finger, vice versa. Therefore, reliable and accurate feature extraction and matching is the overall challenge in any fingerprint recognition system.

(a) Left loop (b) Right loop (c) Whorl

(d) Plain arch (e) Tented arch

Figure 2.6: Different types of fingerprint classified by their global shapes.

2.4 Components in Feature Extraction and Matching

There are many components in feature extraction and matching parts of a fingerprint recognition system. A typical fingerprint feature extraction and

matching procedure may include the following stages (as shown in Figure 2.7):

- Segmentation. It refers to the separation of fingerprint area (foreground) from the image background. An elegant segmentation technique should be able to separate the reliable area in a fingerprint image for further processing.

- Image pre-processing (or called pixel-wise enhancement). It refers to adjusting the pixel intensity values of a fingerprint image to the desired intensity values depending on some parameters (e.g. mean intensity and intensity variance). So that all the fingerprint images has a uniform distribution of intensity values in the same range, which will be used as the input images in the contextual filtering stage. One of the most popular image pre-processing technique in fingerprint recognition field is image normalization developed by Hong et al. [HWJ98].

- Local ridge orientation and frequency estimation. Local ridge orientation $\theta(i, j)$ at pixel (i, j) refers to the angle that the ridge crosses through a small neighborhood with horizontal axis where local ridge frequency at pixel (i, j) refers to the inverse number of ridges per unit length along a hypothetical segment centred at (i, j) and orthogonal to the local ridge orientation $\theta(i, j)$.

- Contextual filtering. In contextual filtering stage, the filter (e.g. Gabor filter and Log-Gabor filter) characteristics change according to the local context like local ridge orientation and frequency. It is the major stage for image enhancement and noise removal. Binarization

of fingerprint images could be performed after this stage in order to facilitate the minutiae extraction.

- Minutiae/feature extraction. The extracted minutiae are used in minutiae based fingerprint recognition systems for matching while the patterns may be used in a pattern based fingerprint recognition system. Other features like singular points may also be extracted for fingerprint alignment and matching.

- Fingerprint alignment and matching. In this stage, the above feature information is used to compare the registered fingerprint and query template to obtain a matching score. Before the matching process, the two fingerprints may need to be aligned to the same position and direction.

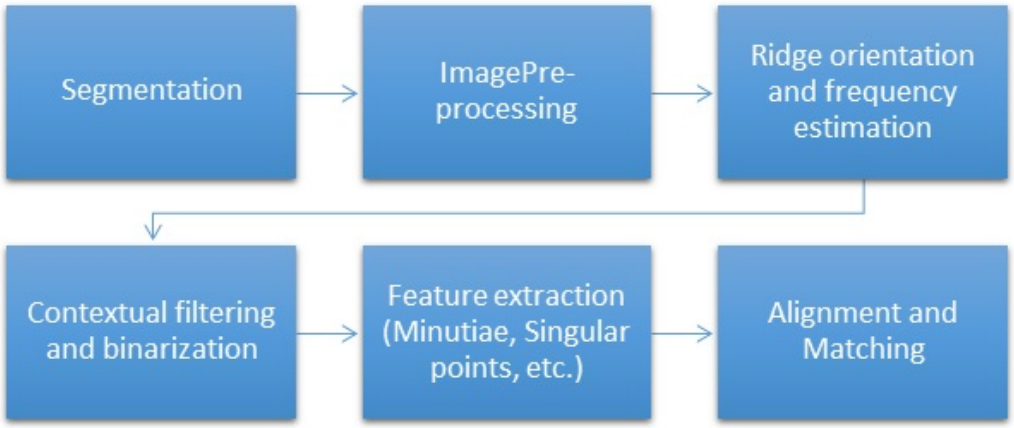

Figure 2.7: The procedure of feature extraction and matching in a fingerprint recognition system.

In the following sections, each stage of a fingerprint recognition system will be described in detail.

2.4.1 Fingerprint image segmentation

Segmentation refers to separating a fingerprint image into foreground and background. Foreground means the recoverable ridge and valley areas of a fingerprint image while background means the unrecoverable, non-ridge and non-valley areas [MMJP09]. After segmentation, a mask is generated to shield the background. Figure 2.8 shows two samples of segmentation from Ratha et al.'s [RCJ95] and Chen et al.'s [CTCY04] approaches. Ratha etal's segmentation method processes a fingerprint image block by block with a size of 16 x 16, based on the intensity variance and mean intensity. Thus, the boundary of the segmentation mask does not exactly fit the boundary of the fingerprint as show in Figure 2.8a. Chen et al. [CTCY04] trained a linear classifier to select foreground (ridge and valley areas), then a post-processing stage is performed to regularize the results. The segmentation mask of Chen et al.'s method has a smooth boundary that Ratha et al's method does not have as shown in Figure 2.8.

Segmentation removes the interferences of non-fingerprint or/and noisy areas in a fingerprint image. It is important for the accuracy of feature extraction in the subsequent stages, because features extracted from non-ridge, non-valley or/and noisy areas are not reliable for the matching.

(a) (b)

Figure 2.8: Two segmentation techniques: (a) an example of fingerprint segmentation by Ratha's [RCJ95] approach; (b) an example of fingerprint segmentation by Chen et al.'s [CTCY04] approach;

The fingerprint features that can be used in a fingerprint segmentation are listed as follows:

- *Mean intensity*: Mean intensity of a block indicates the grey level of that block. Because foreground area contains ridges which usually have lower intensity values than background areas. The calculation of mean intensity for a window with size of w x w is illustrated in equation 2.1 [RCJ95, BG02]:

$$M = \frac{1}{w^2} \sum_{w} I \tag{2.1}$$

where M denotes the mean intensity and I denotes the intensity of each pixel in the chosen window.

- *Intensity variance*: Because foreground of a fingerprint image contains ridges and valleys, and the intensities of ridge and valley are quite distinctive. Thus the intensity variance of foreground will be higher than background. The calculation of intensity variance for a window with size of w x w is illustrated in equation 2.2 [RCJ95, BG02]:

$$V = \frac{1}{w^2} \sum_{(I-M)^2} I \tag{2.2}$$

where V denotes the intensity variance.

- *Coherence*: Coherence was first used in fingerprint segmentation by Bazen and Gerez [BG02] to evaluate how well the gradients are pointing in the same direction. Coherence usually is higher in the foreground than background, because the ridges and valleys are continuous and parallel. The coherence is also used to evaluate the reliability of a selected fingerprint area. If the coherence value is low, then the selected area is probably a noisy or non-ridge and non-valley area. Thus, it is also used for fingerprint image quality estimation [CDJ05, ZYHZ05]. The calculation of Coherence is illustrated in equation 2.3.

$$Coh = \frac{\sqrt{(G_{xx} - G_{yy})^2 + 4G_{xy}^2}}{G_{xx} + G_{yy}} \tag{2.3}$$

where Coh denotes the coherence value, and G_{xx}, G_{yy}, and G_{xy} are averaged squared gradient components over a window w, which are calculated as $G_{xx} = \sum_w G_x^2$, $G_{yy} = \sum_w G_y^2$ and $G_{xy} = \sum_w G_x G_y$, respectively. And G_x and G_y are gradient components, which indicate the gradient values on x-axis and and y-axis, respectively.

- *Local ridge orientation patterns.* The local ridge orientations in the foreground should contain a dominated orientation, while background usually does not have one.

Most segmentation methods use more than one of above features to calculate the segmentation mask. Much research has been reported for segmentation of fingerprint images. Those approaches can be classified into several categories, which are: feature value thresholding based segmentation approaches [MMKC87, MC89, MM97, XZWG12, FDJ12, ZZYJ13, HWJ98] and learning-based segmentation approaches [BG02, CTCY04].

Feature value thresholding approaches use global or local thresholding of features in a fingerprint to separate background and foreground. Mehtre et al. [MMKC87] separate the fingerprint images by calculating the histogram of ridge orientation in each 16X16 block. The presence of a significant peak in a histogram denotes an oriented pattern, whereas a flat or near-flat histogram is characteristic of an isotropic signal. Maio and Maltoni [MM97] use the average magnitude of the gradient in each 16X16 block to separate a fingerprint image. Ratha [RCJ95] uses the intensity variance in the orthogonal direction to the ridge orientation. The example of Ratha's approach is shown in Figure 2.8a. Hu [HYZ+10] performs adaptive threshholding segmentation after applying the log-Gabor filtering to the im-

age, which achieves better result than directly applying the segmentation method. Fleyeh et. al [FDJ12] and Zhao et. al [ZZYJ13] define several fuzzy rules to select the thresholds of parameters. Fleyeh et al. claim that 96% of tested fingerprint images from FVC2000 databases are correctly segmented, but the size of test dataset is relatively small since only 100 images are selected for testing. Zhao et. al admit that their method perform well on high quality images, but not well on some low quality images. One problem of feature value thresholding methods is that the segmentation boundary does not fit the fingerprint boundary which is square like and not smooth as learning based methods as shown in Figure 2.8a and 2.8b. This is because a fingerprint image is processed blockwisely in these methods. Wang et al. [WBGS10] uses a median filter to smooth the boundary of segmentation to obtain a result similar to learning-based methods as shown in Figure 2.9. This segmentation method is adopted in this research for its simple implementation, fast running speed but satisfactory experimental results.

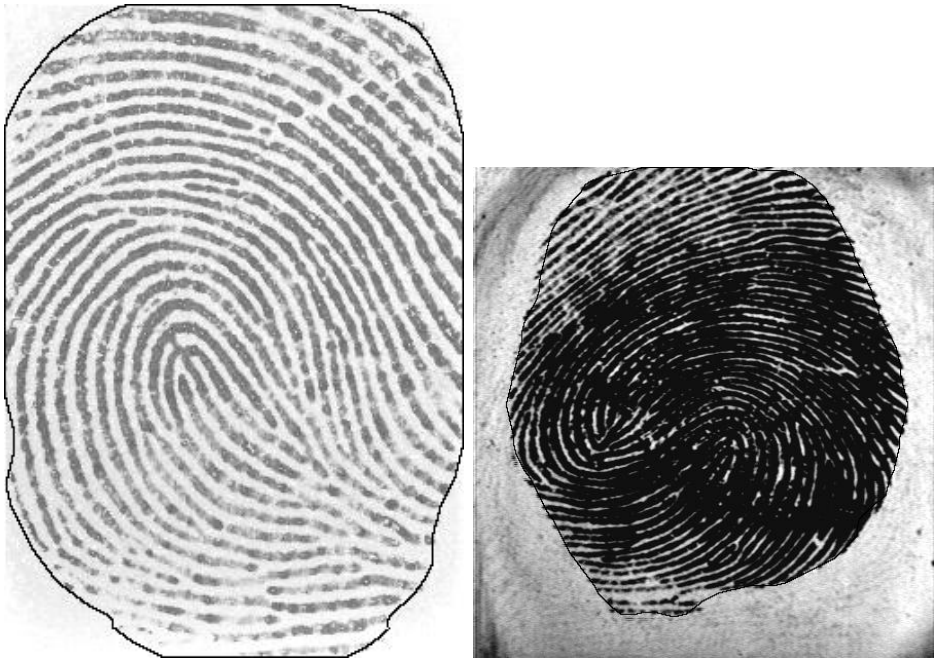

(a) (b)

Figure 2.9: Two samples of segmentation using the method in [WBGS10]. The black line surrounding the fingerprint area indicates the mask boundary. The fingerprint images are from FVC 2002 databases [MMC+02].

Learning-based segmentation approaches usually use linear-classifiers to select background and foreground [MMJP09]. Bazen and Gerez [BG02] proposed a pixel-wise method, where gradient coherence, intensity mean, and intensity variance are computed for each pixel, and a linear classifier associates the pixel with the background or the foreground. Chen et al. [CTCY04] proposed a linear classifier to select foreground blocks based on: the block clusters degree, the difference of local block intensity mean and global image intensity mean, and the block variance. Morphology is then applied during post-processing to regularize the results and reduce the number of classification errors. Figure 2.8b shows an example of fingerprint segmentation by Chen et al.'s [CTCY04] approach. Based on Chen et al's [CTCY04] work, Yang et al. [YZYY10] designed a K-mean based

segmentation method, which does not require the training process. Thus, this method performs faster than Chen et al.'s method.

There are some other interesting methods developed recently. Instead of using mean intensity and variance directly, Zhe et al. [XZWG12] uses the mean shift algorithm to perform the fingerprint segmentation. They define a new feature based on the mean intensity, variance and coherence. However, they only provide a comparison of some samples instead of experimental results on large databases. Another method developed by [BB11] calculates the fingerprint segmentation mask in the frequency domain. They apply a filter to the whole image to get its quality map. Then the segmentation mask is derived from the quality map. They compared their method to coherence based, mean intensity based and intensity variance based methods respectively, and they claimed that the result of their method is the best among those methods. However, they did not compare their method to hybrid segmentation method like the methods based on all of those features. Moreover, due to the fuzzy characteristic of biometrics (e.g. captured fingerprints will not be exactly the same even from the same finger), it is hard to obtain an absolute accuracy score for every segmentation technique. All the experimental results are judged by experts, which may cause errors.

Though fingerprint segmentation is extensively researched, the performance of current techniques could be further improved. The challenges could be summarized as the following points:

- Detect the noise area inside the fingerprint area. Most state-of-the-art fingerprint segmentation methods are able to separate the fingerprint and non-fingerprint area quite accurately. However, to separate the noise area inside the fingerprint is a difficult task. This is because it

is hard to evaluate the noise level to determine whether the areas can be reserved to extract reliable features or not. A quality evaluation process may be a solution to this problem.

- Accuracy versus efficiency. Msiza et al. [MMNM11] have investigated current segmentation methods, and they found that it is hard to achieve both the high accuracy and efficiency. A segmentation algorithm with higher accuracy normally is more complex (e.g. a training process or complex algorithm) and requires more costs of computation.

- Segmentation for latent fingerprint images. The automatic latent fingerprint recognition is a new research area, however, it will not be addressed in this thesis. Latent fingerprints refer to the fingerprints that are not visible immediately by naked eye, like the fingerprints left in a crime scene. Figure 2.10 shows two examples of latent fingerprints images. Both images contain lots of useless informations other than the fingerprints.

(a) (b)

Figure 2.10: Two examples of latent fingerprint images.

2.4.2 Image pre-processing

After the segmentation, image pre-processing is conducted to improve the contrast of the image and uniformly distribute the intensity values into selected ranges. Image pre-processing in fingerprint recognition is also called pixel-wise enhancement which refers to assigning a new value to each pixel depending on its previous value and some parameters (e.g. mean intensity and intensity variance) [MMJP09]. Thus, this stage belongs to image processing measures in the spatial domain. Pixel-wise techniques act as an initial processing stage followed by a further image enhancement algorithm (referring to contextual filtering techniques). There are many pixel-wise enhancement techniques which have been used in fingerprint recognition systems including histogram equalization [WCT98], Wiener filtering [GAKD00] and normalization [HWJ98], adaptive normalization [KP02], and a method based on the analysis of finger skin profile [SG06].

The most popular pixel-wise enhancement is normalization introduced by Hong et al.[HWJ98]. It adjusts the intensity values of a fingerprint image to have the desired range of intensity values and variances. The distribution of intensity values of fingerprint images are normally different even scanned by the same type of scanners depending on the environment (light condition, wetness, finger pressure on the scanner etc.) during the scanning . But this normalization technique is able to adjust the intensity values of all the images into the same range to facilitate further processing. The detailed algorithm is described as follows:

$$I[x,y] = \begin{cases} m_0 + \sqrt{I[x,y] - m)^2 * v_0/v} \text{ if } I[x,y] > m \\ m_0 - \sqrt{(I[x,y] - m)^2 * v_0/v)} \text{ if } otherwise, \end{cases} \tag{2.4}$$

where m and v are the image mean and variance and m_0 and v_0 are the desired mean intensity and variance after normalization. Figure 2.11 shows an example of normalization described in [HWJ98].

(a) (b)

Figure 2.11: An example of normalization described in [HWJ98].

Kim and Park [KP02] improved the above normalization method by dividing the image into blocks and calculating the mean intensity and variance block by block.

The purpose of this stage is to make the distributions of ridge and valley intensities fall in the different ranges which give the image a better clarity. The limitation of the above image pre-processing techniques focuses on the increase of the image contrast rather than removing noise. However, in our study, we found that removing certain amount of noise (e.g. Gaussian noise and other nonuniform noise) in this stage is able to obtain a better processing result in the subsequent contextual filtering stage. Therefore, designing a fingerprint image pre-processing method which is supportive to successive contextual filtering (e.g. Gabor filtering), for better enhancement

results and feature (e.g. minutiae) extraction is a challenge in fingerprint recognition.

2.4.3 Ridge orientation and frequency estimation

Local ridge orientation and frequency are two features required in subsequent filtering process. Local ridge orientation $\theta(i, j)$ at pixel(i, j) refers to the angle that ridge crosses through a small neighborhood with horizontal axis. And local ridge frequency at pixel (i, j) refers to the inverse number of ridges per unit length along a hypothetical segment centred at (i, j) and orthogonal to the local ridge orientation $\theta(i, j)$ [MMJP09]. Figure 2.12 shows a demonstrated result of local orientation estimation, where Figure 2.12a is a fingerprint image and Figure 2.12b is the plot of ridge orientation. Figure 2.13 shows the calculation of local ridge frequency at pixel (x_i, y_j) [HWJ98]. Local ridge orientation field and ridge frequency can be estimated by the gradient based method with the following steps which was proposed by Kass and Witkin [KW87], Hong et al. [HWJ98] and Bazen and Gerez [BG02]:

(i) Divide the input image into w x w size blocks (16 x 16 is an empirical size used by authors);

(ii) Compute $G_x(i, j)$ and $G_y(i, j)$ which are two gradient components along x and y direction at pixel (i, j) respectively. They are computed by convoluting with horizontal and vertical Sobel operator [GW01] and for each block. G_{xx}, G_{yy}, and G_{xy} are averaged squared gradient components over a window w. We define:

$$G_{xx} = \sum_{w} G_x^2, \tag{2.5}$$

$$G_{yy} = \sum_{w} G_y^2, \tag{2.6}$$

$$G_{xy} = \sum_{w} G_x G_y, \tag{2.7}$$

(iii) The local ridge orientation of point (i, j) is calculated by:

$$\theta(i,j) = \pi/2 + 1/2 * tan^{-1}(2G_{xy}/(G_{xx} - G_{yy})) \tag{2.8}$$

(iv) Construct a 1-D wave by projecting the grey levels of all pixels in each block along the direction orthogonal to block orientation as shown in Figure 2.13. Let $T(i,j)$ ($T(i,j) = (s_1 + s_2 + s_3 + s_4)/4$) be the average number of pixels between five consecutive peaks ($s_{1,2,3,4}$) in the constructed 1-D wave (see Figure 2.13b), then the frequency $f(i,j) = 1/T(i,j)$.

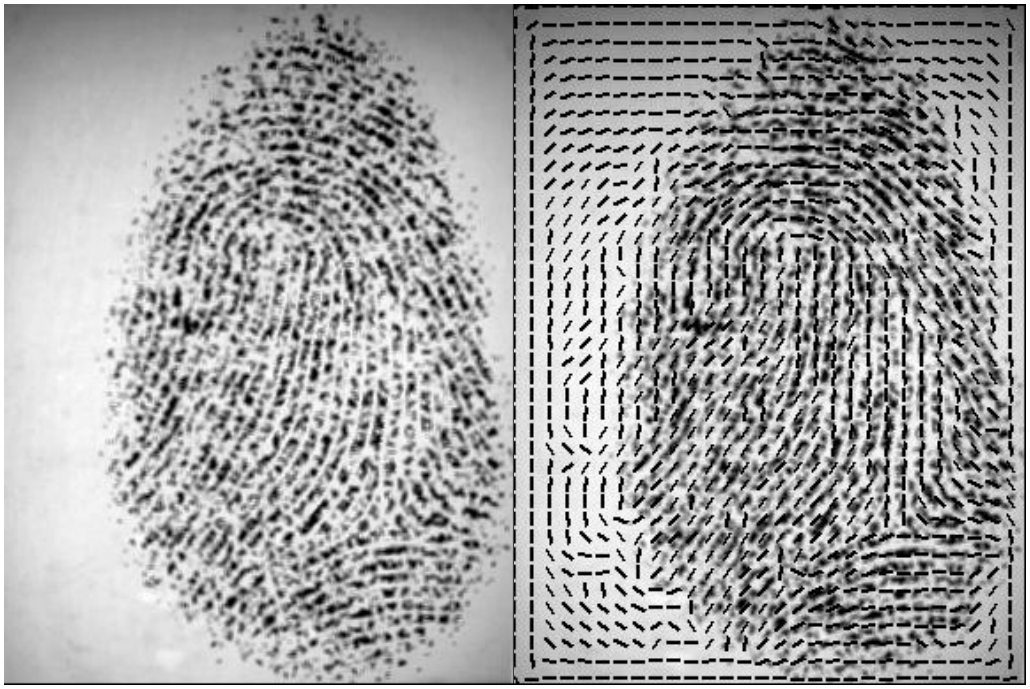

(a) (b)

Figure 2.12: The result of local orientation estimation: (a), a fingerprint image and (b), the plot of ridge orientation.

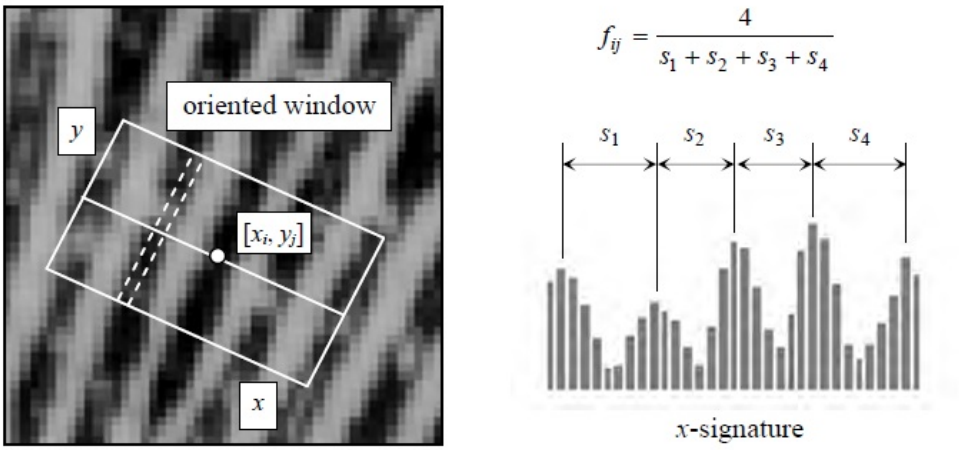

(a) (b)

Figure 2.13: (a), An oriented window centered at pixel (x_i, y_j); (b), The x-signature on the right clearly exhibits five peaks; the four distances between consecutive peaks are averaged to determine the local ridge frequency (from [HWJ98])

The orientation estimation methods include two major categories: local based orientation estimation and global based ones. Most traditional methods are local based methods. Some other orientation estimation methods are developed other than using the gradient of an image. Ji [JY08] developed an orientation estimation method based on the pulse coupled neural network (PCNN) and ridge projection. They firstly divide the fingerprint image into 16x16 blocks then detect the primary ridge using PCNN, then they estimate the ridge orientation based on the detected primary ridge. Finally they will correct the orientation value based on a 3x3 neighbour field. They observe that their method can improve the accuracy at a rate of 3.6% to Hong et al.'s [HWJ98] system. However, their system is only able to provide 4 different orientations of each block and the block size is fixed to 16x16. Therefore, it may not be enough to show the accurate ridge orientation by only using 4 different orientation values. Zhu [ZYHZ06] developed a neural network based method to learn the correctness of orientation of the gradient based method. They claim that their method will improve the accuracy of minutiae detection. However, they did not apply their method to large databases for evaluation.

Chikkerur [CR05] developed an orientation field estimation method in the Fourier domain by short time Fourier transformation (STFT) analysis. Then, Wang and Hu [WHP07] proposed a fingerprint orientation model based on 2D Fourier expansions (FOMFE) in the phase panel. They firstly generated a coarse orientation field in a grey scale image based on a gradient method, then FOMFE is used to reconstruct the orientation field in the global level of a image. Based on the FOMFE method, Tao et. al [TYC+10] designed a weighted-FOMFE method for orientation estimation, and they

claimed that their method improves about 3.6% of accuracy comparing to FOMEE method.

In conclusion, although many methods have been proposed in the literature, it is still an ongoing problem especially for those low quality images. Local ridge orientation field is one of the input of the contextual filtering techniques (e.g. Gabor filtering), and it is used to calculate the singular points of the fingerprints which is important to alignment and fingerprint classifications.

2.4.4 Contextual filtering

In contextual filtering stage, the filter characteristics change according to the local context like ridge orientation and frequency [MMJP09]. Contextual filtering is widely used for fingerprint image enhancement. Much research has been reported for contextual filtering. The most popular filtering technique is Gabor filter, adopted by Hong et al. [HWJ98], Lee and Bhattacharjee [LB09], Greenberg et al. [GAKD00] and Jang et al. [JPLK06]. Besides, some other filters have been designed for contextual filtering such as log-Gabor filter [WLHF08], directional Fourier domain filter [SMM94], directional median filter [WSG04], curved Gabor filter [Got12b, Got12a] and oriented diffusion filtering techniques [GS12].

The 2-demensional Gabor filter is introduced in the following equations. We adopt it for contextual filtering in our work as it is a well known and effective context filtering technique. The 2-dimensional Gabor filters have the properties of both orientation and frequency selectiveness. The equations

for 2-D even symmetric Gabor filters are as follows [MMJP09, JRL97]:

$$G(x, y; \theta, f) = exp\{-1/2(\frac{x_\theta^2}{\sigma_x^2} + \frac{y_\theta^2}{\sigma_y^2})\}cos(2\pi f x_\theta) \tag{2.9}$$

$$x_\theta = xsin\theta + ycos\theta \tag{2.10}$$

$$y_\theta = -xcos\theta + ysin \tag{2.11}$$

where f and θ denote the frequency and orientation of local ridges respectively, whereas σ_x and σ_y represent the standard deviation of Gaussian envelope along x and y axes respectively. Therefore, before using Gabor filters, two parameters that should be estimated are local ridge orientation and frequency. The selection of $\sigma_x$and σ_y determines the performance of 2-D Gabor filters. The larger values chosen for σ_x and σ_y may be better for removing noise, but it may produce some spurious ridges, the smaller values chosen for σ_x and σ_y may not effectively remove noise [MMJP09]. Hong et al. [HWJ98] suggest 4 is a good choice for both σ_x and σ_y by observing their empirical data. Figure 2.14 shows the graphical representation (lateral view and top view) of the Gabor filter defined by the parameters θ = 135 degrees, f = 1/5, and $\sigma_x = \sigma_y = 3$. Figure 2.15 shows an example of fingerprint image processing results by Gabor filtering.

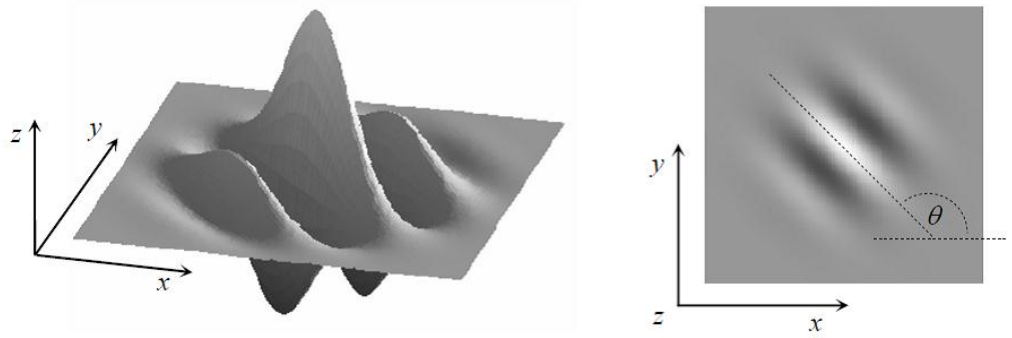

Figure 2.14: Graphical representation (lateral view and top view) of the Gabor filter defined by the parameters θ= 135 degrees, f = 1/5, and σ_x= σ_y = 3 (from [MMJP09]).

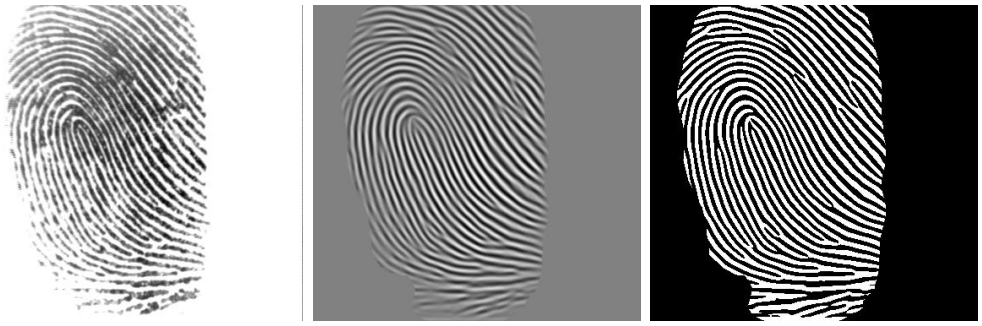

(a) (b) (c)

Figure 2.15: An example of fingerprint image processing results by Gabor filtering: (a) the original fingerprint image is from FVC 2002 database; (b) the processed fingerprint image after Gabor filtering; and (c) is the binarized image. Note the above images are segmented, and $\sigma_x = \sigma_y = 2$.

Contextual filtering is the most important image processing stage for fingerprint images in a fingerprint recognition system. It is able to enhance the fingerprint images for extracting the binarized fingerprint images afterwards, which can be used to extract minutiae or other important features in the matching stage. Most of the contextual filtering techniques are able to fulfil the requirements of fingerprint image enhancement. However, their

performance is highly depended on the previous stages especially on the local ridge orientation estimation and local ridge frequency estimation.

2.4.5 Singular point detection

Singular points could be used for fingerprint alignment (as reference points to superimpose two fingerprints) and fingerprint classification (to determine the fingerprint types).

Plenty of research has been reported for singular point detection. The most popular approach is based on Poincaré Index which was first proposed by Kawagoe and Tojo [KT84]. It is a simple and effective approach to detect the singular points. However, it is well recognized that the accuracy of this approach highly depends on the quality of fingerprint images. For low quality fingerprint images, this approach can generate a large number of spurious singular points [MMJP09]. The spurious singular points may influence the accuracy of fingerprint alignment and classification. Several improved approaches have been proposed to overcome the problem of spurious singular points in recent years. Karu and Jain [KJ96] smooth the orientation field of fingerprints by averaging to reduce the number of detected singular points based on the observation that a fingerprint of an individual contains same number of cores and deltas. It improves the accuracy of singular points detection since most fingerprints do not have more than 2 core-delta pairs. The problem with this approach is that smoothing the fingerprint images may cause detected singular points some pixels away from of original ones as noticed by Wang et al. [WLN07]. In some cases, over smoothing of the ridge orientation field may cause the miss detection of genuine singular points, because the detected singular points may shift away

from the genuine location. Therefore, Wang et al. [WLN07] investigated the relationships between singular points and their neighborhoods and establish a theorem named "zone Could-be-in" which indicates the areas that may contain singular points to address the above problem. Zhou et al. [ZGZ07] proved that a fingerprint should have the same number of cores and deltas, and they computed the Poincaré Index combining with a technique named Differences of the Orientation values along a Circle (DORIC). They use the Poincaré Index method first to detect the singular points, then the optimal singular points are selected to minimize the difference between the original orientation field and the model-based orientation field reconstructed from the singular points. Bo et al. [BLE09] proposed an approach based on orientation field which can detect regions possibly containing singular point to improve the efficiency of Poincaré Index algorithm. Besides the above approaches based on Poincaré Index, some other approaches like detecting singular points by reliability/coherence [CLMM99] and zero-pole model [SM93][CEMM00] [FLW00] have been designed. Ravinde et al. [KCH12] uses the reliability of the local ridge orientation to validate the detected singular points. Their experimental results achieve 92.6% detection rate of genuine singular points, however, the false detection rate is 8.4% which is not counted in the final detection rate. Nilsson and Bigun [NB05] developed an approach based on complex filtering and 1D- projection. Nilsson and Bigun's [NB05] approach achieved the best results, which got the performance having 94% correct fingerprint registration rate. Here the registration rate refers to the rate of fingerprint images that could be registered using the detected singular points with other techniques. However, their singular point detection accuracy is about 83% [NB05].

Above all, most of current detection methods produce numerous spurious singular points depending on the quality of fingerprint images and detection techniques used. The limitations of current singular point detection techniques include: (i), the correct detection rate of current singular point detection methods are not high (normally around 90%); (ii), various image qualities still limit the extraction accuracy. We believe singular point detection and extraction need to be further investigated since the accuracy of detection is not satisfactory in particular for poor quality images. The major challenge of singular point detection is how to remove spurious singular points but retain genuine singular points.

2.4.6 Minutiae extraction

Minutiae is another important feature used for fingerprint matching. The accuracy of minutiae extraction determines the accuracy of minutiae based alignment and matching techniques. Normally, minutiae extraction contains the following steps:

(i) Binarization. It refers to binarizing a grey-level scale fingerprint image to a binary image. It is normally proposed after the contextual filtering such as in [HWJ98], however, there are some approaches proposed to process a grey-level image directly. Figure 2.16b shows a binarization result of figure2.16a by Maio and Maltoni's approach [MMC+02].

(ii) Thinning operation. Binary images will be further processed by thinning the ridges lines to one pixel width ridge lines, and a skeleton image may obtain after the process. Figure 2.16c shows a skeleton image obtained after binarization and thinning of Fig 2.16b.

(iii) Minutiae detection. Once a skeleton image is obtained, minutiae may be detected by calculating the cross number $cn(p)$ of a pixel p which is defined by Arcelli and Baja [ADB85]. Figure 2.17 shows cross number values and their respective representations and the cross number cn(p) may be calculated by the following equation:

$$cn(p) = 1/2 \sum_{i=1}^{8} |val(p_{i \bmod 8}) - val(p_{i-1})| \tag{2.12}$$

where $p_0, p_1, ...p_7$ are the pixels belonging to an ordered sequence of pixels defining the eight neighborhood of p and $val(p) \in \{0, 1\}$ is the pixel value.

(iv) Post-processing. It refers to processing the detected minutiae in order to remove spurious minutiae. It is an essential stage because many spurious minutiae points may be extracted.

(a) (b) (c)

Figure 2.16: A sample fingerprint binarization and thinning process. (a) A fingerprint grey-scale image(from FVC2002 DB1a database); (b) the image obtained after binarization of the image in (a); (c) skeleton image obtained after a thinning of the image in (b).

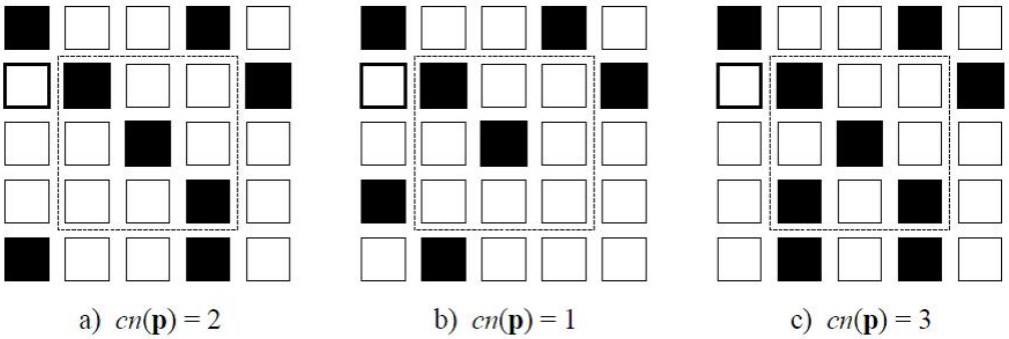

Figure 2.17: Minutiae detection by cross number, when: (a), cn(p) =2, the pixel is in a normal ridge line; (b), cn(p) = 1, the pixel is a ridge ending; (c), cn(p) = 3, the pixel is a ridge bifurcation.

The thinning and cross number based method is one of the most popular minutiae extraction techniques. There are some other minutiae extraction techniques which extract the minutiae directly from grey scale images such as Maio and Maltoni's [MM97] method. These methods work by tracking the local ridge lines in grey scale level. However, these methods do not take the advantage of context filtering, such as ridge rejoining of discontinuities and noise removing. Therefore, minutiae may be mistakenly detected or missed.

Besides, another minutiae extraction technique has been developed by Shin [SHC03, SHC06] based on run length encoding. Run length encoding is a very simple data compression technique [Smi97]. The authors use it to detect the minutiae from the binarized image without thinning. The idea is similar with the methods on the grey scale images, which tracks the ridge lines. But this technique is applied to binarized images (after contextual filtering) instead of grey scale images. In Figure 2.18 shows the example of how run length encoding works to detect the minutiae. It contains two runs of run length encoding which are vertical run and horizontal run re-

spectively for each fingerprint image. The major advantage of this method is that it preserves the geometric information of the ridge structure. The thinning based methods cannot preserve this information properly because the ridge is shrunk to an one-pixel width. Thus the detected minutiae points may have several pixels' shifting comparing to the locations of true ground minutiae points. This problem is well addressed by the above method. This method is adopted in our research, this is because our matching method using binarized minutiae blocks which contains texture information and a minutiae point in the center of a block. Thus the accurate minutiae location (no position shifting in the traditional thinning based minutiae extraction methods) is important to our matching method.

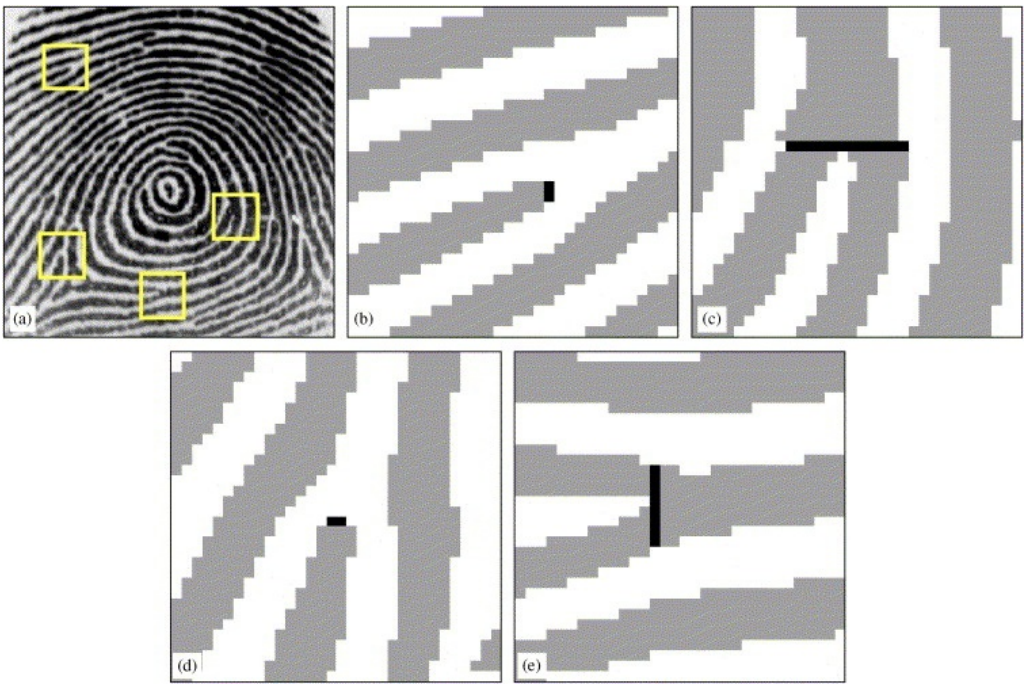

Figure 2.18: Fingerprint minutiae in run representation: (a), input grey fingerprint image; (b), ridge ending in horizontal ridge detected by vertical run; (c), ridge bifurcation in vertical ridge detected by horizontal run; (d), ridge ending in vertical ridge detected by horizontal run; and (e), ridge bifurcation in horizontal ridge detected by vertical run.(from [SHC06])

Regardless of which minutiae detection method is used, more or less spurious minutiae will be detected. Therefore, the more important part of minutiae extraction is how to remove the spurious minutiae but reserve the genuine ones. Post-processing is crucial to all minutiae detection methods. Zhao and Tang [ZT07] introduce several spur minutiae types which usually appear before the post-processing. Figure 2.19 shows examples of these spur minutiae. After minutiae extraction, resultant minutiae will directly be used for alignment or matching. Thus, spur minutiae will decrease the accuracy of alignment or matching. How to effectively extract reliable minutiae is still an on-going challenging problem.

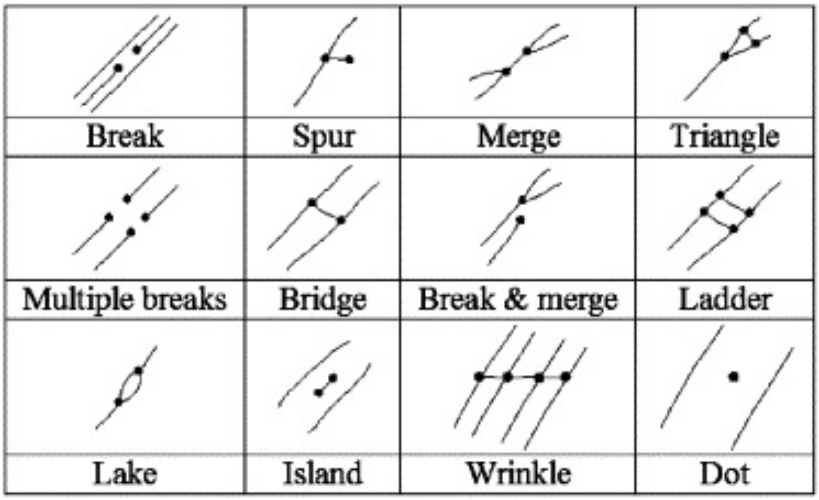

Figure 2.19: Examples of false minutiae (black dots).(from [ZT07])

2.4.7 Fingerprint alignment and matching

After fingerprint features are extracted, then comparisons will be performed between different fingerprint images. Then the alignment problem arises due to the rotation and displacement of fingerprints during the scanning stages. Fingerprint alignment is a difficult problem in fingerprint recogni-

tion. Matching problem could be simplified if alignment is perfectly conducted between two different fingerprints.

2.4.7.1 Fingerprint alignment

There are two categories of alignment methods which are global alignment (using level 1 features) and local feature (level 2 feature) based alignment. Global alignment usually uses some reference points, and singular points are perfect candidate reference points in this case. Thus, how to extract reliable and accurate singular points is a challenging problem which needs to be addressed as well. In local feature based alignment, some local features are extracted for comparison. Local minutiae structure is the most popular feature in this case. Both global and local methods have their inherent advantages and disadvantages.

Though a perfect pre-alignment may greatly improve the efficiency of a fingerprint recognition system and reduce a complex match algorithm to a simple minutiae point pairing problem, there are difficulties to realize such a perfect algorithm. Global pre-alignment methods have two types: i), absolute pre-alignment which pre-align every fingerprint to the fixed rotation angle and position; and ii), relative pre-alignment which align the query fingerprint template according to the template stored in the database. Most absolute pre-alignment methods use core position to translate fingerprint images. However, reliable detection of core point is very difficult due to the various qualities of fingerprint images [MMJP09]. Furthermore, arch fingerprints do not contain a core point which restricts this method to be applied to all fingerprints. A more robust option is to use a relative pre-alignment approach based on a dynamic selection among different alignment

techniques such as by superimposing the singularities, correlating the orientation images and comparing ridge features [YA06].

Due to the time and resource constraints and difficulty of global matching, researchers [WCT98, HM90, FLW00] have developed local minutiae matching approaches which do not need to consider the global transformation such as translation and rotation. Local minutiae matching consists of comparing two fingerprints according to local minutiae structures. These structures include ridge distance, ridge count between the central minutiae and the number, distance and angles of minutiae falling inside some regions [MMJP09]. Because these methods do not require pre-alignment of two fingerprint images, they are also called alignment free methods (e.g.[WH12, LYC+10]).

2.4.7.2 Fingerprint matching

A fingerprint matching algorithm compares two given fingerprints and returns either a degree of similarity or a binary decision (matched/non-matched) [MMJP09]. Most of the matching algorithms are performed on binaraized images or after minutiae extraction.

Matching fingerprint images is a very difficult problem due to the variations of the impressions of the same finger as we introduced before. The aim of matching algorithms is to find the maximum number of matches of minutiae (or patterns) and get a similarity score between two fingerprint images and set a threshold to check whether the similarity score exceeds the threshold.

Fingerprint matching techniques can be coarsely classified into three families[MMJP09]:

- Correlation-based matching (e.g. [LELJSM07, KAN08]): two fingerprint images are aligned and overlapped according to their displacements and rotations, then the correlation between the corresponding pixels is computed. The correlation between two fingerprint images is computed on the grey scale images. If the correlation value between two fingerprints is high, then these two fingerprint is possible a match; otherwise these two fingerprints may not from the same finger.

- Minutiae based matching (e.g. [JY00, HWJ98, CFM10]): this is the most popular and widely used technique. It is an analogy of the fingerprint comparison made by fingerprint examiners. Minutiae are extracted from the two fingerprints and stored as sets of points (e.g. $(x_i, y_j; \theta_{ij})$). Minutiae-based matching tries to find the alignment between the template and the input minutiae feature sets that result in the maximum number of minutiae pairings [MMJP09]. It can be classified into two types for minutiae based matching, which are: global pre-alignment using reference points then for matching, and local minutiae structure based matching. The local minutiae structure based matching methods can be further classified into nearest neighor-based and fixed radius-based matching methods. The nearest neighor-based methods explores the relationships between the selected minutiae and a number of its nearest surrounding minutiae, e.g. the method proposed by Jiang and Yau [JY00]. The drawback of nearest neighor-based methods is that the tolerance to spurious and missed minutiae is low [CFM10] (the local minutiae structure may not be reliable if there is spurious minutiae surrounding the central minu-

tiae). Slightly different with nearest neighor-based methods, fixed radius based methods define a fixed radius R. All the minutiae in the radius R of the selected minutiae are considered as its neighbors, e.g. the method proposed by Ratha et al. [RB00]. This matching method family has better tolerance to spurious and missed minutiae to nearest neighor-based methods. Because all the surrounding minutiae inside the radius R contributes to the formed local minutiae structure, a small number of spurious minutiae inside the radius will not dominate the overall local minutiae structure. However, there are some new issues introduced in fixed radius based methods. One major issue is that a sophisticated local matching mechanism is required due to the increase of the minutiae number inside the radius R. Another issue is that border errors may occur in these methods [CFM10]. In particular, a minutiae close to the radius border of the central minutiae in one fingerprint may be outside the border in another fingerprint, due to the non-linear distortion or location inaccuracy, and this may cause a mismatch with that minutiae.

- Non-minutiae based matching (e.g. [ZWZ07, GZY06]): it is suitable for the situations when the quality of fingerprint images is extremely low. In this case, some other features (e.g., local orientation and frequency, ridge shape, texture information) may be extracted more reliably than minutiae. However, the distinctiveness of these features is lower than minutiae, which causes that lower matching accuracy which is not as good as minutiae based methodsfor medium or high quality fingerprint images. Theoretically, correlation-based matching

techniques could be conceived of as a subfamily of non-minutiae feature based matching techniques [MMJP09].

Table 2.3 illustrates the advantages and disadvantages of the above three types of matching techniques. Correlation-based matching based techniques normally require pre-alignment of two fingerprint before the comparison. This constraint limits the matching performance of partial fingerprints. Besides, the tolerance of non-linear distortion is not as high as minutiae based techniques [FZ11]. This is because the minutiae is local feature and the non-linear distortion could be mitigated by setting a tolerance threshold such as distance and angle differences between minutiae pairs. But the advantage of this matching is that it has high image noise resistance [MMJP09]. Furthermore, this matching tries to get a correlation score between two whole fingerprint image, which means that the fingerprint global structures are used for comparison. Thus it increases the reliability of the matching results since the complete fingerprint image information is used for comparison. For minutiae based matching, it has the disadvantage of low tolerance to image noise. If the image quality is low, then the minutiae extraction is not so reliable for matching. Non-minutiae based matching addresses this issue because other ridge pattern features could be reliably extracted easier (e.g. ridge patterns and local ridge orientation). Therefore this matching is suitable to extremely low quality fingerprint images. However, these features do not have as high distinctiveness as minutiae. Thus the performance of this matching is not as high as minutiae based matching in case the image quality is high [FZ11].

Table 2.3: The advantages and disadvantages of three categories of matching methods

Techniques	Advantages	Disadvantages
Correlation based	Reliable global structure comparison; high tolerance to (local) image noise	Require pre-alignment; computation cost is high; low tolerance of non-linear distortion; partial fingerprint comparison is an issue.
Minutiae based	High tolerance to non-linear distortion; an analogy to expert based matching; pre-alignment is nonessential; fast and low computation cost; High distinctiveness of inter-class fingerprint pairs.	Low tolerance to image noise; highly depends on the accuracy of minutiae extraction
Non-minutiae based (excluding correlation based)	Other ridge pattern features could be reliably extracted easier (e.g. ridge patterns and local ridge orientation); suitable to low quality images.	Distinctiveness of inter-class fingerprint pairs is relatively lower.

2.4.7.3 State of art matching techniques

Fingerprint matching is one of the hottest areas in the research of fingerprint recognition. Many matching algorithms have been designed and reported

with acceptable experimental results. In the following part, we introduce several current fingerprint matching methods.

Jiang and Yau [JY00] designed a matching method based on both global and local structures. Because the global minutiae structure shows the uniqueness of fingerprints, but the local minutiae feature has the advantage of rotation and translation invariant, they use the local minutiae structure pair with the highest similarity as a reference point for alignment, then a global comparison is performed. They claim that their method achieves an error equivalent rate (EER) (indicates the overall matching error rate) of 0.45% from a total 2260512 matching. However, they did not mention the database used in their experiments.

Wahby and Ahmad [WSOA13] proposed a multilevel structure technique which firstly decomposes an image into regions based on global features and then formulates multilevel features from both global and local features. Their result shows that this method get average EER of 3.79% of FVC2002 DB1, DB3 and DB4.

Cappelli et al. [CFM10] proposed a minutiae matching method by cylinder code, and they claimed that it is one of the most accurate methods up to now. Figure 2.20 shows the representation of minutiae cylinder code (MCC) in a fingerprint template. They get an average EER of 0.29% of on FVC2006 database based on the best minutiae extractor from FVC2006 campaigns. Feng et. al [FZ11] evaluated the performances of several minutiae based matching methods. Their results indicate that the MCC method is ranked the first in most cases except the fingerprint dataset with the small common region between two enrolled fingerprint images.

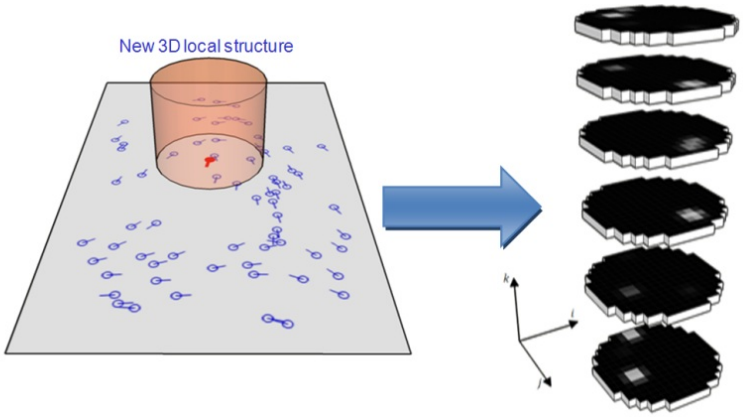

Figure 2.20: Minutiae cylinder code representation associates a local structure with each minutiae. This structure encodes spatial and directional relationships between the minutiae and its (fixed-radius) neighborhood and can be conveniently represented as a cylinder whose base and height are related to the spatial and directional information, respectively.(from [CFM10])

Because of the different minutiae/feature extractors and databases used for above matching methods, it is difficult to compare the performance of each method at the same bench mark. Recently, the trend of matching methods is combining different levels of features. Though fingerprint matching has been extensively researched, how to design a reliable and accurate matching algorithm is still an on-going challenge. In summary, an excellent matching algorithm should have good tolerance to image noise, non-linear distortion and feature extraction errors.

2.5 Matching Metrics to Evaluate a Fingerprint Recognition System

There are two types of comparisons between fingerprints in fingerprint recognition. When a pair of fingerprints from the same finger is compared, it is named as intra-class comparison. If two fingerprints are from different fin-

gers, then this type of comparison is named as inter-class comparison. The purpose of fingerprint recognition techniques is to increase the similarities in the intra-class comparisons and amplify the dissimilarities in the inter-class comparisons. If an intra pair of fingerprints is considered as a non-match by a fingerprint recognition system, then this match is called false non-match error. If an inter pair of fingerprint is considered as a match, this match is called false match error.

False non-match rate (FNMR) and false match rate (FMR) are two main metrics to evaluate the matching accuracy of a fingerprint recognition system. Figure 2.21 shows the matching score distributions of intra-class matching (genuine user profile) and inter-class matching (impostor profile). The difficulty is that the range of matching score produced by two query individuals, one genuine and one impostor, compared to a registered template, are likely to overlap. Hence a threshold t is selected to decide whether two fingerprints are a match or not. For a given threshold t, if the matching scores of genuine pairs are smaller than t, then these pairs are considered to be a false non-match. The FNMR is the percentage of pairs in the genuine distribution whose matching scores are smaller than t. If the matching scores of impostor pairs are larger than t, then these pairs are false matched with genuine users. And the FMR is the percentage of pairs in the impostor distribution whose matching scores are larger than t.

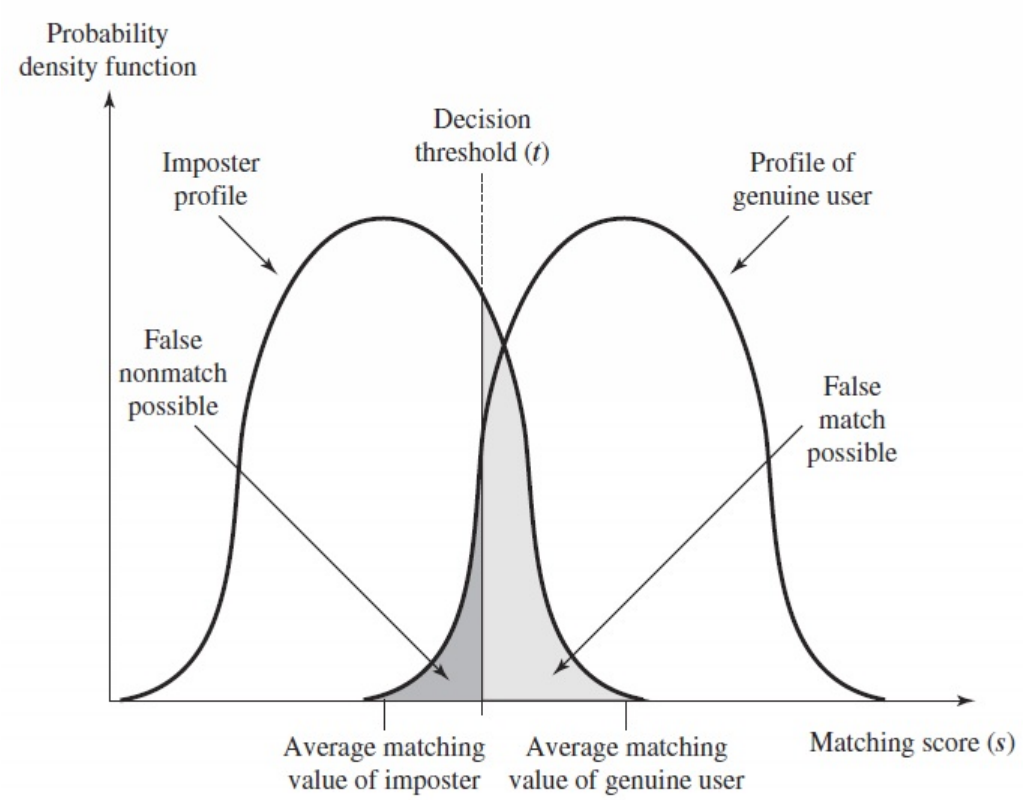

Figure 2.21: Matching score distributions between impostor profile (inter-class) and genuine user profile (intra-class). If the matching scores are greater than a preassigned threshold t, then we call these templates and query templates matched (from [SB11]).

The metrics for the evaluation of a fingerprint recognition system include the following [**?**]:

- **False match rate (FMR)**: It is also named as false acceptance rate (FAR) in biometrics. It refers to the probability that the system incorrectly matches the input pattern to an impostor template in the database. It measures the percent of invalid inputs which are incorrectly accepted. In case of similarity scale, if the person is impostor in real, but the matching score is higher than the threshold, then he is treated as genuine that increase the FAR and hence the performance

also depends upon the selection of threshold value.

- **False non-match rate (FNMR)**: It is also named as false reject rate (FRR). It refers to the probability that the system fails to detect a match between the input pattern and a genuine template in the database. It measures the percent of valid inputs which are incorrectly rejected.

- **Equal error rate (EER)**:It refers to the rate at which both false accept and false reject errors are equal (the matching error rate when FMR = FNMR). The value of the EER can be easily obtained from the ROC (receiver operating characteristic) curve. The EER is a quick way to compare the accuracy of matching methods with different ROC curves. In general, the matching methods with the lowest EER is most accurate.

- **FMR100**: the lowest FNMR for FMR <= 1%.

- **FMR1000**: the lowest FNMR for FMR <= 0.1%.

- **ZeroFMR**: the lowest FNMR for FMR = 0%.

FMR and FNMR are usually used to indicate the accuracy of a biometric system. Different systems have different requirement for FMR and FNMR. For example, in a fingerprint criminal identification system, the police officer would like to shortlist all possible criminals for that single fingerprint, then this system needs a sufficient low value of FNMR. Thus, the potential criminal may not escape from this identification system. In another case, in a high security authentication system, the FMR should be sufficiently low so that a masquerader will not be granted access to the system. FMR100,

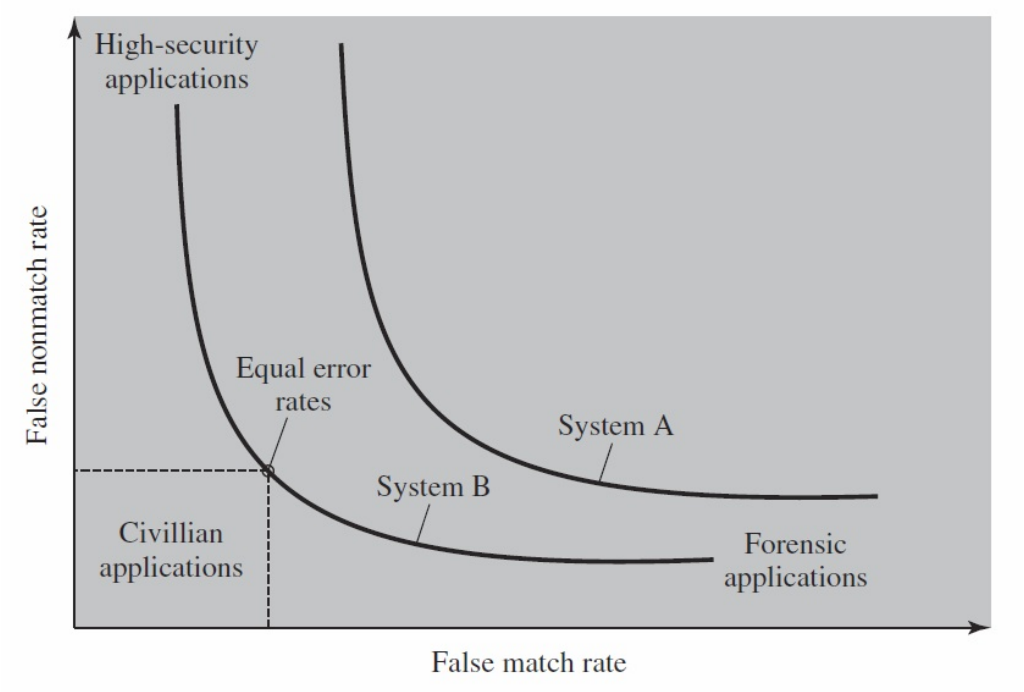

Figure 2.22: The receiver operating characteristic (ROC) curve of two fingerprint recognition systems.

FMR1000 and zeroFMR could be used as metrics to evaluate the system performance according to their accuracy requirement. If a system requires that the FMR should be at least smaller than 1%, then FMR100 could be a useful metric to evaluate this system. But if a system requires the highest security standard with 0 tolerance to false match errors, then zeroFMR would be the suitable metric. In our case, all of these metrics will be used to evaluate the proposed algorithms. Figure 2.22 shows a sample receiver operating characteristic (ROC) curve of FMR and FNMR for two fingerprint recognition systems. A ROC curve is a graphical plot "which illustrates the performance of a binary classifier system as its discrimination threshold is varied" [Bra97]. ROC curves are widely used in the field of medicine, radiology, biometrics etc.[BD06]. In the figure, we can see that

high security applications require low FMRs. And forensic applications require low FNMRs. But EER is the metric to evaluate the overall accuracy, so a fingerprint with low EER is suitable for civilian applications.

2.6 Databases for Experiments

Fingerprint Verification Competition(FVC) databases [MMC+02, MMC+04, FOTG07] are used for performance evaluations of designed fingerprint recognition techniques in this thesis. FVC aims to track performance of state-of-the-art fingerprint matching algorithms. The FVC databases are widely accepted by researchers currently. Thus it is possible to compare the results of research in this field across the whole scientific community.

Specifically, in FVC2002 databases, the acquisition conditions were the same for each database which are: interleaved acquisition of different fingers to maximize differences in finger placement, no care was taken in assuring a minimum quality of the fingerprints and the sensors were not periodically cleaned. During some sessions, individuals were asked to: a) exaggerate displacement or rotation or, b) dry or moisten their fingers [AFF09]. Therefore, the fingerprint images in these databases contain plenty of variations and noise, which means that they are specially suitable for the evaluations of fingerprint recognition algorithms. Table 2.4 shows the specification of the databases used to evaluate the performance of our algorithms in this thesis. Some sample fingerprint images with different levels of quality are provided in Appendix A.

Table 2.4: The specifications of the FVC databases used in this thesis. In the column of image numbers, the first number indicates the number of fingerprint groups in which the fingerprints are from the same finger, and the second number indicates the number of fingerprint images in each group.

Database	Image numbers	Image size	Image resolution	Sensor
FVC 2002 DB1a	100*8	388*374	500	Optical Sensor
FVC 2002 DB2a	100*8	296*560	569	Optical Sensor
FVC 2002 DB3a	100*8	300*300	500	Capacitive Sensor
FVC 2002 DB4a	100*8	288*384	500	SFinGe v2.51 [Mal04]
FVC 2006 DB2a	140*12	400*560	569	Optical Sensor

2.7 Conclusion

This chapter explores the literature of all aspects of a fingerprint recognition system. Firstly, we have described the characteristics of fingerprint as a biometric, and have discussed the importance of fingerprint recognition. Secondly, we have introduced the fingerprint features in detail, and the factors which cause the fingerprint variations during the feature extraction. Thirdly, components of feature extraction and matching are introduced and discussed. These components include fingerprint segmentation, local orientation and frequency estimation, contextual filtering, minutiae extraction, fingerprint alignment and matching. Finally, the databases and commonly used metrics by researchers for experimental evaluations are also described.

In this chapter, we have summarized the existed issues and challenges in each component of fingerprint feature extraction and matching. Though every component could be further improved by addressing these issues, our research focuses on three major challenges which are: (i), designing a fingerprint image pre-processing method which enables successive contextual filtering (e.g. Gabor filtering) to perform with improved results, and ultimately makes possible enhanced feature (e.g. minutiae) extraction; (ii), designing a reliable singular point detection method with a high correct detection rate of singular points, so that the detected singular points can be used as reference points for fingerprint alignment or for fingerprint classification in a fingerprint identification system; (iii), designing a reliable fingerprint matching method which is accurate and has a high tolerance to noise and feature extraction error. How to achieve the above three objectives is the focus of this thesis. This thesis will address each of research objectives above, and design and develop unique solutions and with experimental results to show how the above major issues have been dealt with.

In the next chapter, we will address the first research objective, which aims to improve the performance of the image pre-processing stage in fingerprint recognition, and enables successive contextual filtering (e.g. Gabor filtering) to perform with improved results, and ultimately makes possible enhanced feature (e.g. minutiae) extraction. A new image pre-processing method is proposed in order to address the issue that the current fingerprint image pre-processing techniques only focus on the image contrast enhancement instead of improving the clarity of ridge and valley structures. The initial purpose of image pre-processing is to uniformly distribute the intensity values into the selected range, and then the resultant images could

become the input of the contextual filtering stage. Thus, current image pre-processing method focus on normalize the image intensities into a selected intensity range rather than noise reduction and image quality improvement. In our opinion, image pre-processing could play a more important role in fingerprint image enhancement, which may improve the performance of subsequent contextual filtering stage, and ultimately to improve the feature extraction results.

Chapter 3

Image Pre-processing for Image Quality Enhancement

In the previous chapter, we have reviewed the techniques used for fingerprint recognition, and have identified three major research challenges in fingerprint recognition which need to be addressed in this work, which are: (i), designing a fingerprint image pre-processing method which enables successive contextual filtering (e.g. Gabor filtering) to perform with improved results, and ultimately makes possible enhanced feature (e.g. minutiae) extraction; (ii), designing a reliable singular point detection method with a high correct detection rate of singular points, so that the detected singular points can be used as reference points for fingerprint alignment or for fingerprint classification in a fingerprint identification system; (iii), designing a reliable fingerprint matching method which is accurate and has a high tolerance to noise and feature extraction error.

In this chapter, we will address the research challenge with respect to fingerprint image pre-processing. Image pre-processing aims to pre-process

the image to allocate the pixel intensities into the desired range, and then to obtain a better image contrast [MMJP09]. Image pre-processing is necessary in fingerprint recognition, because the distribution of grey level intensities of fingerprint images may fall in the different ranges (due to the variations during the fingerprint capturing stage and the differences in fingerprint scanners). And the resultant images of image pre-processing are the input to the subsequent contextual filtering stage. The major limitation of current fingerprint image pre-processing techniques (e.g. normalization [HWJ98] and adaptive normalization [KP02] techniques) is that they only focus on the image contrast enhancement instead of improving the clarity of ridge and valley structures. In our opinion, image pre-processing could play a more important role in fingerprint image enhancement besides the image contrast improvement, which may improve the performance of subsequent contextual filtering stage, and ultimately to improve the feature extraction results. This chapter proposes a method which addresses the above limitation of current image pre-processing techniques. This method is developed based on the analysis of histograms of fingerprint images from FVC 2002 databases. All pixels in a fingerprint image could be separated into three grey level ranges, which are: (i), ridge areas; (ii), valley and background areas; and (iii), the possible noise area and the edges between ridge and valleys. The proposed method is able to separate these three areas automatically, and then three designed equations are applied to these three intensity ranges, respectively, to improve the clarity of ridge and valley structures. This method is able to normalize the fingerprint image to a fixed range of intensities, and to enhance the clarity of ridge/valley structures, especially for wet and smudged fingerprint images.

This chapter is organized as follows: First, an overview of the research problem is described. Then, the procedure of the proposed method is described in detail. Finally, the experimental results are also provided and discussed to demonstrate the effects of this algorithm.

3.1 Overview

Image pre-processing in fingerprint recognition is also called pixel-wise enhancement which refers to assigning a new value to each pixel depending on its previous value and some parameters (e.g. mean intensity and intensity variance) [MMJP09]. Thus, this stage belongs to image processing measures in the spatial domain. Pixel-wise techniques act as an initial processing stage followed by a further image enhancement algorithm (referring to contextual filtering techniques).

Recent research in the area of fingerprint pre-processing has been introduced in Section 2.4.2 including one of the most popular image-processing methods called normalization [HWJ98, KP02, HB12]. However, normalization and other current fingerprint image pre-processing methods only aims to enhance the image contrast instead of noise reduction and image quality enhancement. The basic reason for not proposing any noise reduction techniques in this stage is because that the subsequent context filtering stage is able to handle the noise removal task in normal circumstance. However, in some cases, especially when the fingerprint is scanned in a wet/smudged condition, solely using the context filtering techniques may not perform well, as shown in Figure 3.1. This figure shows an example of fingerprint image processing by Gabor filtering on a wet type fingerprint. Figure 3.1a

is a fingerprint image sample from the FVC2002 database DB3a. This image is noisy between ridge lines. Figure 3.1b is the binarized image after applying the Gabor filtering technique and the segmentation technique ([HWJ98, WBGS10]). The binarized image contains several spurious islands and incorrect joint points between ridge lines. This is because the Gabor filtering technique cannot eliminate the influence of noise at this level. It consequently reduces the accuracy of feature extraction which will directly influence the matching accuracy. Therefore, some solutions need to be implemented to address this problem. Current solutions are more focused on the post-processing of binarized images and minutiae extraction (see Section 2.4.6). A appropriate post-processing method will significantly reduce the influence of noise. But if we can reduce the noise level in the image pre-processing stage, the result may be better than only using post-processing techniques. Ultimately, it will improve the final fingerprint matching accuracy, because the feature extraction is more reliable if more noise is eliminated.

3.2 Proposed algorithm for enhancement of fingerprint images

In this section, we will first introduce two background techniques, used in the proposed image pre-processing method, which are power-law transformation and contrast stretching. Power-law transformation and contrast stretching are image processing techniques used for control image brightness and image contrast, respectively. In this research, the proposed image

pre-processing algorithm is designed based on the above two techniques in order to improve the clarity of fingerprint ridge and valley structure. Gabor filtering and binarization techniques are also implemented to show the effect of this image pre-processing method. Because image processing techniques aim to enhance the image quality and make possible reliable feature (mainly minutiae) extraction (which normally extracted from binarized images) in the subsequent minutiae extraction stage, the clarity of the obtained binarized images may determine the accuracy of minutiae extraction, which will ultimately influence the fingerprint matching accuracy. Therefore, evaluation of obtained binarized fingerprint images which are obtained after the contextual filtering stage is able to demonstrate the advancement of this image pre-processing method.

3.2.1 Power-law transformation and contrast stretching

Power-law transformation and contrast stretching are techniques used in digital image processing to improve the contrast and brightness of an image [GW01]. The equation of power-law transformation is as follows [GW01]:

$$s = cr^{\gamma} \tag{3.1}$$

where s is the output grey level, r is the input grey level, c and γ are positive constants used to control the shape of the transformation.

When $\gamma < 1$, a narrow range of dark input intensity values map into a wide range of output values. It means that the output image becomes brighter than the input image. When $\gamma > 1$, the effect of the generated

curve is opposite of the curve obtained when $\gamma < 1$. Therefore, power-law transformation controls the brightness of the output image by selecting different values of γ. Figure 3.2 shows the plots of power-law transformation with $c = 1$ and different values of γ. In the proposed approach, power-law transformation is not applied uniformly to the entire input image but to parts of the image with a specific range of intensity value. This approach will be described in next section.

Contrast stretching is a linear function which can increase the contrast of an image [GW01]. Due to its linear property, this transformation does not lose data information other than intensity values. Figure 3.3 shows typical contrast stretching where L is the grey level of an image and is equal to 256, r is the input pixel intensity, s is the output pixel intensity, (r_1, s_1) and (r_2, s_2) are two points that control the shape of the transformation [GW01]. the The following equation is used in contrast stretching:

$$s = \begin{cases} \dfrac{rs_1}{r_1} & \text{if } r < r_1 \\ \dfrac{(s_2 - s_1)r}{(r_2 - r_1)} + \dfrac{(s_1 - s_2)r_1}{(r_2 - r_1)} & \text{if } r_1 < r < r_2 \\ \dfrac{(L-1-s_2)r}{L-1-r_2} + \dfrac{(L-1-s_2)(L-1)}{L-1-r_2} & \text{if } r_2 < r < L-1 \end{cases} \tag{3.2}$$

Because the input intensity in the range of $[r_1, r_2]$ is mapped to a wider range $[s_1, s_2]$, the contrast of an image is improved. However, two pairs of points (r_1, s_1) and (r_2, s_2) have to be moderately selected, and their best values depend on different images, which make implementation challenging. Normally, the selection of (r_1, s_1) and (r_2, s_2) is based on the observation of image histograms. Contrast stretching could be used for image normalization as well [GW01]. In particular, if we select $s_1 = 0$ and $s_2 = 255$, and r_1

and r_2 as the 5th and 95th percentile in the histogram, respectively (that is, 5% of the pixel in the histogram will have values lower than r_1, and 5% of the pixels will have values higher than r_2), then the image is normalized after this transformation (that is, 10% of pixels are saturated to prevent outlying pixels). Contrast stretching and power-law transformation have been widely used for adjusting the contrast and brightness in digital image processing [GW01]. Based on them, we develop a new equation to reduce noise and enhance fingerprint images. The next section illustrates how this algorithm works.

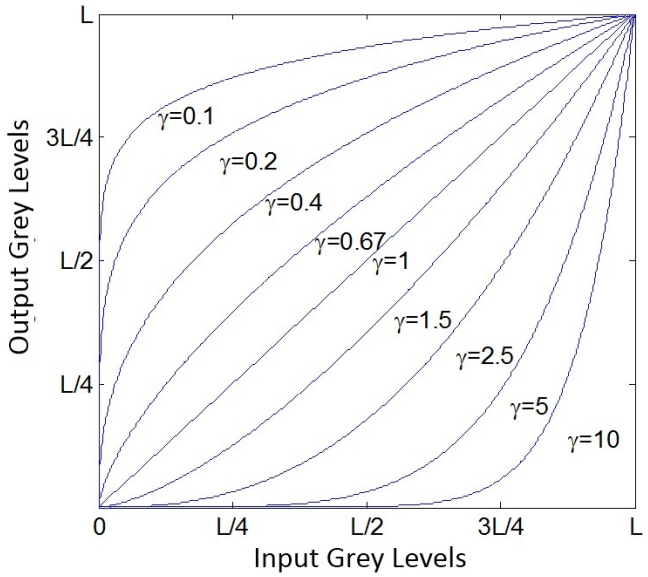

Figure 3.2: Plots of power-law transformation with different values of γ.

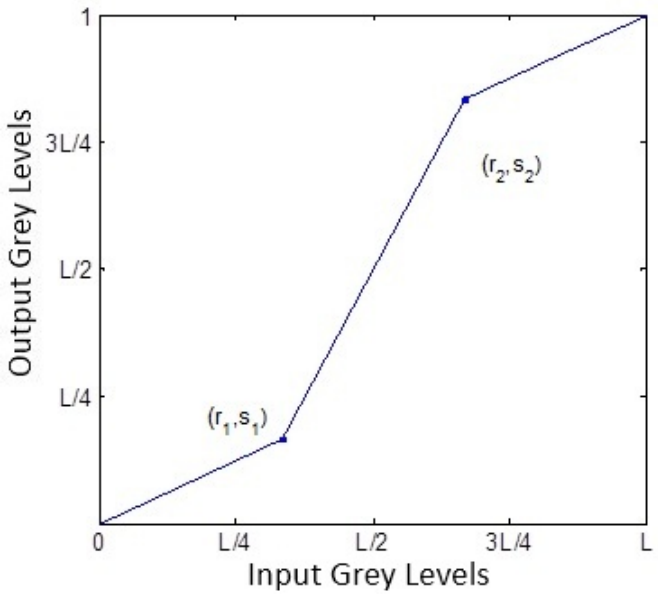

Figure 3.3: Plots of typical contrast stretching, where r denotes the input grey levels (the x-axis), and s denotes the output grey levels (the y-axis)

3.2.2 Proposed algorithm for fingerprint image enhancement

Analysing the histogram of fingerprint images of FVC2002 databases has led to the proposed algorithm. An image histogram is a graphical representation of the tonal distribution in a digital image [GW01]. Thus, a grey level fingerprint image's histogram indicates the distribution of grey levels. Figure 3.4 shows the histogram of Figure 3.1a. We can see that two peaks in this histogram around grey level 40 and 100 along the x-axis roughly divide the grey level into three parts. The first part can be regarded as the grey levels of ridges, and the second part as the grey levels of edges of ridges and noise, while the last part is the grey levels of the valleys and background. This is because the intensities of a grey scale fingerprint image can

be roughly classified into two parts which are ridge and non-ridge. Normally noise is darker than background but brighter than ridge lines, which means it has lower intensity values than the background but has higher intensity values compared to ridges lines. Though in some cases, like in latent fingerprints, there are some other non-ridge components like handwriting (seen in Figure 2.10) other than naturally generated noise existing in fingerprint images. However, these circumstances are not considered in this work, as normally these non-fingerprint areas are unreliable and can be separated from the fingerprint image by segmentation techniques.

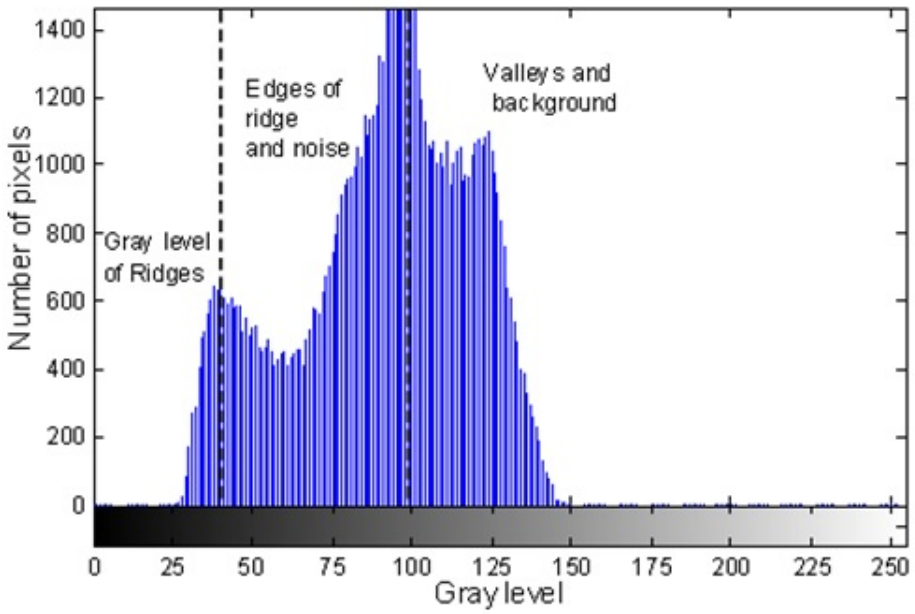

Figure 3.4: Histogram of fingerprint image from Figure 3.1a.

Based on the above observation and analysis, we construct a new equa-

tion to improve fingerprint images as follows:

$$s = \begin{cases} \dfrac{rs_1}{r_1} & \text{if } r < r_1 \\ \dfrac{(s_2 - s_1)r^\gamma}{(r_2^\gamma - r_1^\gamma)} + \dfrac{s_1 r_2^\gamma - s_2 r_1^\gamma}{r_2^\gamma - r_1^\gamma} & \text{if } r_1 < r < r_2 \\ L - 1 & \text{if } r_2 < r < L - 1 \end{cases} \tag{3.3}$$

where we apply power-law transformation between (r_1, s_1) and (r_2, s_2), and we set $s_2 = 255$, then the input values bigger than r_2 are clipped because we regard this part as valley and background regions.

The three parts of equation 3.3 are applied to three different ranges of input grey levels as shown in Figure 3.4. Figure 3.5 shows the plots of the proposed algorithm with $\gamma < 1$. This algorithm is similar to contrast stretching except that non-linear transformation is applied in the middle part. That is because contrast stretching can improve the contrast of a fingerprint image, but it does not change the data information except the intensity values. Therefore, information about noise is still kept by applying contrast stretching. By applying power-law transformation, the noise level can be reduced better than with linear transformation, by selecting γ according to the noise level. The implementation of our algorithm is shown in the following steps:

(i) Firstly, a typical contrast stretching is performed in order to distribute grey levels of an image to [0, 255]. That is because not all fingerprint images occupy the full grey levels of [0,255] as shown in Figure 3.4. It is performed by applying equation 3.2 as $r_1 = min(r)$, $s_1 = 0$, $r_2 = max(r)$ and $s_2 = 255$. Note 5% of the data is first saturated at low and high grey levels of the original image in order to remove the

interference caused by such a small amount of pixels.

(ii) We then apply the algorithm on the remaining image, block by block, with a block size of 16x16. The reason we process the image block by block is that there are different levels of noise even in one fingerprint image. Therefore, different values of parameters can be selected for different blocks in order to obtain an improved result. The rules of parameter estimation are introduced in the next section. Figure 3.6 shows the result of our approach with $r_1 = s_1 = 50$, $r_2 = 160$ and $\gamma = 1$. Note that this image is segmented to mask the non-ridge and non-valley areas.

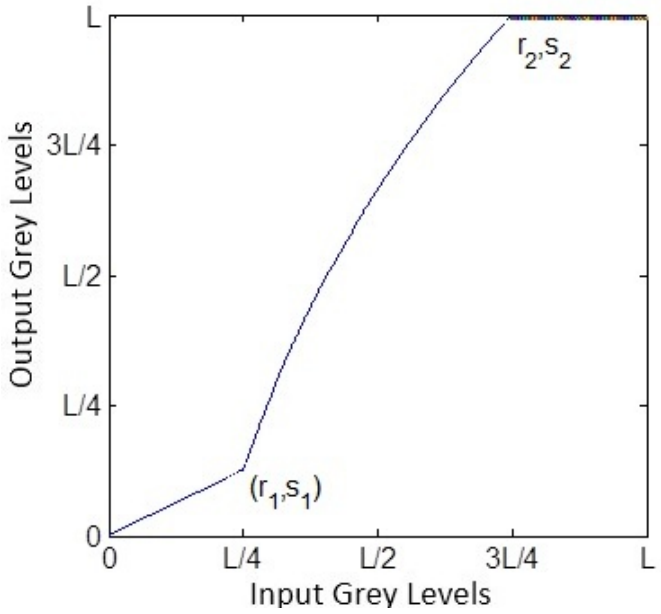

Figure 3.5: Plot of equation 3.3 with $\gamma < 1$.

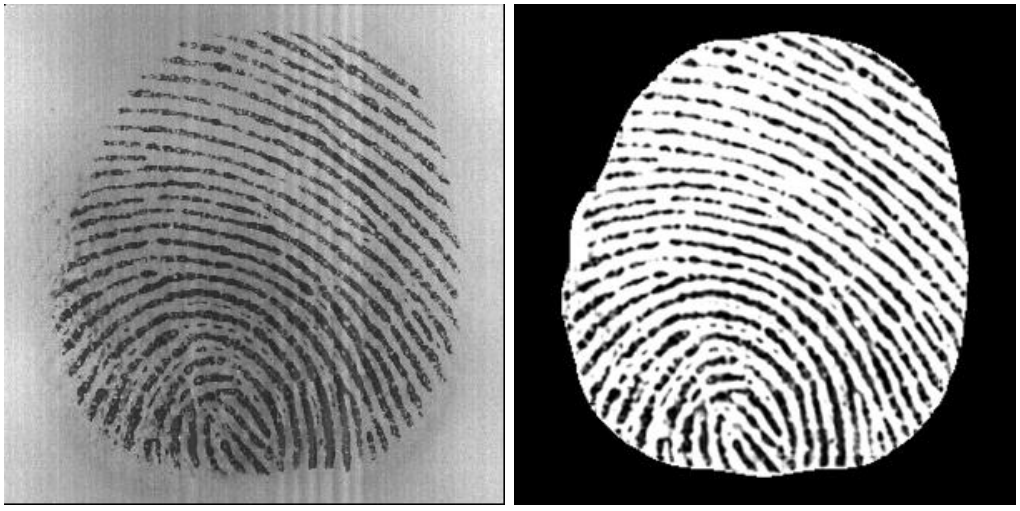

(a) (b)

Figure 3.6: Resultant images after being processed by this method: (a), original image; (b), the result after the segmentation and the image pre-processing approach with $r_1 = s_1 = 50$, $r_2 = 160$ and $\gamma = 1$.

3.2.3 Parameters estimation

There are a number of undefined parameters in equation 3.3 which are r_1, s_1, r_2 and γ. For different blocks, the best choice of these parameters may be different. Therefore, a scheme which can automatically estimate the best values for parameters is needed. We use several variables to adjust the values of parameters as shown in Table 3.1.

Table 3.1: Variables for parameters estimation.

Variables	Description
Mean intensity(M)	Mean value of grey levels for each block.
Variance (V)	Variance of grey levels for each block.
Reliability of block orientation (R) (also named as Coherence)	The reliability of orientation for each block. High reliability shows the ridge and valley areas are clear, and low reliability shows noise level is high.

Calculation of mean intensity M, variance V and reliability R has been described in section 2.5. The value R is low for noisy and corrupted regions and high for good quality regions [MMJP09]. For low reliability blocks, if the mean intensity M is low than the mean intensity of the whole fingerprint image then γ should be set smaller than 1 to increase the mean intensity and contrast; and if the mean intensity M is high than the mean intensity of the whole fingerprint, then we set γ bigger than 1 to decrease the mean intensity and increase the contrast. The reliability R generated near singular points is normally low [MMJP09], and the mean intensity M also is relatively lower than other regions in the same fingerprint image, so the quality of singular point areas can be improved by setting *gamma* smaller than 1. Table 3.2 shows our estimation based on the experiments of different sets from the FVC2002 fingerprint databases. Figure 3.7 shows the resultant image of Figure 3.6a using automated parameter selection.

Table 3.2: Estimation of parameters in equation 3.3.

Parameter	Rules of estimation
r_2 selection	if $M > 200, r_2 = M + V;$ else if $150 < M <= 200, r2 = M + V/2;$ else if $128 < M <= 150, r_2 = M;$ else if $M <= 128, r_2 = M - V/2;$
r_1 and s_1 selection	$r_1 = \max(M - V, 25);$ $s_1 = r_1;$
γ selection	if $M >= 200, \gamma = 1.2;$ else if $R >= 0.7, \gamma = 1;$ else if $R <= 0.5, \gamma = 0.5;$ else if $0.5 < R < 0.7$ & $M > 150, \gamma = 1.2;$ else if $0.5 < R < 0.7$ & $100 <= M <= 150, \gamma = 0.8;$ else if $0.5 < R < 0.7$ & $M < 100, \gamma = 0.6;$

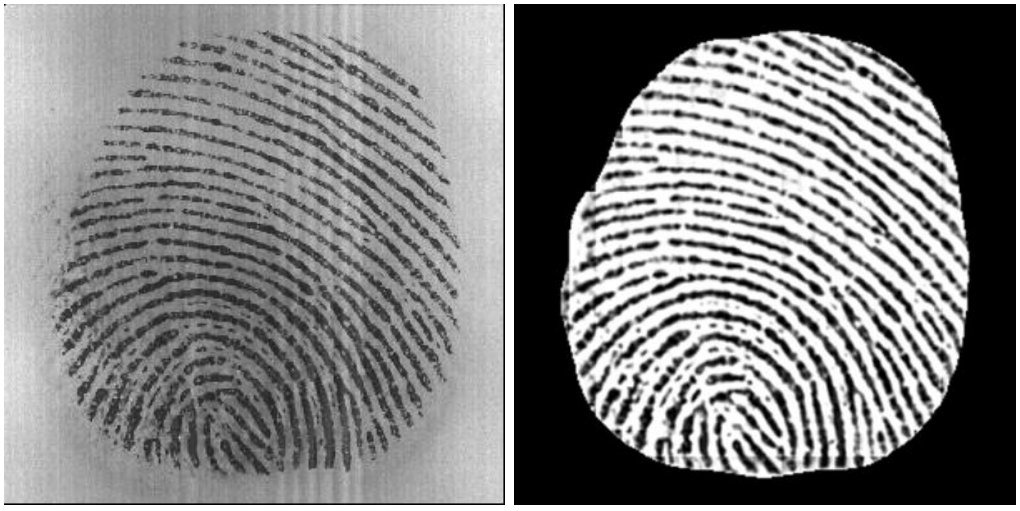

(a) (b)

Figure 3.7: Resultant images after being processed by our method by automated parameter selection. (a) is the original fingerprint image, and (b) is the resultant image.

3.2.4 Result of Gabor filtering and binarization

We divide the image into 16x16 blocks and calculate the average orientation and frequency of each block as input to the Gabor filter. Then, a Gabor filter bank of 60 filters with angle increment of 3 degrees is designed for image processing. For each block, the block is convoluted with a Gabor filter with a chosen angle from the designed Gabor filter bank. The details of Gabor filtering and binarization techniques are described in Section 2.4.4. Figure 3.8 shows a sample result after applying Gabor filtering technique to Figure 3.7b.

Figure 3.8: Gabor filtering and binarization of the sample fingerprint image in Figure 3.7b.

Figure 3.9a is a original noisy fingerprint image which is also an intra-class (from the same finger) fingerprint of the image in Figure 3.7a. Figure 3.9b is the resultant image after applying our method to the original image, and Figure 3.9d is the resultant image after Gabor filtering and binarization. By comparing Figure 3.9c and 3.9d, the latter image is much clearer and has less spurious islands. After applying our method, the binarized noisy sample image is almost the same as the fine sample image as shown in Figure 3.8. The result shows that much of the noise has been removed and ridges and valleys are smoother and clearer, so that the detected minutiae will be more reliable since many spurious minutiae have been removed.

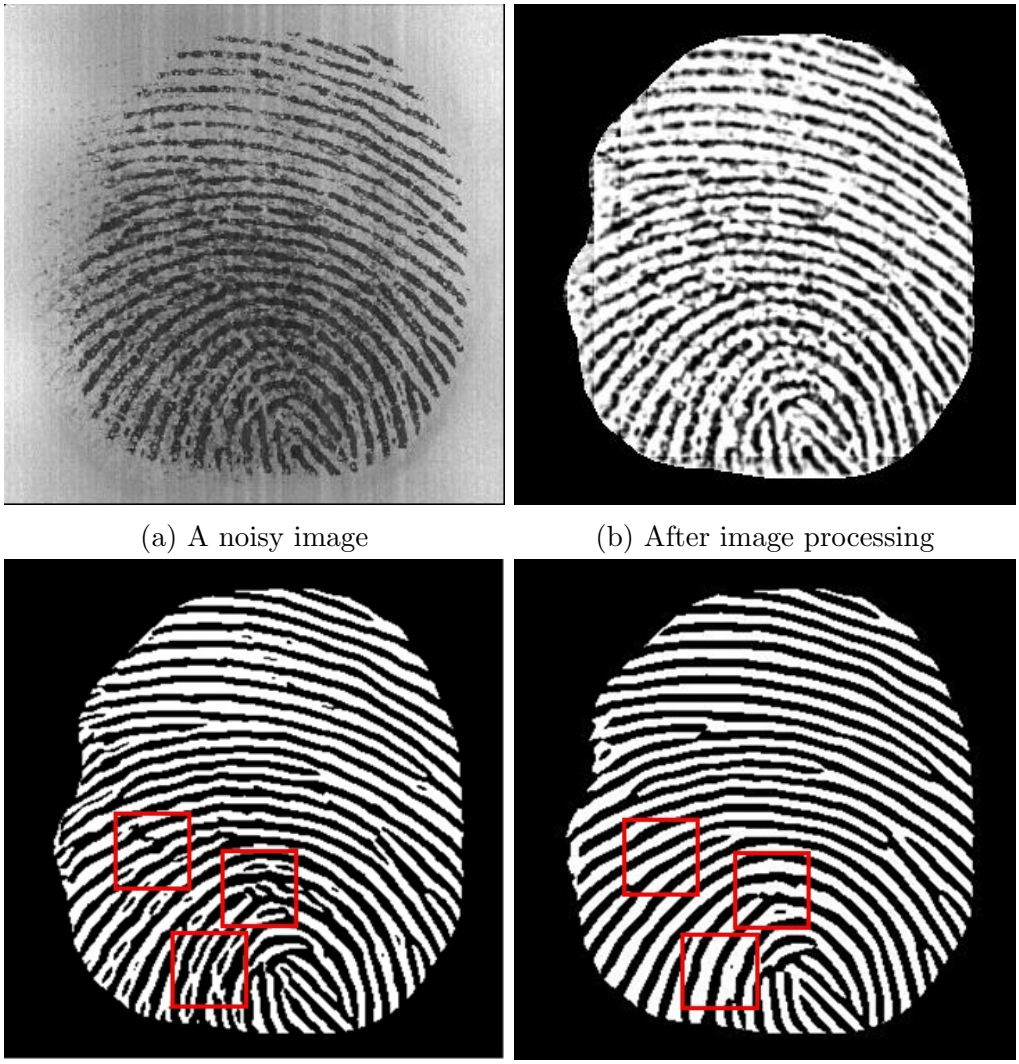

(a) A noisy image (b) After image processing

(c) Without the proposed method (d) With the proposed method

Figure 3.9: Gabor filtering and binarization of a noisy and smudged sample fingerprint after applying our image pre-processing method: (a), the original image with corrupted fingerprint areas; (b), the resultant image after applying our image pre-processing method; (c), Gabor filtering and binarization without the proposed image pre-processing method; d), binarized image with our image pre-processing methods. The red squares show the improved areas by our method.

3.3 Experimental results

Database DB3a of FVC2002 is used to evaluate the result of this approach. This sub-database contains more wet type fingerprints than any other databases in the FVC 2002 databases. For good quality fingerprint images such as in Figure 3.7a, an image quality enhancement is not required. However, when the noise level is high, our proposed approach can significantly reduce the noise level and improve the accuracy of further minutiae detection as shown in Figure 3.9. More examples are shown in Figure 3.10. The left column shows the noisy original images, the middle column shows the binarized images without applying our method and the right column shows the resultant images after applying our image precessing method. We can see that our method is able to remove noise significantly on those wet type and noisy fingerprint images.

We also use a goodness index (GI) [CDJ05] to evaluate the performance of this proposed approach. The GI is defined by Chen et al. [CDJ05] as follows:

$$GI = \frac{p}{t} + \frac{a+b}{u} \tag{3.4}$$

where p represents the total number of paired minutiae and t represents the ground truth minutiae in a given fingerprint image; a and b are the number of missed and spurious minutiae respectively, and u is the total number of detected minutiae. GI indicates the minutiae extraction accuracy after the image processing. If a GI value is high, then it indicate the minutiae extraction accuracy is high. GI is a expert based method to evaluate the image quality after the image enhancement [CDJ05]. Hence normally only a small number of fingerprint samples are selected for evaluation.

We calculate GI by applying our fingerprint image pre-processing method to 20 random selected sample fingerprints in DB3a of FVC2002 containing both high and poor quality images. Table 3.3 shows the results of GI by comparing our proposed method with traditional approaches that use the normalization techniques [HWJ98, KP02]. Thus, GI is adopted by researchers (e.g. [ZT07, ZGLR01, ZT07, BL10]) to evaluate the performance of fingerprint image processing techniques. From this table, we can see that our proposed approach followed by Gabor filtering technique can detect minutiae more accurately than the traditional Gabor filter based approaches and can improve the performance by 9% on average. Especially, our proposed approach can improve the accuracy of minutiae detection of poor quality fingerprint images, such as sample 4 and 12 in which the GI is enhanced by more than 40%. Table 3.4 shows the comparison between our proposed approach and other approaches. The average GI is 0.69 which is better than other other reported results in Table 3.4, and it is about 14% improvement over other methods. However, GI computation is conducted manually by an expert, that means human errors are inevitable. Furthermore, the samples selected for experiments are also different in different research (in Table 3.4, which introduces the difficulty to do a comparison. However, several very poor quality images (refer to Figure 3.10) are used for evaluation for our method, which indicates that our method is superior than the methods in Table 3.4. Besides, we also provide the fingerprint matching results by incorporate this method into a simple fingerprint verification system in Chapter 5.

The advantages of this image pre-processing method could be summarized as follows:

- This method avoids complex computation such as the successive Gabor filtering technique, but utilizes the characteristic of grey level distribution of ridges and valleys. Different equations apply to the ridge and valley areas respectively to reduce the noise.

- This method can effectively improve the image quality of wet or smudged fingerprints (refers to the samples in Figure 3.10)

- This method will retain the important information of ridges and valleys of good quality images as shown in Figure 3.8.

- The values of parameters in this method are automatically selected according to the designed parameter selection scheme. It is suitable to process fingerprint images scanned by 500dpi (The standard used in FVC 2002 databases).

Table 3.4: Comparisons between other approaches and our proposed approach

Methods	Minimum GI	Maximum GI	Average GI
Hong et al. [HWJ98]	0.29	0.55	0.39
Zhao and Tang [ZT07]	0.18	0.75	0.50
Simon-Zorita et al. [ZGLR01]	0.33	0.76	0.55
Bhattacharjee and Lee [BL10]	0.31	0.75	0.55
Proposed	0.48	0.84	0.69

Table 3.3: Comparison of the GI results without and with our method respectively, based on Gabor filtering techniques.

Image No.	Goodness Index	
	Traditional approach based on Gabor filtering without our method	Proposed approach
1	0.60	0.60
2	0.65	0.65
3	0.75	0.67
4	0.29	0.50
5	0.72	0.79
6	0.71	0.71
7	0.79	0.69
8	0.56	0.48
9	0.74	0.72
10	0.60	0.75
11	0.50	0.68
12	0.43	0.83
13	0.42	0.68
14	0.55	0.84
15	0.67	0.72
16	0.49	0.59
17	0.69	0.72
18	0.72	0.78
19	0.40	0.70
20	0.74	0.72
Average	0.60	0.69

3.4 Conclusion

In this chapter, we have presented a new image pre-processing approach, which is able to improve the clarity of ridge and valley structures in a fingerprint image. This approach is able to improve the image contrast as well as to remove noise and unnecessary information, such as valueless ridges, which often exist on wet/smudged fingerprints. Furthermore, the values of parameters in this method are automatically selected by the parameter

selection scheme, which is designed based on the experimental observation and analysis on FVC 2002 databases. The experimental results show that this approach can effectively improve the quality of fingerprint images especially for wet and smudged fingerprint images. The GI is improved by 9% by using this image pre-proessing method before the contextual filtering stage in our experiment. The experimental results also indicate that removing adequate noise in image pre-processing stage enables the subsequent image processing stage (Gabor filtering) to have a better enhancement result, which ultimately improves the performance of feature extraction and matching.

In the next chapter, we will address the second research objective of this work, which aims to design accurate and reliable singular point detection techniques. Because most of current detection methods produce numerous spurious singular points depending on the quality of fingerprint images and detection techniques used. The limitations of current singular point detection techniques include: (i), the correct detection rate of current singular point detection methods are not high (normally around 90%); (ii), various image qualities still limit the extraction accuracy. We believe singular point detection and extraction need to be further investigated since the accuracy of detection is not satisfactory in particular for poor quality images. The major challenge of singular point detection is how to remove spurious singular points but retain genuine singular points. Therefore, two different singular point detection methods are proposed in order to address this challenge in the next chapter.

(a) (b)

Figure 3.1: An example of fingerprint image processing results using the Gabor filtering and binarization technique: (a), original fingerprint image is from FVC 2002 database; (b), the processed fingerprint after Gabor filtering and binarization. The clarity of the ridge and valley structure is not high in this image, especially the area inside the red square.

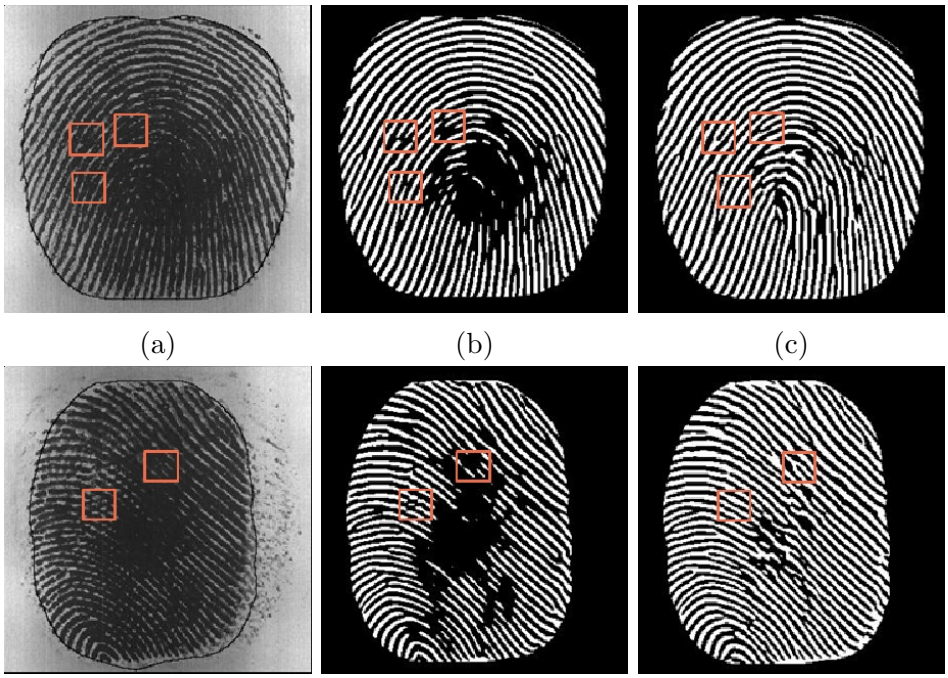

(a) (b) (c)

(d) (e) (f)

Figure 3.10: Two groups of samples, the left column shows the noisy original images, the middle column shows the binarized images without applying our fingerprint image pre-processing method and the right column shows the resultant images after our fingerprint image pre-processing method.

Chapter 4

Reliable Singular Point Detection

In the previous chapter, we have addressed the issue in fingerprint image pre-processing stage, and presented a method to improve the image quality. This image pre-prcessing method is able to improve the image contrast as well as to remove noise and unnecessary information, such as valueless ridges, which often exist on wet/smudged fingerprints. The experimental results show that the Goodness Index (GI) is improved by 9% after applying this method. In this chapter, we will address the research objective of reliable singular point (SP) detection.

SP is an important feature in fingerprint recognition. SPs could be used for fingerprint alignment as reference points to superimpose two fingerprints as well as for fingerprint classification (to determine the fingerprint types). Reliable and accurate SP detection is important in some fingerprint matching methods, because these matching methods are based on fingerprint pre-alignment, which uses SPs as reference points. Furthermore, reliable and

accurate SP detection is also important in a fingerprint identification system, because most reported fingerprint classification systems use SPs to identify the fingerprint types (e.g. left loop, right loop, whorl and arch type fingerprints) [AM09, AG14]. SPs can help in reducing the search time and space in large databases by classifying the fingerprints into different types [KJ96, AB12]. An accurate classification algorithm may also play a role in speeding up the matching process by quickly rejecting different types of fingerprints. Therefore, SP detection techniques are important to fingerprint recognition, and reliable and accurate SP detection techniques are able to improve the performance of a fingerprint recognition system. However, current SP detection techniques suffer the problem that the correct detection rate of SPs is relatively low, mostly around 90% or even lower (e.g. [NB05, ZGZ07, LML13]), due to various reasons (e.g. noise, partial fingerprint and displacement).

In this chapter, two different singular point (SP) detection approaches have been developed to address this research issue. The first SP detection approach proposed in this work uses the Poincaré Index based method for SP detection, then a post-processing procedure is designed to remove spurious SPs, in order to increase the correct detection rate. The experimental results show that it significantly increases the correct detection rate of SPs compared to the original and other Poincaré Index based methods. However, Poincaré Index based techniques have the inherent disadvantages of containing numerous spurious singular points. This is because the Poincaré Index based techniques try to detect the singular point locally (searching them from the whole image blockwisely) instead of treating them as global features. Therefore, we have designed the second method, a new singular

point detection method based on the analysis of the local ridge orientation field. This method detects singular points by analyzing the global structure of the local ridge orientation field. This method obtains better experimental results than the designed Poincaré Index based method.

This chapter is organized as follows: Firstly, the improved Poincaré Index based approach is described including the experimental results. Furthermore, the new SP detection approach based on analysis of the local ridge orientation map is introduced. Subsequently, the experimental results and discussions are provided. The final section is the conclusion of this chapter.

4.1 A Rule Based Post-processing Method for Poincaré Index Based SP Detection

In this approach, a Poincaré Index value calculation is performed on the local ridge orientation map to detect the SPs, then the calculation is followed by two techniques to validate the detected SPs. One validation technique is based on segmentation which shields the non-ridge/valley areas and the second is based on smoothing the gradient field to prevent false SPs. Furthermore, a rule based approach is used to post-process the detected SPs.

4.1.1 Poincaré Index implementation

Before describing the Poincaré Index calculation, local ridge orientation map needs to be computed, and core/delta points are two forms of convergence of oriented ridge lines. The local ridge orientation $\theta(i, j)$ at pixel (i, j) refers to

the angle of which the ridge crosses through a small neighborhood with the horizontal axis. It is generated by calculating the gradient of the intensity values of a fingerprint image [KW87, BG02]. The details of the local ridge orientation calculation has been described in Section 2.4.3. Figure 4.1 shows the result of local orientation estimation, where Figure 4.1a is a fingerprint image and Figure 4.1b is the plot of orientation. Figure 4.1c indicates the detected SPs where red circles and blue triangles refer to the core and delta points, respectively, using Poincaré Index calculation.

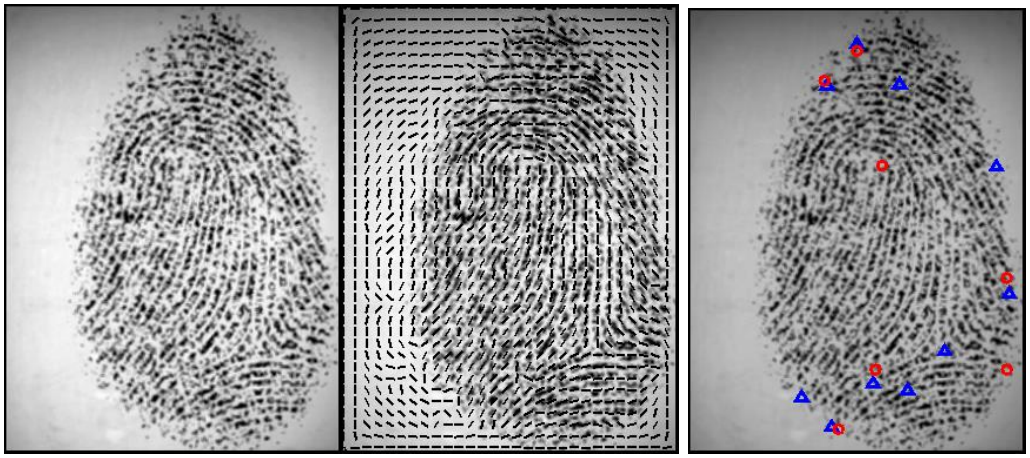

(a) (b) (c)

Figure 4.1: The local ridge orientation of a fingerprint image: (a), the original image; (b), plot of orientation of (a); and (c): the result of SPs detection without smoothing of gradient field and other validation techniques (red circles denote core points and blue triangles denote delta points).

The calculation of the Poincaré Index values is based on the local ridge orientation of a fingerprint. According to [MMJP09], the Poincaré Index values of a core point, delta point and normal ridges are $1/2, -1/2$ and 0, respectively. Figure 4.2a, 4.2b and 4.2c show the orientation of a core point, delta point and normal ridges. Let $d_{1,2...8}$ denote the directions of 8 pixels anti-clockwise around the pixel (i, j), its Poincaré Index value of (i, j) may

be computed as:

$$Poincaré(i,j) = 1/2\pi \sum_{k=1...8} angle(d_k, d_{k+1} mod\ 8) \tag{4.1}$$

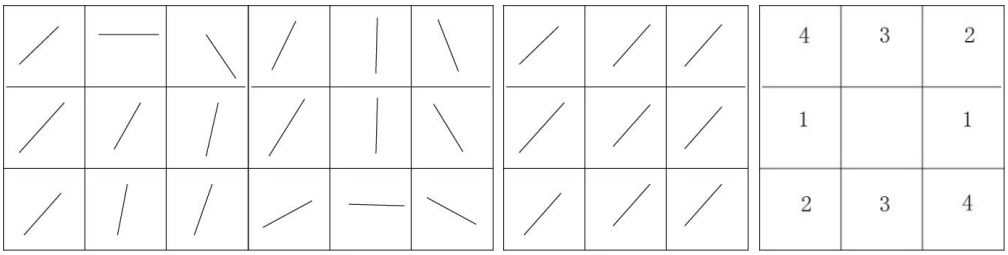

(a) (b) (c) (d)

Figure 4.2: The orientation map of a: (a), core point; (b), delta point and (c), normal ridges. (d) is the designed four directions to calculate the Poincaré Index value.

In implementation, four directions of ridge lines are used to calculate Poincaré Index values as shown in Figure 4.2d. It means that the orientation of each pixel will be assigned the value of the closest direction. Figure 4.1c shows the result of SPs detection without any smoothing techniques, in which red circles and blue triangles denote core points and delta point. respectively. We can see that the result is far from satisfactory because many false SPs are detected. According to Zhou et al. [ZGZ07], the Poincaré Index based approach can detect not only all genuine SPs but it will also detect a number of spurious SPs. Therefore, removing spurious SPs but retaining genuine SPs is a challenge.

4.1.2 Validation and selection of detected SPs

Two techniques are used to remove the spurious SPs: one is segmentation and the other is a rule based approach. Segmentation can effectively remove SPs in non-ridge/non-valley areas while a rule based procedure is used to determine whether a SP should be removed. The rule based post-processing approach is used to validate the detected SPs, and unreliable SPs will be discarded.

4.1.2.1 Segmentation

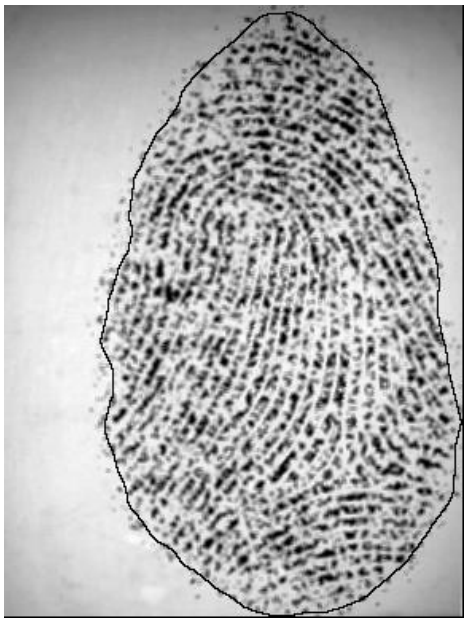

Figure 4.3: Mask generation of Figure 4.1a, and the black lines indicate the boundary of the mask.

Segmentation refers to separating a fingerprint image into foreground and background, of which foreground refers to the recoverable ridge and valley areas of a fingerprint image while background refers to the unrecoverable, non-ridge and non-valley areas [MMJP09]. The segmentation tech-

niques have been described in Section 2.4.1 using the method in [HWJ98, WBGS10]. After segmentation, a mask is generated to shield the background. Figure 4.3 shows the result of segmentation of Figure 4.1a.

4.1.2.2 Post-processing for SPs validation

Because there are numerous spurious SPs detected by the Poincaré Index technique, how to remove these SPs is an issue. Therefore, a rule based post-processing method is developed to validate the detected SPs in this work. This post-processing approach is designed by observing the effects of smoothing the gradient field. A Gaussian filter is used to smooth the gradient field in order to remove the spurious SPs generated by local irregular gradient presentations (such as SPs caused by image noise). The equation of the Gaussian filter is shown in Equation 4.2:

$$g(x, y) = 1/(2\pi\theta^2)e^{-(x^2+y^2)/(2\theta^2)} \tag{4.2}$$

where x and y is the distance from the origin in the horizontal axis and vertical axis, respectively, and θ is the standard deviation of the Gaussian distribution. The variable θ in the Gaussian filter controls the levels of smoothness of an image. In the proposed approach, we use the Gaussian filter to smooth the gradient field of a fingerprint image. It means that the vertical and horizontal gradient components of the gradient field are convoluted with the Gaussian filter. Then the orientation field is computed after the smoothing. We have tested our approach on the FVC 2002 [MMC+02] databases and found that when $\theta = 24$, most false SPs are removed. However, when a big value of θ is chosen, one or two genuine SPs may also be

removed mistakenly in some cases. Furthermore, the detected SPs may be located away from the real SPs by several pixels. Because of the inaccuracy of the detected position, these SPs cannot be used further for alignment of fingerprints for a match. Figure 4.4 shows the effect of smoothing and the circles indicate SP areas. We can see that the most irregular areas in Figure 4.4a are removed in Figure 4.4b. However, the SP areas are slightly away from their original regions, as is also noted by Wang et al. [WLN07]. It will cause the detected SPs to be marked at incorrect places.

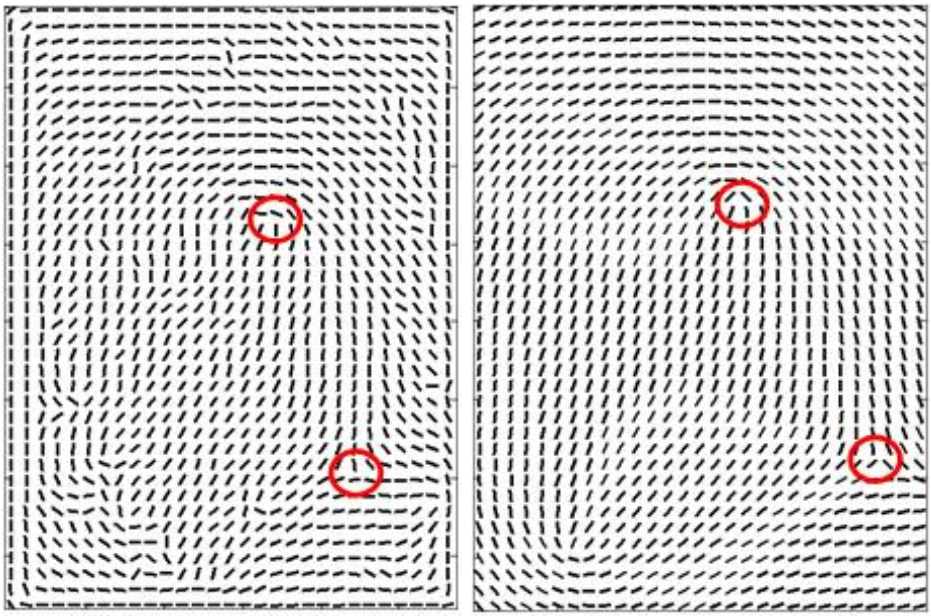

(a) (b)

Figure 4.4: The orientation field of Figure 4.1a) where the circle indicates the SP areas. (a), the original orientation field; (b), the smoothed orientation field with $\theta = 24$.

Therefore, we propose a validation scheme to remove spurious SPs and relocate the detected SPs based on experimental observation as follows:

(i) Set $\theta = 5$ and $k = 1$, where k denotes the sequence number of core and delta data sets, which means the kth smoothing. Choosing $\theta = 5$

is an appropriate start value as reported by Bazen and Gerez [BG02], at which most genuine SPs will be retained.

(ii) Detect SPs using the Poincaré Index calculation, and remove any cores outside the segmentation mask. Next store SPs as: $C_k = \{(x_1, y_1), (x_2, y_2), ...(x_{Mk}, y_{Mk})\}$, $D_k = \{(x_1, y_1), (x_2, y_2), ...(x_{Nk}, y_{Nk})\}$ where C and D are set of cores and deltas respectively; (x_i, y_i) is the position of a core or delta point; M and N are the number of cores and deltas respectively, and M_k and N_K denote the number of cores and deltas in the *kth* iteration respectively.

(iii) Set $\theta = \theta + 4$, $k = k + 1$. Repeat the same procedure as in step (ii) above until $\theta >= 24$.

(iv) If $(N_k <= M_k <= 2 \& M_k = M_{k-1} \& N_k = N_{k-1})$ or $\theta = 24$, then we choose the last core and delta sets as the final result, else we redo step (ii).

(v) We get k pairs of core and delta points sets from the above steps which are $C_1...C_k$ and $D_1...D_k$. For data sets $C_1...C_k$, we map the core points from C_k to C_1 in sequence by selecting a pair of core points with the minimum distance. Take an example, for a point (x, y) in set C_k, we calculate the distance between (x, y) and all points in C_{k-1} using equation 4.3, then a corresponding point (x', y') in C_{k-1} is selected which has the shortest distance to the point (x, y). Next we do the same step until we find the corresponding point of the point (x, y) in C_1. For the delta point part, the procedure is the same as the core point part. Finally, the refined positions of validated SPs are

obtained.

$$distance = \sqrt{(x_2 - x_1)^2 + (y_2 - y_1)^2} \tag{4.3}$$

$\theta = 5$ is chosen as the smallest value for SP detection, because if $\theta < 5$ there are too many spurious SPs detected as illustrated by Bazen and Gerez [BG02]. Then we set the values of θ in the range [5, 24] based on the research in [BG02] and experimental observation (the θ values are 5, 9, 13, 17, 21, 24 which are selected in step (ii) of the above procedure). The increase in θ may cause the missing of genuine SPs. Therefore, we chose 4 as the incremental step of θ until valid SPs are found. So most images do not need to be smoothed with $\theta = 24$. Furthermore, step (v) defines a simple method to relocate the accurate position of valid SPs. The above procedure also defines rules to validate SPs which are:

- **Rule 1**: cores near mask or border of the image within 5 pixels should be removed;
- **Rule 2**: a fingerprint image should not contain more than 2 pairs of cores and deltas unless 3 or more cores are still detected when $\theta = 25$;
- **Rule 3**: if a group of cores and deltas are possibly the genuine SPs, then the subsequent group should have the same number of cores and deltas.

We only remove core points near the mask or border of an image in **rule 1**, because a fingerprint image may not contain a complete fingerprint. However, core points are normally in the centre of a fingerprint and most of the core points will not be near the mask or border of an image. Therefore, core points near the mask or border are highly likely to be spurious points.

Rule 2 is defined according to the work of Karu and Jain [KJ96] and Zhou et al. [ZGZ07]. They found and proved that the number of core and delta points should be the same in a fingerprint, and most fingerprints will not have more than 2 pairs of core and delta points. However, if there are 3 or more pairs of core and delta points, as in some special cases, so we set that if 3 or more cores are found when $\theta = 24$, we keep that result as the final result. **Rule 3** is a constraint, such that detected SPs will be validated only if results of two subsequent smoothings are the same, which means that the detected SPs are reliable. We find that a pair of false core and delta points may be retained only if both rules 1 and 2 are used in some cases. Rule 3 eliminates this kind of situation. Figure 4.5 shows the result after segmentation and validation of Figure 4.1a also shows some more sample detections for poor quality images selected from the FVC 2002 database.

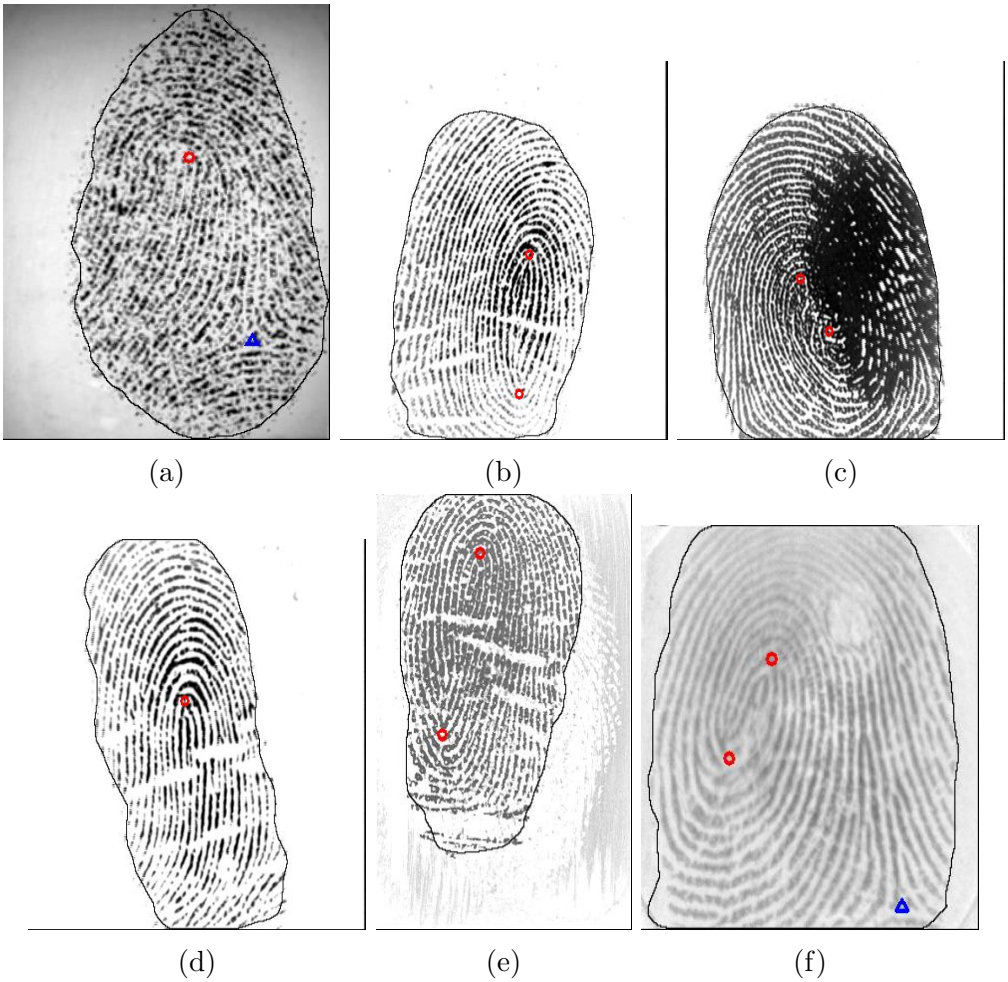

Figure 4.5: The results of the proposed approach: (a) is the result of Figure 4.1a ; (b), (c), (d), (e) and (f) are five selected poor quality images from the FVC 2002 databases.

4.1.3 Experimental Results

The FVC2002 [MMC+02] DB1a and DB2a databases have a total 1600 images to test this approach. FVC (Fingerprint Verification Competition) is an international competition to evaluate fingerprint recognition techniques, and its databases contain various quality fingerprint images [MMC+02]. Table 4.1 shows the specifications of these databases.

Table 4.1: The specifications of FVC 2002 DB1a and DB2a databases

Database	**Sensor type**	**Image size**	**Image numbers**	**Image resolution**
FVC2002 DB1a	Optical Sensor	388x374	800	500
FVC2002 DB2a	Optical Sensor	296x560	800	569

The experiment is conducted by checking the detected core points and delta points with human experts. The SPs are marked by human experts and initially considered as genuine SPs, then the experiment results are compared to those marked points to calculate the detection rate. If a core/delta point is in the range of 16 pixels (which is a threshold adopted by various researchers, e.g. [ZWZ06]) to a correct core/delta point, we consider this point is correct, otherwise it is a false one. If a genuine core/delta point is not detected, we call this point a missed one. The plain arch type of fingerprints do not contain SPs. Therefore, if there are no SPs detected in an arch fingerprint image, then we say that this image is correctly detected as an arch fingerprint.

Table 4.2 shows the experimental results of our approach. From Table 4.2, we can see that the total error rate of core and delta point detection is 10.52%. And average 91.50% of the fingerprint images are detected without false/missed SPs by our approach. Table 4.3 shows the comparison of experimental results with other Poincaré Index based methods, we can see that our method is better than these reported results. In this table, Bazen and

Gerez's [BG02] approach uses the Poincaré Index approach without post-processing, so the results show the normal possible error rate of Poincaré Index based approaches. However, the miss rate of our approach is close to their approach. We have analyzed our results and found that we remove the SPs close to the border of the mask using rule 1. Therefore, some SPs near border of the mask are removed, but these points are considered as genuine ones as they could be easily determined by experts.

Table 4.2: The results of the approach on databases FVC 2002 DB1a and DB2a

Database	**Miss rate**	**False rate**	**Total error rate**	**Correct image rate**
FVC2002 DB1	4.79%	1.67%	6.46%	92.25%
FVC2002 DB2	10.82%	3.75%	14.57%	90.75%
Average	7.81%	2.71%	10.52%	91.50%

Table 4.3: Experimental results comparison with other reported Poincaré Index methods.

Approach	**Miss rate**	**False rate**	**Total Performance**
Bazen and Gerez [BG02]	5%	13%	82%
Ohtsuka et al. [OWT+08]	-	-	86.67% (FVC 2002 databases 1, 2 and 4; extended version of Poincaré Index method introduced in [MMJP09])
Li et al. [LML13]	-	-	82.95%
Our method	6.81%	2.71%	89.48%

4.1.4 Advantages and disadvantages

By analysing the results, we have found some reasons why the SPs are missed or falsely detected in our approach:

- False delta points are detected near the borders of images. e.g. in Figure 4.6b, a false delta point is detected in the right down side of the image.

- In a whorl type fingerprint, if two core points are too close, then one core point may be shifted too far from the correct position due to the smoothing of the orientation field, e.g. in Figure 4.6c, the second core is obviously detected far from the genuine position. This also happens

in the situation if a fingerprint has more than two genuine cores.

- If the quality of a fingerprint is poor, then the detected position is not very accurate. However, in this case, the detected core/delta positions are normally not far from the correct position, so they can still be used for fingerprint classification.

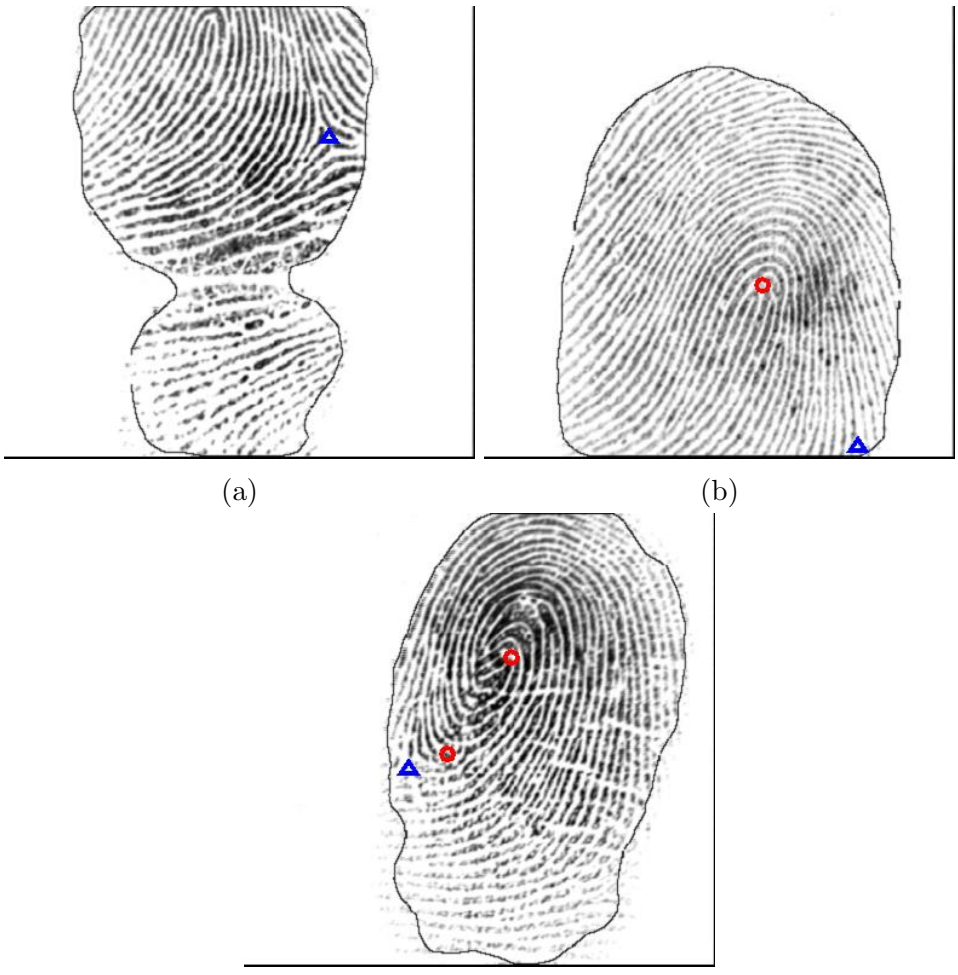

(a) (b)

(c)

Figure 4.6: Examples of missed or false detection of SPs.

One of the reasons that causes the above miss/false detection is that the Poincaré Index calculation processes an image block by block (or pixel

by pixel) which ignores the global structure of ridge/valley lines. In order to solve the above existing problem in Poincaré Index methods, a new SP detection method based on the analysis of the overall local ridge orientation map is introduced in the next section.

4.2 A Method for SP Detection Based on Local Ridge Orientation

In this section, a new SP detection approach is developed based on analyzing the pattern in the fingerprint local ridge orientation map in order to address the problems encountered with the Poincaré Index based methods. Furthermore, this approach is also able to locate a reference point for arch types of fingerprints or even partial fingerprints.

In the following section, the detailed reference point detection approach is described first. Next we shall introduce the reference point detection for arch type fingerprint images. This will be followed by a method to detect reference points for partial fingerprints. Finally, experimental results and analysis are provided to confirm the accuracy of detection of reference point using this proposed method.

4.2.1 The proposed approach for SP detection

As we mentioned before, a SP is a global feature of a fingerprint. It could be a core or delta point. Both core and delta points are formed due to the direction changes of ridge lines. Therefore, the local ridge orientation surrounding a core or delta point changes in the orientation map as shown

in Figure 4.7

In our approach, we categorize a ridge orientation map into four values which are 0, $\pi/4$, $\pi/2$ and $3\pi/4$. The local ridge orientation value of a fingerprint is in the range $[0, \pi)$ instead of $[0, 2\pi)$, which is because local ridge orientation is not directional. The local ridge orientation can be represented by the following equation:

$$O_{x,y} = \begin{cases} 0 & if\ O_{x,y} < \pi/8 \quad or \quad O_{x,y} >= 7\pi/8 \\ 3\pi/4 & if\ O_{x,y} < 3\pi/8 \quad or \quad O_{x,y} >= \pi/8 \\ \pi/2 & if\ O_{x,y} < 5\pi/8 \quad or \quad O_{x,y} >= 3\pi/8 \\ \pi/4 & if\ O_{x,y} < 7\pi/8 \quad or \quad O_{x,y} >= 5\pi/8 \end{cases} \tag{4.4}$$

where $O_{x,y}$ indicates the ridge orientation at pixel (x,y).

Figure 4.7 shows the ridge orientation map after the previous stage. We can see that the orientation map is segmented into four distinctive areas, where black areas represent orientation value of 0, dark grey areas represent orientation value of $\pi/4$, light grey areas represent orientation value of $\pi/2$, and white areas represent orientation value of $3\pi/4$. There are several joint points between orientation segments. If a joint point is connected to four orientation blocks which have four different values, then this point is possibly a SP. In Figure 4.8, those joint points are marked as a red star.

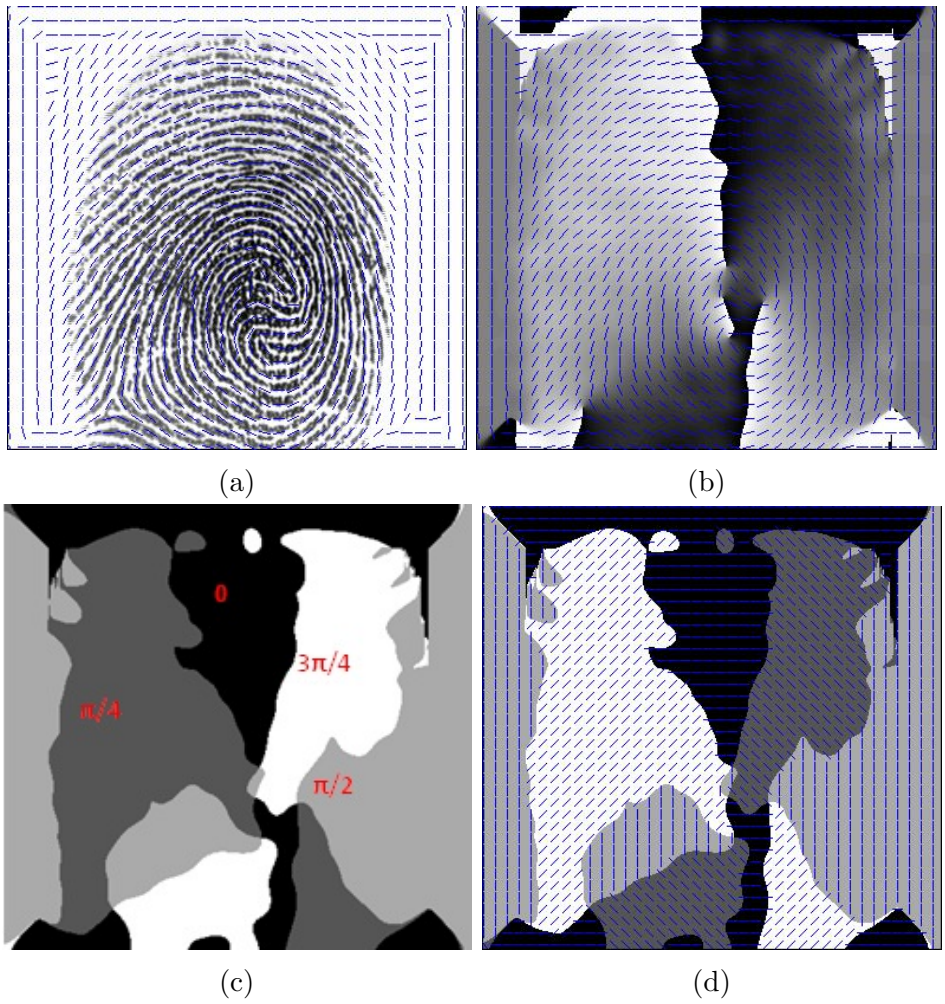

Figure 4.7: An example of local ridge orientation field transformation into four local ridge orientation values. The blue dash lines show the directions of ridges. (a), the original image; (b), the local ridge orientation field; (c) and (d) are the orientation map after the orientation value transformation. The values of orientation lie in the range of $[0, \pi)$ mapping to the color from white (0) to black (π).The orientation map after being segmented into four values. The orientation values of black, dark grey, light grey and white segments are 0, $\pi/4$, $\pi/2$ and $3\pi/4$ respectively.

Here we divide the orientation values into only four values instead of eight or more values. This is due to the following reasons: Firstly, four values are enough to observe the changes of the orientation in the SPs areas. Secondly, eight or more values cannot eliminate sufficient noise, especially in

some poor quality fingerprint images, which may produce a small number of small size of unreliable orientation segments. Finally, using only four values will make the orientation segments have sufficient size, which is easier for SP validation which is introduced in the next part.

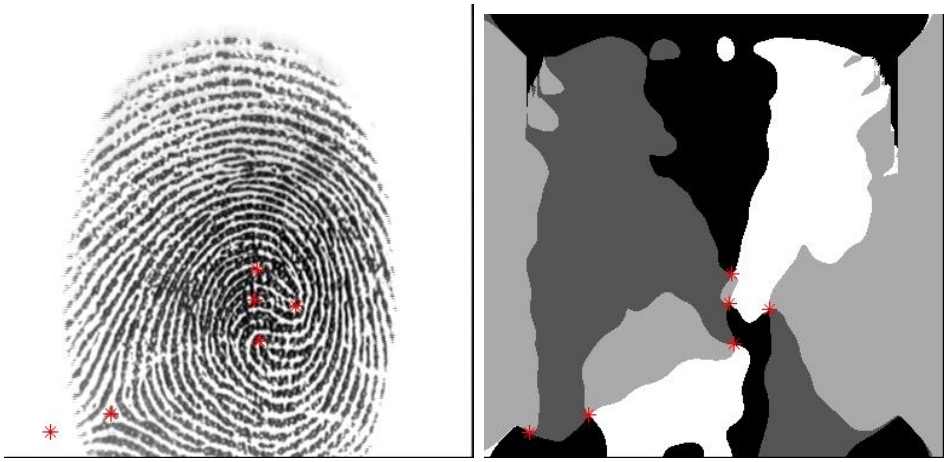

(a) (b)

Figure 4.8: Detected reference points plotted in the (a) original image and (b) orientation map (marked as a star).

4.2.1.1 Recognize the SP types

If we want to use these detected SPs as reference points for fingerprint classification, then we have to correctly recognize SP types either as core or delta.

Figure 4.9 shows the surrounding area of a core point and delta point in the orientation map. We can see that: a core point has a feature that it's surrounding orientation values increase from 0 to $3\pi/4$ anticlockwise; while a delta point has its surrounding orientation values increase from 0 to $3\pi/4$ clockwise. This idea is similar to Poincaré Index. Thus, we define a SP type by following rules in our approach.

1. If four orientation blocks surrounding a SP are placed in an order of $0 \rightarrow \pi/4 \rightarrow \pi/2 \rightarrow 3\pi/4$ in the anticlockwise direction, then this point is a core point (see Figure 4.9a).

2. If the joint 0 value orientation segment is below the detected core point, then this core point is the secondary core point in a whorl type fingerprint.

3. If four orientation blocks surrounding a SP are placed in an order of $3\pi/4 \rightarrow \pi/2 \rightarrow \pi/4 \rightarrow 0$ in the clockwise direction, then this point is a delta point (see Figure 4.9b).

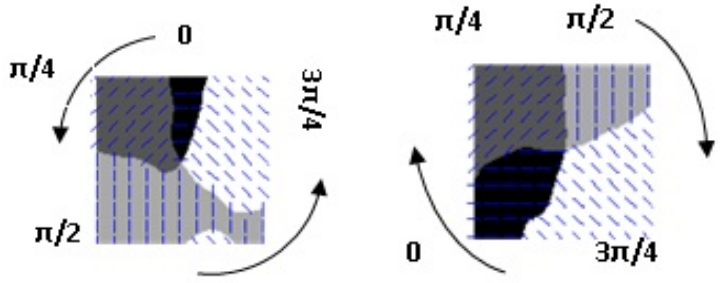

(a) A typical core point at the centre

(b) A typical delta point at the centre

Figure 4.9: Patterns of a core and delta point in the orientation map.

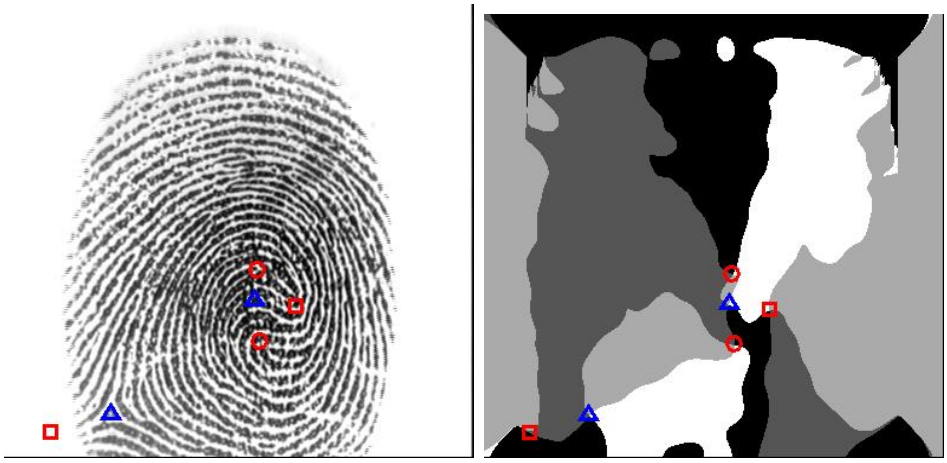

(a) (b)

Figure 4.10: The reference points are classified (note we use a red square to mark the secondary core point). (a), the marked singular points in the original image; (b), the marked singular points in the segmented local ridge orientation map.

Figure 4.10 shows the image after SP classification. We use red circles, red squares, and blue triangles to indicate the main core points, the secondary core points and delta points respectively. Because whorl type has two core points, here we use the term "main" and "secondary" to distinguish between them. The core point with its ridge loop direction pointing to the top is considered the main core point while the one with its ridge direction pointing to the bottom is considered the secondary core point.

4.2.1.2 Validation of detected SPs

Not all joint points are genuine SPs. Some of them are formed due to noise (as seen in Figure 4.10). In this case, it is necessary to remove those false SPs. One possible method is segmentation. Segmentation of fingerprint images is used to remove singular points outside the mask boundary. After segmentation, a mask is generated to shield the background. The detail of

the segmentation algorithm can be seen in [WBGS10]. Figure 4.11 shows the result of the segmentation. It can effectively remove false SPs outside the mask boundary. Figure 4.11a shows the segmentation boundary of a fingerprint image. Figure 4.11b illustrates that a core point is discarded because it is outside of the mask.

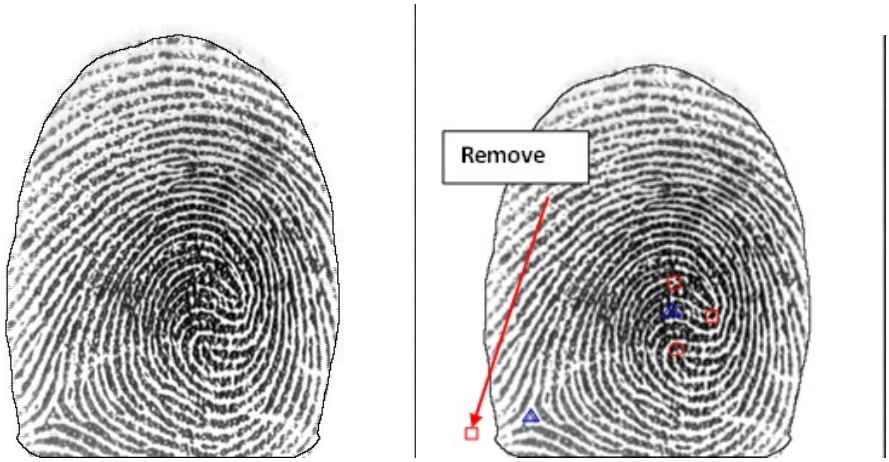

(a) (b)

Figure 4.11: If the detected SPs are outside the mask, then these SPs are removed.

4.2.1.3 Validation of SPs based on patterns of orientation segments

After segmentation, the rest of the SPs need to be further investigated. Based on the analysis of the pattern of the orientation segments, a validation scheme is designed as follows:

1. Pairing the core and delta points: Divide the singular points into two groups: paired and non-paired. The criterion of pairing is to check whether two SPs are connected by any orientation partition excluding the 0 value segments. This is because 0 value segments are normally

on the top of a core point, thus it is not a valid pair if a core point and a delta point is connected by a 0 value segment.

2. For paired SPs: A fingerprint image should only contain one core point excluding the secondary core points in a whorl type fingerprint. If there are more than two cores detected, we will only keep the most reliable core point and its relevant delta point pair. The other core/delta pairs are removed. The reliability of a core/delta is decided by the sizes of its connected orientation segments and their distances. For example, the Euclidean distance between a spurious pair of core point and delta point is relatively closer than a genuine pair of core and delta point (see Figure 4.12a). Besides, for a spurious pair core and delta point, there may be one or more joint segments whose area is small as shown in Figure 4.12a. Though in several rare cases, there are more than three genuine core and delta pairs in some fingerprints. However, our method only chooses the two most reliable core and delta pairs.

3. For non-paired SPs: If a SP is not close to the boundary of the mask (let us say 25 pixels), then it should be connected to at least three large size orientation segments (here we set the size of the segments as 625 pixels based on experimental observation of 500 dpi fingerprint images). Otherwise it is possibly generated by noise. In the case a SP being close to the boundary of a mask, then it should be connected to at least two large size orientation segments.

4. Additional rule: Delta points should be below all core points, and core points should be above all delta points. This assumes that the fingerprint images are not placed in a up-down direction.

Step 1 is the pairing step which is an essential part of the validation part. Normally for a complete fingerprint, the number of core points and delta points are the same [MMJP09]. Based on our observation, if there are some spurious singular points detected in a fingerprint, these points contain the same number of core and delta points. Therefore, we make the following assumption:

Among the detected SPs, if the fingerprint is complete (non-partial) and naturally produced (non-artificial), then in a loop type fingerprint, any core point has one and only one corresponding delta point to make them a match, and in a whorl type fingerprint, any core point has one or two corresponding delta points to make them a match (both core points may be a match with either delta point in a whorl type fingerprint). Based on this assumption,

(a) (b)

Figure 4.12: The example of pairing the reference points: (a), remove the unreliable SP pairs; (b), detected reference core point.

we could remove false pairs of SPs. False pairs of SPs are determined by the smallest size of their connected orientation segments and their distance as defined in step 2. For non-paired singular points, because the orientation values surrounding a genuine SP are changing smoothly, genuine SPs are usually connected to those orientation segments with sufficient size, which is defined in step 3. The major aim of step 4 is to remove spurious SPs from non-fingerprint areas as in some cases a fingerprint image may contain the impression of other parts of a finger. Figure 4.12 shows the image after singular point paring. We use red circles, red squares, and blue triangles indicate the main core points, the secondary core points and delta points respectively.

4.2.1.4 Reference point detection for arch fingerprints

In some cases, a fingerprint image does not have a core nor delta point. There are two kinds of these fingerprint images: one is arch type fingerprints, and the other is partial fingerprints. Figure 4.13 shows an arch fingerprint image.

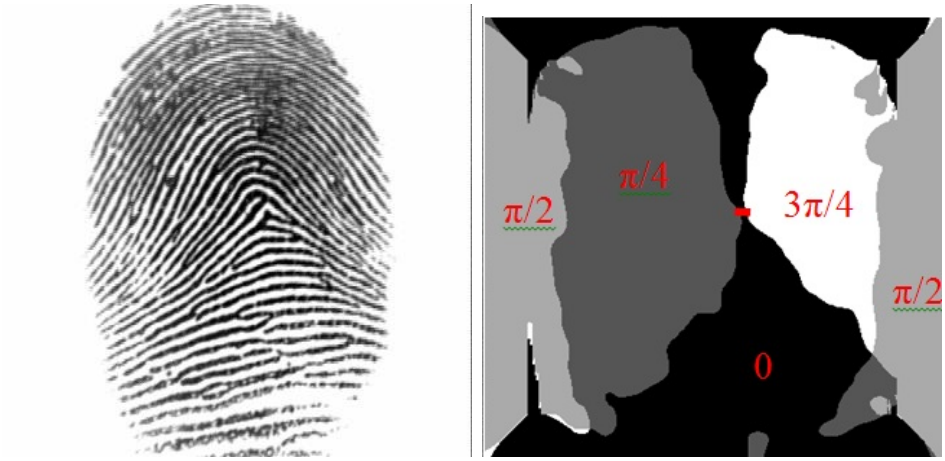

(a) (b)

Figure 4.13: An example of (a), an arch fingerprint and (b), its orientation map.

An arch type fingerprint has no loop of ridge lines as shown in Figure 4.13a, so there is no joint point of four different orientation segments in its orientation map . However, because of no loop or delta, the major orientation segments are placed in a sequence of $\pi/4$, 0, and $3\pi/4$ as shown in Figure 4.13b. Therefore, we simply find two points which have the shortest distance between the major $\pi/4$ orientation and $3\pi/4$ orientation segments as indicated as red line in Figure 4.13b). Then we choose the middle point of this line as a reference point. Arch type fingerprints do not have joint points between different orientation segments and there are only three major orientation segments with different orientation values instead of four in other types of fingerprints as shown in Figure 4.13b. To find a point which is located in the middle orientation segment and closest to the other two orientation segments could be a reference point. For an intra-class group of arch type fingerprints, the locations of detected reference points are very close to each other because the distributions of orientation segments are

similar. Figure 4.14 shows an example of reference points detection for two arch type fingerprints from an intra-class group. We can see the locations of two detected reference points which are close to each other.

(a) (b)

Figure 4.14: Two examples of reference point detection for arch type fingerprints. These two fingerprints are a pair of intra-class fingerprints (from the same finger).

4.2.2 Experimental Results

FVC 2002 [MMC+02] databases are used once again for evaluation of this singular point detection method as these databases contain a wide rang of fingerprint images with different levels of quality.

We use the FVC 2002 databases DB1a and DB2a to evaluate our approach. Each of these databases has 800 fingerprints, so the total number of fingerprints is 1600 (refer to the Table 4.1). Because SPs are global features, it is hard to find the exact position of a SP. Therefore, we define that if a detected SP is inside the defined SP area (an area centered at the location of the genuine singular point with a selected radius R), then we consider it is correctly detected. The SP area radius R is not formally defined in

fingerprint recognition, a distance within 10 - 20 pixels to the genuine SP location is accepted in the literature. For example, Li et al. [LML13] choose ±14 pixels as the radius of SP area, but Weng et al. [WYY11] choose ±20 pixels as the radius of SP area. In our case, we consider some small pixel(±16) shifts of SPs as acceptable. Figure 4.15b is an example of false detection of the core point, because its position is shifted from its true position by more than 16 pixels. In this case, even though it still works for fingerprint classification or coarse alignment, we still regard it as falsely detected. Furthermore, since our aim of reference point detection is for alignment and classification, the consistency of detected positions of SPs is the most important concern. For example, in Figure 4.15a, the core point should be located on the "inner most loop" [MMJP09] of a ridge, but the detected core point is located between the second and third inner most loop of ridges. However, we still consider it as correctly detected, since all other intra-class fingerprints have the same detected position and it is still within the distance of ±16 pixels of the genuine core point area.

(a) (b)

Figure 4.15: Two samples of SP detection: (a) is considered as correctly detected while (b) is considered as falsely detected.

We have already given an example in Figure 4.12, where a false pair of core and delta points are removed by our approach. Figure 4.16 shows some more examples of comparisons between our improved Poincaré Index based approach introduced in Section 4.1 and this approach. The first column is the results of SP detection by Poincaré Index approach, and the second column shows the results using our approach. We can see that those images with false SPs in the first column are correctly detected in the second column.

Table 4.4 shows the experimental results on the FVC 2002 databases DB1a and DB2a. The second column shows the miss detection rate of SPs, which refers to the percentage of SPs that is not detected, the third column shows the false detection rate of SPs which refers to the percentage of SPs that are falsely detected; the fourth column is the overall correct rate of SP detection; and the last column shows the percentage of fingerprint images without miss/false detected SPs. From the table, we can see the average miss rate is higher than the average false detection rate. One major reason is the segmentation errors where some SPs (especially delta points) are outside or close to the boundary of masks. Among the falsely detected SPs, some points are a little far away from the true positions like the core point in Figure 4.15a. That is because the orientation maps are not accurate enough due to noise. We have also examined the fingerprint with missed or falsely detected SPs. Most of these images have at least another SP correctly detected, which can be used for coarse alignment in the next stage. However, there may still be some fingerprint images which have no correctly detected SPs. We need to further investigate those images in order to reduce or remove the influence on alignment or classification in the future.

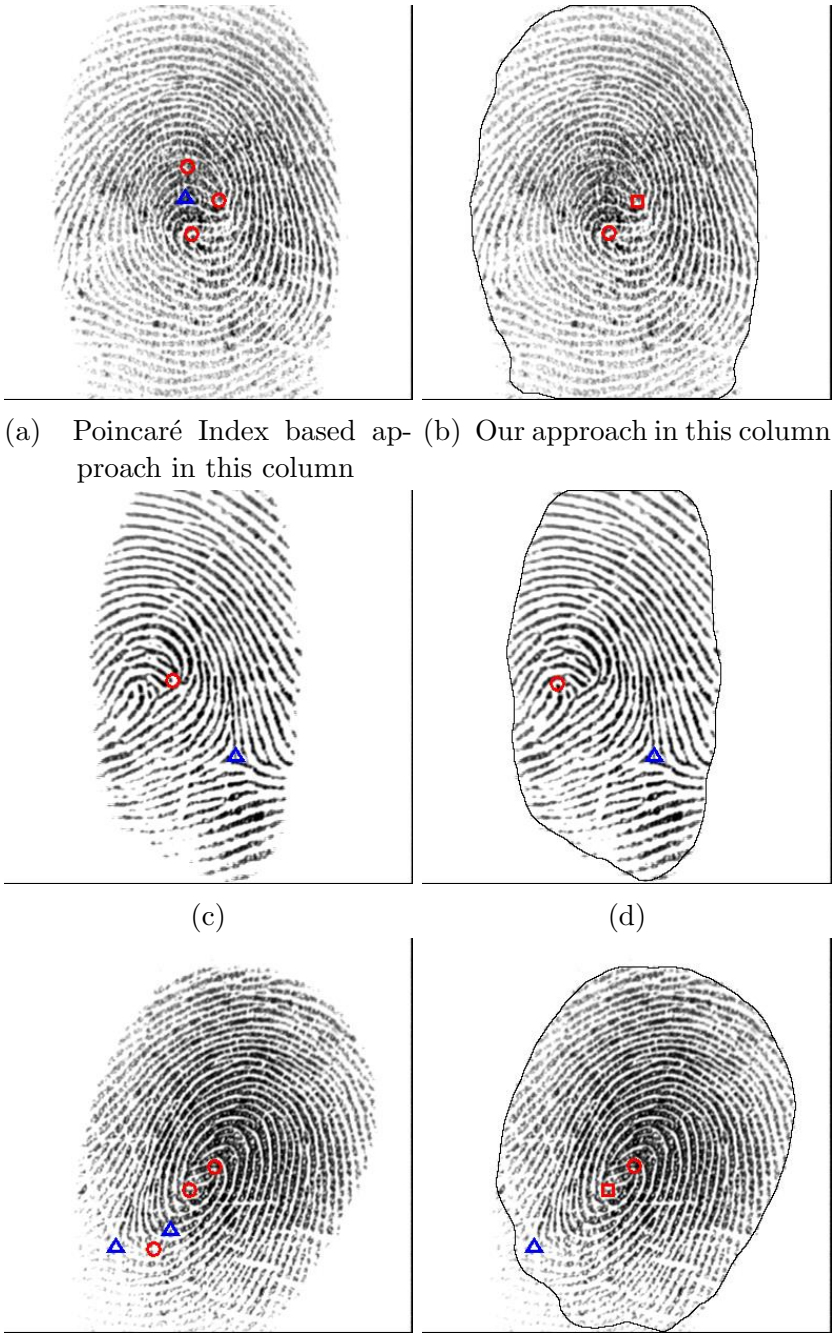

(a) Poincaré Index based approach in this column

(b) Our approach in this column

(c)

(d)

(e)

(f)

Figure 4.16: Comparison of results between the Poincaré Index based approach and our approach. The first column is the Poincaré Index based approach, and the second column is our approach.

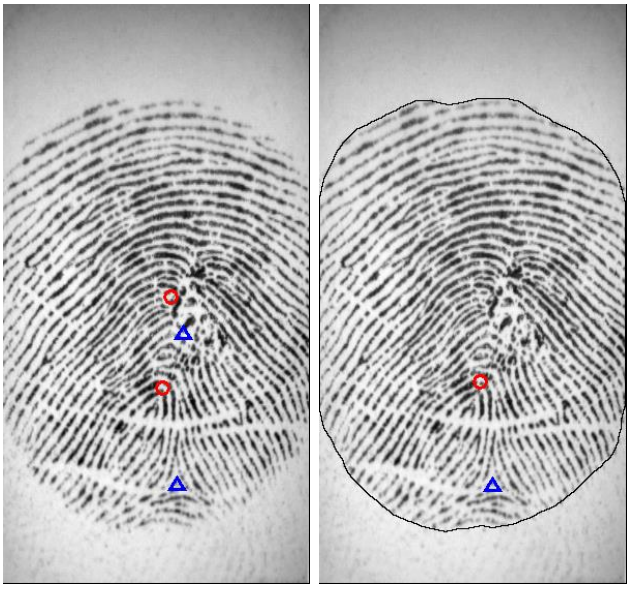

(g) Poincaré Index based approach in this column

(h) Our approach in this column

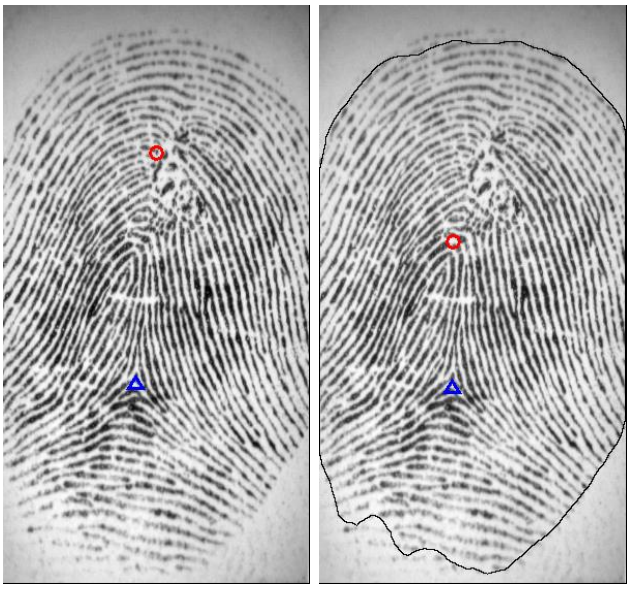

(i)

(j)

Figure 4.16: Comparison of results between the Poincaré Index based approach and our approach. The first column is Poincaré Index based approach, and the second column is our approach.

Table 4.5 shows the comparison between our approaches and other published results. From this table, we can see that our second approach is better than other approaches. However, because of the fuzziness feature of the SP positions that is different fingerprint experts may point out different genuine SP position, it is hard to provide accurate comparisons. A better way is to incorporate the singular/reference point detection approaches into alignment and matching algorithms to obtain a final False Acceptance Rate (FAR) and False Rejection Rate (FRR). We will investigate this in the next chapter.

Table 4.4: The results of the approach on database FVC 2002 DB1a and DB2a databases

Database	**Miss rate**	**False rate**	**Total correct rate**	**Correct image rate**
FVC2002 DB1	4.48%	0.85%	94.66%	94.25%
FVC2002 DB2	2.96%	3.59%	14.57%	93.45%
Total average	3.72%	2.22%	94.05%	93.31%

Table 4.5: Comparisons with other approaches

Approaches	**Miss SP**	**False SP**	**Total correct rate**
Bazen and Gerez [BG02]	5%	13%	82%
Nilsson and Bigun [NB05]	-	-	83%
Zhou et al. [ZGZ07]	14.6%	4.8%	81.6%
Zheng et al. [ZWZ06]	7.8%	4.9%	87.3%
Ohtsuka et al. [OWT+08]	-	-	92.15% (FVC 2002 databases 1 and 2)
Weng et al. [WYY11]	7.03% in total		92.97% (FVC 2002 databases 1 and 2)
Ravinder et al. [KCH12]	-	-	92.6% (FVC 2002 databases 1 and 2, 3 and 4)
Li et al. [LML13]	-	-	82.95%
Proposed Poincaré Index approach	7.81%	2.71%	89.48% (FVC 2002 databases 1 and 2)
Second proposed approach	3.72%	2.22%	94.05% (FVC 2002 databases 1 and 2)

4.3 Conclusion

In this chapter, we have presented two SP detection methods, which are able to obtain high correct detection rate of SPs. The first approach develops a rule based validation scheme after the Poincaré Index calculation. The experimental results show that this approach obtain better results than other reported Poincaré Index based approaches. The overall correct detection rate of SPs achieves 89.48% on the FVC 2002 DB1a and DB2a databases, which is about 3% improvement or more over other reported Poincaré Index based approaches. Furthermore, in order to address the limitations of Poincaré Index based approaches, a new SP detection method is developed afterwards. This approach is based on the analysis of the patterns of a fingerprint's local ridge orientation field. The experimental results show that this method obtains 94.05% correct detection rate of SP detection and 93.31% of fingerprints are without missed/falsely detected SPs which is better than the previous Poincaré Index based approach and other report results tested on the same databases. Furthermore, we extended this approach to arch type fingerprints. Thus, it is possible to locate a reference point for an arch fingerprint which can be used for fingerprint alignment or/and fingerprint classification.

The next chapter will address the third research objective of this work which aims to design an accurate and reliable fingerprint matching method. Because our overall research objective is to improve the overall matching accuracy of an automatic fingerprint recognition system, a reliable and accurate matching method or metric needs to be designed to achieve this objective. Though fingerprint matching has been extensively researched, how

to design a reliable and accurate matching algorithm is still an on-going challenge. An excellent matching algorithm should have good tolerance to image noise, non-linear distortion and feature extraction errors. In order to address this challenge, a new fingerprint matching metric named binarized minutiae block is proposed for fingerprint matching. Furthermore, four fingerprint global similarity calculation methods are designed based on this matching metric to evaluate its reliability and accuracy for fingerprint matching.

Chapter 5

Fingerprint Matching Using Binarized Minutiae Blocks

In Chapter 3 and 4, we have taken many steps to improve the performance of fingerprint feature extraction including fingerprint image quality enhancement and reliable singular point (SP) detection. The experimental results show that: (i), our image processing method improves the image quality by 9%, in terms of Goodness Index (GI), which is a metric used to evaluate the image quality of fingerprint images; and (ii), our second singular point detection method obtains 94.05% correct detection rate of singular points, which is better than other report results tested on the same databases. After fingerprint feature extraction, fingerprint matching is performed to obtain the final matching score to determine whether a pair of fingerprints match or not. Both the feature extraction and matching stages contribute to the final matching accuracy of a fingerprint recognition system. Thus, a reliable and accurate fingerprint matching method could significantly improve the overall performance of a fingerprint recognition system.

In this chapter, we aim to design a fingerprint matching method which is accurate and has a high tolerance to non-linear distortion and feature extraction errors. Fingerprint matching is one of the most important process in a fingerprint recognition system, because it may determine the final matching accuracy of this system. Fingerprint matching is a stage after the feature extraction in fingerprint recognition. The features (e.g. SPs and minutiae information) extracted in the previous stages are input information to a fingerprint matching algorithm. The accuracy of a fingerprint matching method may be influenced by two factors: the reliability and accuracy of input features; and the techniques used for the matching method itself (e.g. tolerance to non-linear distortion and the ability to address the displacement problem of fingerprint matching). Since the reliability of input feature is out of the scope to fingerprint matching, how to improve the accuracy and reliability of fingerprint matching method is an issue to be dealt with in fingerprint recognition.

In order to address this challenge, a new matching metric is designed for fingerprint matching, and is named a "binarized minutiae block" (BMB). It is a binarized fingerprint image block with a minutiae point in the center. Besides, all BMBs are normalized to make all the minutiae has the same direction for fast and easy local minutiae similarity calculation. Unlike minutiae based, correlation based or other non-minutiae based methods, BMB utilizes both minutiae and texture information for matching. Thus, the BMB method has the advantages of minutiae based and correlation based (which compares grey level texture information) methods. The main advantage of this BMB metric are: (i), more information has been taken into consideration in fingerprint matching compared to other

minutiae based (no texture information) and correlation based (no minutiae information) matching methods, which increases the reliability of local minutiae similarity. (ii), the calculation of local minutiae similarity is based on the comparison of BMBs using the Hamming distance [Ham50] calculation, which is a simple XOR operation that could be implemented in one CPU cycle. (iii), high tolerance to missing and spurious minutiae. Minutiae is not the only information in a BMB, and this metric is not a local minutiae structure based method. Missed and spurious minutiae only influence the BMB generation, and spurious minutiae is not probable to obtain low hamming distance values during the comparison of BMBs (the lower hamming distance indicates the higher BMB similarity, vice versa). (iv), high tolerance to non-linear distortion. Unlike correlation based methods, only the surrounding texture information of minutiae points is used for matching rather than using the texture information of a whole fingerprint. Thus, the tolerance to non-linear distortion of this method is as high as other minutiae based methods, which are much higher than correlation based methods (non-linear distortion may cause shifts of ridges and valleys on some areas of a fingerprint image, which could not be well addressed in correlation based methods because they takes the whole image for comparison). Furthermore, four global similarity calculation methods are proposed to obtain the final matching scores and evaluate the designed matching metric, BMB.

The rest of the chapter is organized as follows: First, the process of fingerprint template generation based on binarized minutiae blocks is described. Then, how to generate the local minutiae similarity is introduced. Subsequently, four global similarity score calculation methods are described, Finally, experimental results are provided, and a comparison with the ex-

perimental results of other reported matching methods is analyzed and discussed.

5.1 Fingerprint Matching based on the Binarized Minutiae Blocks

In this section, we first introduce template generation using binarized minutiae blocks which are used to calculate the local similarity of minutiae pairs. Next the global matching similarity methods, which aim to obtain the final matching score between two fingerprint templates, are illustrated in detail. Finally, experimental results and discussions are discussed in detail.

5.1.1 Generating fingerprint template

In this matching method, the texture information (binarized ridge and valley flows) is used for fingerprint matching. Texture information has been used in correlation based methods for fingerprint matching (grey level texture information) [LELJSM07, KAN08]. The advantage of using texture information for fingerprint matching is that the texture information is the raw information of a fingerprint containing not only minutiae information but also other information such as structure of ridge and valley [MMJP09], thus makes the comparison more reliable than using only minutiae. However, using texture information for fingerprint comparison has some issues [MMJP09], which are: (i), non-linear distortion makes impressions of the same finger significantly different in terms of global structure. Because a 3-D finger is mapped to a 2-D image, the global structure of a fingerprint

may be different from another fingerprint of the same finger (e.g. shifts of some ridges). Therefore, global correlation based methods may fail if the non-linear distortion of a fingerprint is high. (ii), skin condition and finger pressure cause image brightness, contrast, and ridge thickness to vary significantly across different impressions. The above issues are well addressed by using the BMB method. A BMB contains a binarized block of local texture information, which is used for local pattern comparison instead of global texture information comparison. Furthermore, the BMB method does not have concerns over variations of image brightness, contrast, and ridge thickness, because the texture information has been enhanced and binarized by the image processing stage.

For fingerprint template generation, the generated fingerprint template contains not only minutiae information (location and direction) , but also the texture information surrounding the minutiae points. A minutiae point with its surrounding texture information is designed as a matching metric for fingerprint matching, which is named binarized minutiae block (BMB) in this work. The process of fingerprint template generation is shown as follows:

(i) For each minutiae, put a window with size w x w centred at the location of a minutiae point on the binary image. This step is shown in Figure 5.1a and 5.1b, in which a window is selected for a minutiae point.

(ii) Rotate the minutiae window to set the minutiae direction angle at a selected angle value. In this work, the minutiae direction is set to 0 degrees. The purpose of this step is to normalize the minutiae blocks

so that all the minutiae points have the same direction to facilitate the local similarity calculation. This step is shown in Figure 5.1c, in which the selected minutiae window is rotated according to the angle θ of the minutiae point.

(iii) Obtain the minutiae blocks with the size of s x s, where s is the length of the block. After this step, all minutiae blocks have the same size and same direction, then similarity between any two minutiae blocks could be simply compared using exclusive or (XOR) operations (see the equation 5.1). This step is shown in Figure 5.1d, in which a binarized minutiae block (BMB) is generated for the selected minutiae point. For each minutiae point in the binarized fingerprint image, a corresponding BMB will be generated.

Figure 5.1 shows an example of the designed minutiae template generation. Figure 5.1a is a sample binarized fingerprint image from FVC2002 database DB1a, and the red circles and rectangles indicate the detected ridge bifurcations and ridge endings respectively. For each minutiae detected in the image, a window with size of w x w is located at that minutiae. Figure 5.1b shows the chosen window centered at the selected minutiae for a window size of 100 x 100 pixels. Then the selected window is rotated according to the minutiae angle anticlockwise to make the new minutiae angle to the expected angle value. Figure 5.1c shows the minutiae block is rotated in the window to make the minutiae angle equals to 0 degrees after rotation, and the red rectangle is the selected minutiae template block. Finally a smaller block with a size of s x s is obtained from the rotated window. Figure 5.1d shows the obtained BMB with size of 60 x 60 pixels.

(a) A binarized image with detected minutiae. A minutiae is selected for BMB generation, which is centered at the window. The window length w equals 100 pixels.

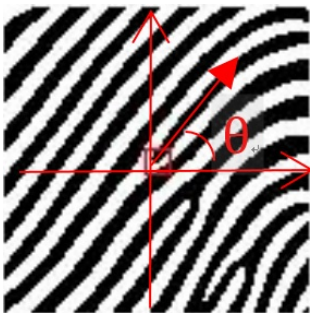

(b) A minutiae window centred at the selected minutiae with window size 100 x 100 pixels.

(c) Minutiae window is rotated to make the minutiae angle to 0. Then a block with length of s is selected.

(d) The BMB of the selected minutiae with block size 60 x 60 pixels.

Figure 5.1: Designed fingerprint template generation steps.

For each detected minutiae, the minutiae template could be generated by the above procedure. Normally when the window length $w = \sqrt{2} * s$, it can fulfil the requirements of the minutiae template block generation. Note the size of minutiae template blocks may influence the matching results.

If the size of a BMB increases, then more texture information is included in the BMB for comparison. Thus, the comparison result of a minutiae pair would be more reliable. However, due to the non-linear distortion introduced during the image capturing stage, the dissimilarity between two BMBs will increase when the size of the BMB increase, which may make the dissimilarity values not so distinguish between a genuine minutiae pair and a false minutiae pair when the size of the BMB is too large (the terms *genuine* and *false* minutiae pair used here mean that two minutiae points are a match or not, respectively, from a pair of intraclass fingerprint images). It means that the tolerance to non-linear distortion will be reduced when the size of the BMB increases. The detailed analysis of the block size influence is described in the experimental evaluation section (Section 5.2.3.1). Because our method not only uses minutiae information but also the core points, the positions of core points are contained in the template. But delta points are not included in the templates. The major reason is that delta points are located at the edge of fingerprints, and are missed in most cases of partial fingerprints. In the case of a fingerprint being incomplete after the scanning stage, the delta points may be missed in the scanned images. For example, numerous fingerprint images in FVC databases have no delta points. Figure 5.2 shows four examples of partial fingerprint from FVC 2002 database DB1a, and these partial fingerprints do not contain a delta point. On an average, there is approximately one fingerprint image having no delta point in each intraclass group based on the observation (total 100 intra groups in this database, and each group has 8 fingerprint images).

Table 5.1 shows a sample fingerprint template generated by our method. The angle of a minutiae point is the direction of the ridges, so the angle

Figure 5.2: Some examples of partial fingerprints in FVC 2002 database DBa1 that having no delta points. On an average, there is approximately one fingerprint image having no delta point in each intraclass group based on the observation (total 100 groups in this database).

values lie in the range of $[0, 360)$ degrees (does not include 360 degrees because the angle of 0 degrees equals the angle of 360 degrees). After the fingerprint templates are generated, the next stage is calculating the possible matching pairs of minutiae.

Table 5.1: A generated minutiae sample template.

Minutiae No.	Position	Angle	Minutiae blocks
1	(x_1, y_1)	θ_1	BMB_1
2	(x_2, y_2)	θ_2	BMB_2
⋮	⋮	⋮	⋮
n	(x_n, y_n)	θ_n	BMB_n
core point	(x_c, y_c)	θ_c	BMB_c

5.1.2 Local Minutiae Similarity Calculation

The minutiae only based methods normally compute the similarity of local minutiae structure (nearest neighbor and fixed radius based methods, see Section 2.4.7.2) as the local minutiae similarity, such as triangular methods [KV00]. In our case, because the texture information is preserved, pairing minutiae by calculating the similarities of texture information between them is much simplified. Hamming distance (HD) is used to calculate the similarity score. HD [Ham50] measures the minimum number of substitutions required to change one string into the other, or the number of errors that transform one string into the other. It has been used in iris recognition for dissimilarity calculation [Dau04, HAD06]. Here we use it to measure the dissimilarity of two binary blocks. Because the blocks for comparison are binarized which consists of 0 and 1, the Hamming distance (HD) can be simply calculated by equation 5.1.

$$HD = ||block_x \oplus block_y||/\text{Size of a block} \tag{5.1}$$

For each BMB in the registered template (template A), it is compared with the BMBs in the query template (template B). Then a HD value is obtained from each comparison using equation 5.1. The HD values indicate the local dissimilarities between each minutiae pair candidate. The local similarity can be easily calculated as $1 - HD$. The minutiae pairs with the top three smallest HD values are reserved as the minutiae pair candidates, but these HD values need to fulfill the condition that $HD <= T_{HD}$. T_{HD} is a decision threshold to decide whether a minutiae pair is probable a genuine pair or not. That means a minutiae pair candidate will be removed from the table while its HD value v is larger than a selected threshold T_{HD}, because the HD value is too large to be considered as a valid pair in this case. The reason why *at most* three possible minutiae pairs are reserved is that a genuine minutiae pair may not always have the smallest HD values (e.g. due to noise or/and non-linear distortion) based on experimental observation. This situation normally happens in noisy fingerprint comparisons and/or if the minutiae block size is too small or too large. By performing this strategy, the possibility of obtaining genuine minutiae pairs will be increased. Daugman [Dau04] reported that a HD threshold between 0.28 and 0.35 is an appropriate decision criterion in iris template comparisons. In this work, the HD threshold is selected as $T_{HD} = 0.35$, which is an appropriate value based on the experimental observation. Figure 5.3 shows the process of generation of minutiae pair candidates. Each minutiae block in template A is compared to each minutiae block in template B, then the valid minutiae pairs with $HD <= T_{HD}$ is stored in the minutiae pair candidate table for further processing as shown in Table 5.2. The variable $\Delta Angle$ ($\Delta\theta_i$) is calculated by the equation $\Delta\theta_i = \theta_i - \theta'_i$ ($i \in 1...m$) where θ_i and θ'_i are angles

of minutiae points (x_i, y_i) and (x'_i, y'_i) in the ith minutiae pair candidate from Table 5.2. This step is also called *local similarity calculation*, because a minutiae point is a local feature in a fingerprint and the HD value indicate the dissimilarity score between a minutiae pair. After the local similarity calculation, the global similarity calculation (the final matching score) could be performed.

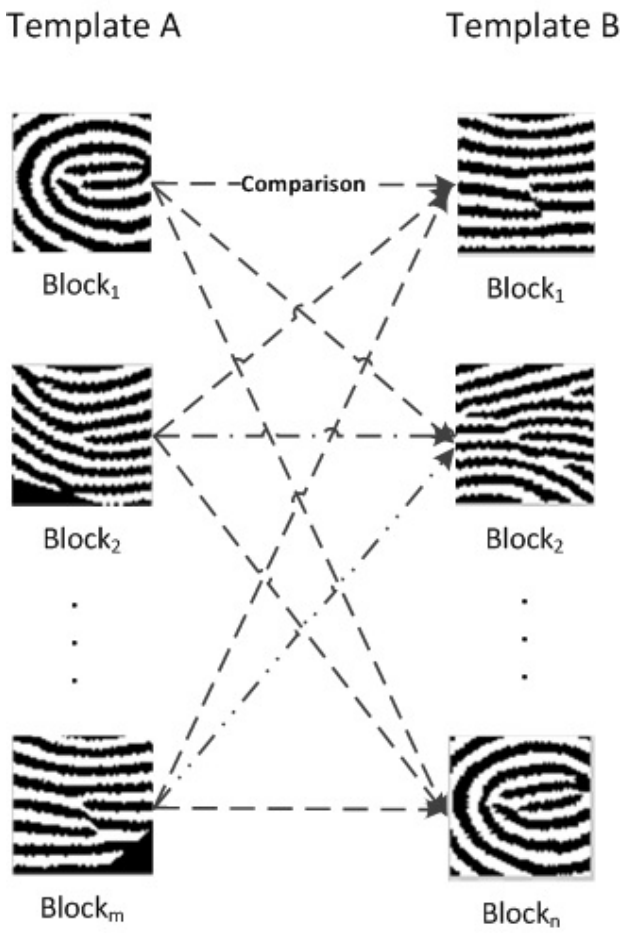

Figure 5.3: Comparisons between the minutiae blocks.

Table 5.2: Generated minutiae pair candidate table. K is the total number of minutiae pair candidates.

Pair No.	HD value	ΔAngle	Template A	Template B
1	v_1	$\Delta\theta_1$	(x_1, y_1)	(x'_1, y'_1)
2	v_2	$\Delta\theta_2$	(x_2, y_2)	(x'_2, y'_2)
⋮	⋮	⋮	⋮	⋮
K	v_K	$\Delta\theta_K$	(x_K, y_K)	(x'_K, y'_K)

5.1.3 Global similarity calculation

Global similarity in fingerprint recognition refers to the overall matching similarity between two fingerprint images. Global similarity is calculated based on the local minutiae similarities in minutiae based matching methods. In this work, the local minutiae dissimilarities are based on the HD values between each minutiae pair in Table 5.2. Thus, the local similarity of a pair of minutiae points equals 1 - HD value. There are several ways to calculate the global similarity between two enrolled fingerprint images.

The traditional fingerprint minutiae based methods use the percentage of matched minutiae as the global matching score. Equation 5.2 of the matching score calculation for minutiae based methods [MMJP09] is as follows.

$$MS = n_p^2/(n_1 * n_2) \tag{5.2}$$

where MS denotes the matching score, n_p is the number of paired minutiae and n_1 and n_2 are the total number of minutiae of template A and B respectively.

However, Liu et al. [LCG+11] argued that using the product of the total number of minutiae from two templates as the denominator in equation 5.2 cannot reflect the reasonable matching score in the case of partial overlapping of two enrolled fingerprint images. Therefore, they modified the matching score calculation as follows:

$$MS = n_p^2/(n_{1\_overlapped} * n_{2\_overlapped}) \tag{5.3}$$

where $n_{1\_overlapped}$ and $n_{2\_overlapped}$) refer to the number of minutiae in the overlapping area of two enrolled templates respectively.

Liu et al. [LCG+11] have found that using equation 5.3 obtains better results than using equation 5.2 in their experiments especially for partial fingerprints. However, if the values of both the numbers $n_{1\_overlapped}$ and $n_{2\_overlapped}$ are small, then this matching score calculation will be unreliable. For example, $n_p = n_{1\_overlapped} = n_{2\_overlapped} = 3$, then the matching score equals 1, which is unreasonable. But equation 5.2 does not have this issue, because the total number of minutiae are usually large even for partial fingerprints.

Some other matching methods explore the interrelationships (local minutiae structure) of minutiae points (e.g. [KV00, TB03, GYZZ11]). The interrelationships of minutiae points refer to the directional difference and distance between each two minutiae points. In particular, if there is a genuine minutiae pair (m_i, m_i') and (m_j, m_j'), then there are some constant relationships between them. For example, the distance between m_i and m_j should equal the distance between m_i' and m_j'. Besides, the minutiae angle difference between m_i and m_j should also equal the ridge angle difference

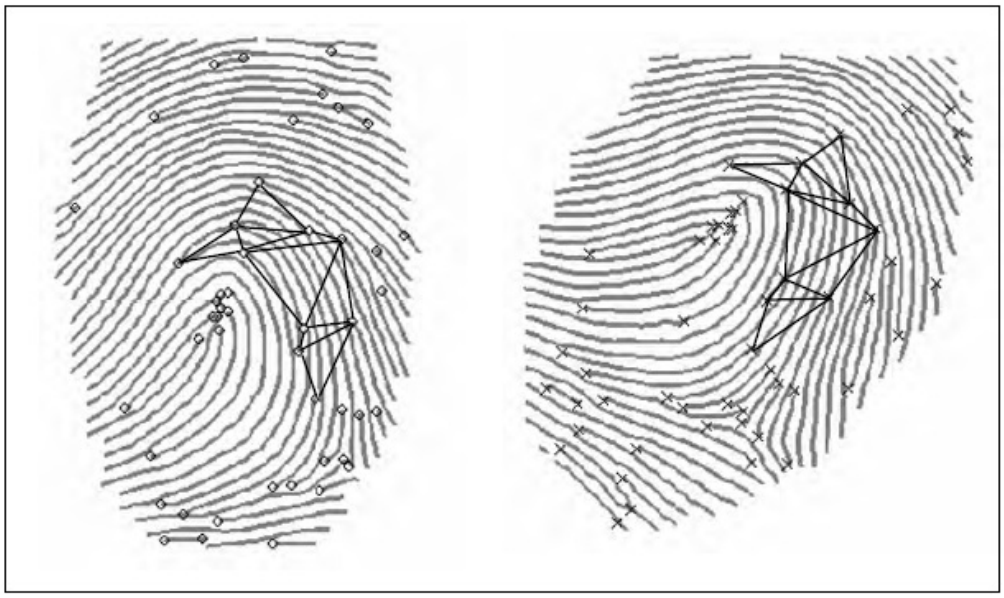

Figure 5.4: An example of using minutiae interrelationships for fingerprint matching proposed by Kovacs-Vajna et al. [KV00]. Each triangle indicates the interrelationships among three selected minutiae points. Two similar triangles from a pair of fingerprint may be a match for the minutiae points composing the triangles.

between m'_i and m'_j. Figure 5.4 shows an example of using interrelationships of minutiae points for fingerprint matching, which is also named local triangular matching [KV00]. In this method, minutiae points are connected by lines to form a graph, which consists of small triangles. Each triangle indicates the interrelationships among three selected minutiae points. By comparing the produced triangles between two fingerprints, it is able to obtain a matching similarity.

Cappelli et al. [CFM10] use local similarity sorting and relaxation techniques to calculate the global matching similarities. They designed several global matching similarity calculation methods based on these techniques. The first method they developed is named local similarity sorting (LSS). This method sorts the minutiae pairs by their local similarities then the top

n_p pairs of minutiae are selected to calculate an average matching score. This method allows duplicate minutiae points in the top n_p minutiae pairs. It means a minutiae point in template A may map to multiple numbers of minutiae in template B. Another method is named local similarity assignment (LSA), in which duplicate minutiae points are not allowed in minutiae pairs. In this case, minutiae points have one to one mapping relationships. Furthermore, the authors have tried to apply the relaxation techniques [RHZ76, FFCS06] to both the LSS and LSA methods. The basis of relaxation techniques are to iteratively modify the local similarities based on the compatibility among minutiae relationships. In particular, given a pair of minutiae a and b, if the global relationships among a and some other minutiae in template A are compatible with the global relationships among b and the corresponding minutiae in template B, then the local similarity between a and b is strengthened, otherwise it is weakened [CFM10]. In brief, relaxation techniques explore the interrelationships among minutiae points in a fingerprint template, then the weight of a minutiae pair is iterative modified according to the interrelationships with other minutiae pairs. In the authors' experiments, the LSA with relaxation techniques achieve the best experimental results with respect to the metric of EER.

In this section, we introduce four methods to calculate the global matching score. The first one uses core points as reference points for pre-alignment then followed by using BMB for a further alignment and matching. The pre-alignment is performed by superimposing two fingerprint images based on the positions of a pair of core points. The second one uses the minutiae interrelationships for validation of minutiae pair candidates. Then the validated minutiae pairs are used for matching. The third method uses the N

number of most reliable minutiae pairs as reference point pairs for fingerprint alignment (the value of N is decided by experimental observations) . Then the highest matching score among those alignments is chosen as the final matching score. Besides, we find that using the average value of the matching score from each alignment obtains better results than just choosing the highest matching score which will be discussed in Section 5.1.4.3.

5.1.3.1 Pre-alignment by SP before the matching

Pre-alignment aims to obtain a superimposed image between two fingerprint images. This method is also introduced in the published paper [WBS12b]. This pre-alignment consists of two steps: 1), a coarse alignment by core points; 2), a refined alignment by pairing the minutiae based on the HD values of the binarized minutiae blocks.

In this pre-alignment, only core points are used as reference points. This is because delta points are often missed in partial fingerprints. This situation is caused by the fact that a core point is normally in the center of a fingerprint, but a delta point is normally on the edge of a fingerprint.

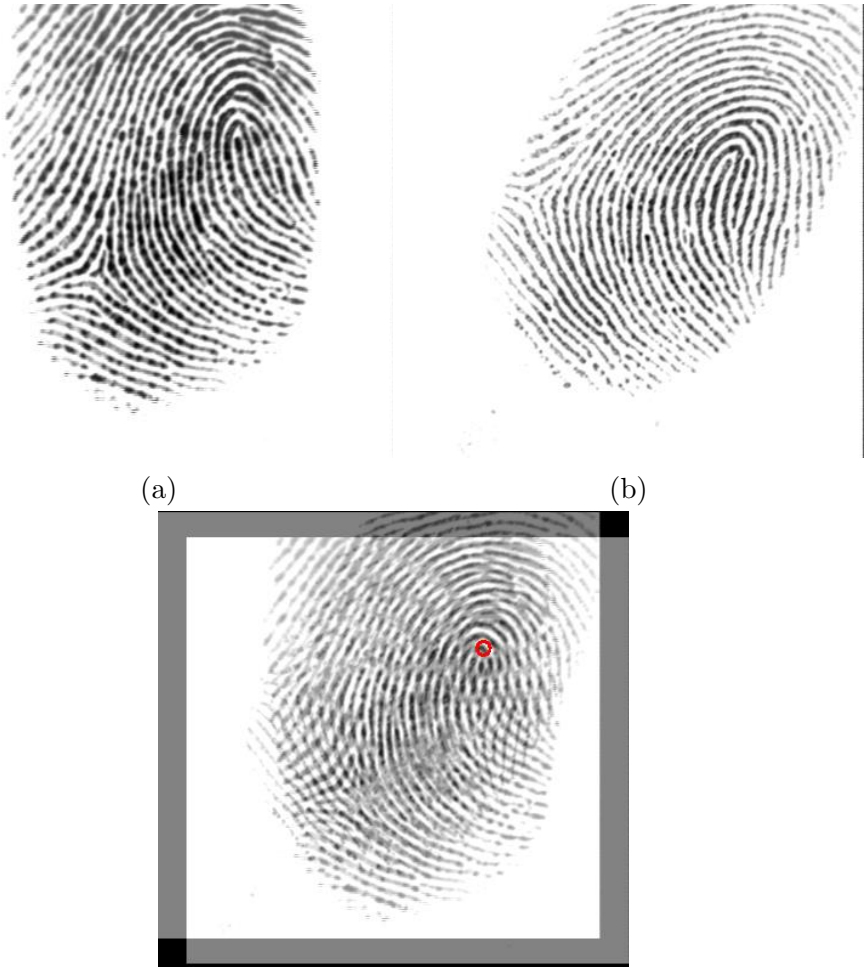

Figure 5.5: Align two fingerprint images using their core points. Though these two images ((a) and (b)) are aligned by their reference points, the rotation angles of these two fingerprints are different as shown in (c). A further alignment needs to be conducted.

In the coarse alignment step, the image of template B will be mapped to the image of template A according to their core point locations. Figure 5.5 shows a sample result after the coarse alignment. Two fingerprint images in this figure are from the same finger (intraclass) with large rotation and displacement between them. From Figure 5.5c, we can see that two fingerprint images are coarsely aligned. However, these two fingerprint impressions are

not placed in the same directions, so some rotations have to be done in the next stage.

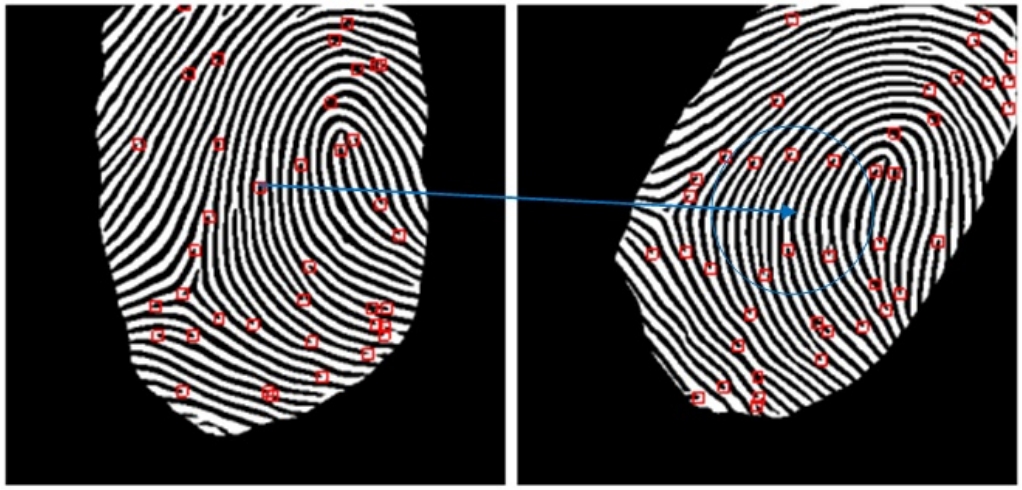

(a) (b)

Figure 5.6: Pairing the minutiae points after the coarse alignment.

After the coarse alignment, a refined alignment is performed based on the minutiae point information. Assume the positions of core points are denoted as C_A:(x_a, y_a) and C_B:(x_b, y_b) from template A and B respectively. Then the shifting amount of positions is $\delta x = x_a - x_b, \delta y = y_a - y_b$. Thus the new minutiae points set M_B of template B could be represented as M'_B $= \{(x_1 + \delta x, y_1 + \delta y),\ (x_2 + \delta x, y_2 + \delta y),...,(x_n + \delta x, y_n + \delta y)\}$ where n is the total number of minutiae points in template B. Then for each minutiae point in template A, several candidate minutiae points could be selected from template B as minutiae pairs. Figure 5.6 shows an example of minutiae pair selections. For a minutiae point m_i in template A, the minutiae points in template B within the radius of a threshold T_r will be listed as the possible minutiae pairs. T_r is a threshold to decide the size of the radius to search the corresponding minutiae pair in template B for each minutiae in template A

as shown in Figure 5.6. This selection is based on the assumption that the fingerprint rotation difference should not exceeds 60 degrees, which is based on the observation of FVC 2002 and 2006 databases. If the minutiae pair with the smallest HD, and the HD value is smaller that a threshold T_{HD}, then this minutiae pair will be selected as the final minutiae pair for rotation and matching. The threshold T_{HD} is used to reject the unreliable minutiae pairs. Then we can obtain an average angle difference of these minutiae pairs which could be used for alignment. Finally we rotate the image B by that average rotation angle (this rotation is not compulsory because the final matching score could be calculated based on the paired minutiae as we will introduce below). Figure 5.7 shows a superimposed image after the alignment of the images in Figure 5.6.

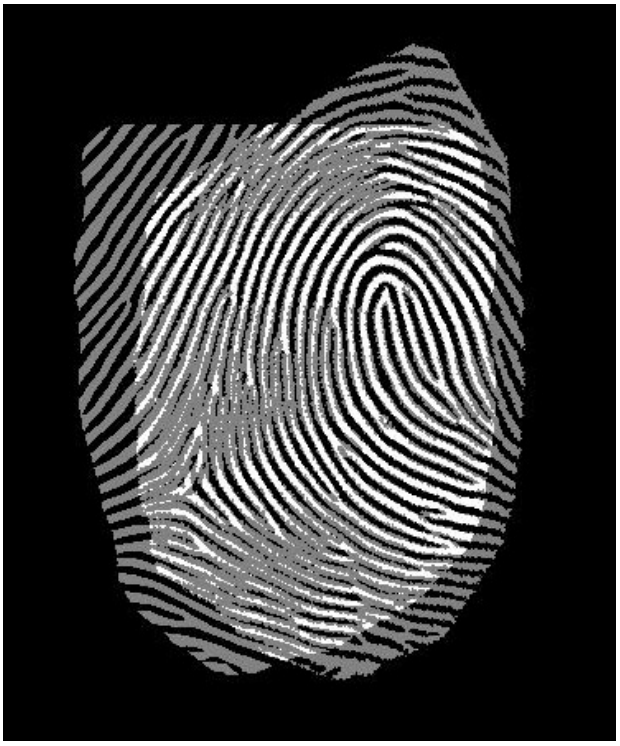

Figure 5.7: Overlapping areas after alignment.

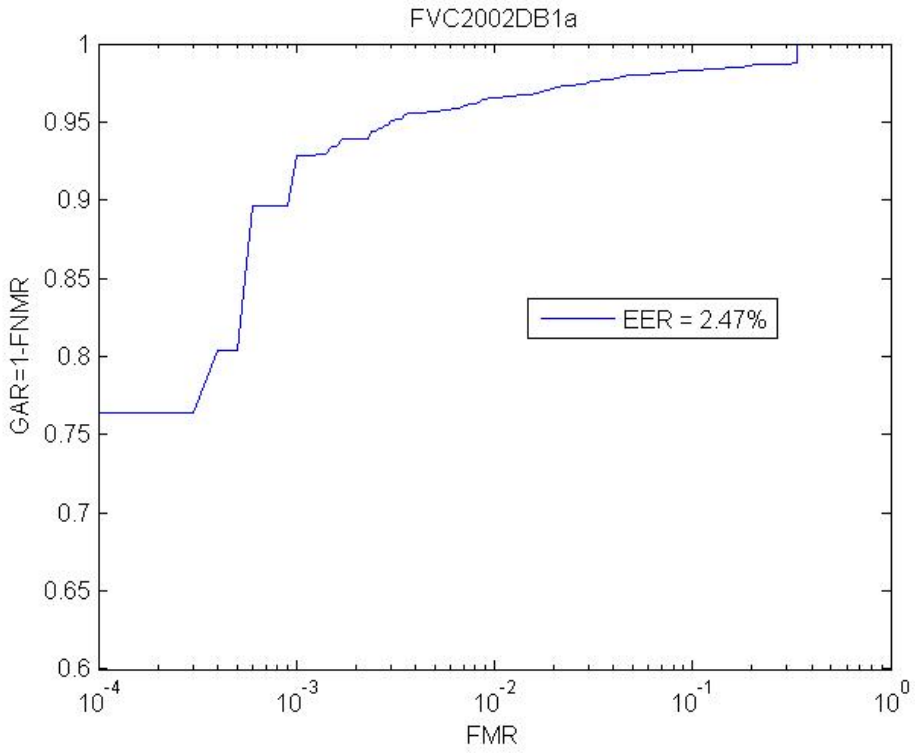

Figure 5.8: Experimental results of FVC2002 DB1a plotted using ROC curve of GAR vs. FMR. (GAR means Genuine Acceptance Rate, GAR = 1-FNMR.

After the minutiae pairing, an overall matching score could be calculated by the equation 5.2. Figure 5.8 shows the receiver operating characteristic (ROC) curve of experiment results of our method. A ROC curve is a graphical plot "which illustrates the performance of a binary classifier system as its discrimination threshold is varied" [Bra97]. ROC curves are widely used in the field of medicine, radiology, biometrics etc. [BD06]. From Figure 5.8, we can see that the equal error rate (EER) of our method is 2.47% for FVC2002 DB1a. EER means the error rate when FMR = FNMR. It indicates the overall performance of a biometric recognition system. The comparison of the matching results with other matching methods is illustrated in Section 5.2.4. For easy comparisons with the other matching method designed in

the following sections, we denote this method as M1.

5.1.3.2 Minutiae pair validation by exploring the minutiae interrelationships

Another global similarity calculation method is based on exploring the interrelationships (include position and direction relationship) among minutiae points. This method uses these minutiae interrelationships to validate the minutiae pairs. Minutiae pairs in Table 5.2 are possible genuine pairs, but the table also contains false pairs. An appropriate minutiae pair validation stage can remove those false pairs. Therefore, validations of minutiae interrelationship are applied to the minutiae pair candidate table. Usually, the angle difference and distance between each two minutiae may be used for validation. Several parameters are defined to evaluate the similarities between minutiae pairs. Table 5.3 shows the parameters and their descriptions. These parameters are generated as per description in Table 5.1. The distance between two minutiae points is calculated by equation 5.4, and the angle between minutiae point (x_i, y_i) and another minutiae point (x_j, y_j) is calculated by the equation 5.5. The values of angle α lie in the range of $[0, 360)$ degrees (or $[0, 2\pi)$).

Table 5.3: Parameters may be used for minutiae validation. The variable K refers to the total number of minutiae pair candidates as shown in Table 5.1

Parameter	Description
$d_{i,j}$	Distance between each two minutiae from the same template according to Table 5.1. $i, j \in \{1...K\}$.
$\Delta\theta_i$	Angle difference of a minutiae pair candidate. It also indicates the possible rotation angle between two enrolled fingerprint images. $\Delta\theta_i = \theta'_i - \theta_i, (i = 1...K)$. It is shown in column $\Delta Angle$ of Table 5.1
$\alpha_{i,j}$	Angle from one minutiae point to another minutiae point. Two minutiae points are from the same template. The angle α calculation refers to equation 5.5

$$d_{i,j} = \sqrt{(x_i - x_j)^2 + (y_i - y_j)^2} \qquad (i, j = 1...K) \tag{5.4}$$

$$\alpha_{i,j} = \begin{cases} atan(-(y_i - y_j)/(x_i - x_j)) & \text{if } x_i >= x_j \text{ and } y_i >= y_j \\ atan(-(y_i - y_j)/(x_i - x_j)) + \pi/2 & \text{if } x_i < x_j \qquad (i, j = 1...K) \\ \pi - atan(-(y_i - y_j)/(x_i - x_j)) & \text{if } x_i > x_j \text{ and } y_i < y_j \end{cases} \tag{5.5}$$

5.1.3.2.1 Minutiae pair validation by distance and angle

One possible method to validate the minutiae pair candidates in Table 5.1 is using the position and direction relationships between each two minutiae pair candidates. Because genuine minutiae pairs are unique (relative posi-

tions and angles), the distances and angle difference between two minutiae points from the same template are constant, if they are from two genuine minutiae pairs. For example, if two genuine minutiae pairs contain minutiae points: (M_i, M_i') and (M_j, M_j') respectively, then we have the distance $d_{i,j} = d_{i',j'}$ and direction angle $\alpha_{i,j} = \alpha_{i',j'}$. Due to non-linear distortions and noise, the distances and direction angles may not be exactly the same in reality. Two thresholds T_d and T_θ need to be assigned to allow for the tolerance in distortions of distances and direction angles respectively (T_d and T_θ are determined by experiment observation, which is introduced in Section 5.2.3). Table 5.4 shows the validation table to determine whether a minutiae pair is valid or not. In this table, i and j refer to the number (No.) of the minutiae pair candidates as shown in Table 5.2 , which means ith and jth rows' minutiae pairs. The variable $\Delta d_{i,j}$ indicates the distance difference between $d_{i,j}$and $d_{i',j'}$. In theory, $\Delta d_{i,j}$ should equal 0, if both ith and jth minutiae pairs are genuine. Because of distortions, this value may have a small range of deviation in the case of genuine pairs. Therefore, one condition to validate the minutiae pairs could be to set a threshold as: $|\Delta d| <= T_d$, which also is shown in equation 5.6. ΔAngle β is the difference in $\Delta\theta_i$ and $\Delta\theta_j$. Because $\Delta\theta$ indicates the rotation angle between two fingerprint images, this value should be constant in theory if any minutiae pair candidate is genuine, and $\Delta\theta_i$ should be equal to $\Delta\theta_j$. In practice, this value may have a small variation due to the non-linear distortions of fingerprint images. Here we get one condition to validate the minutiae pair which is: $|\beta_{i,j}| = |\Delta\theta_i - \Delta\theta_j| <= T_\theta$, which is also shown in equation 5.6. $\alpha_{i,j}$ is the direction angle oriented from one minutiae point m_i to another minutiae point m_j. In theory, the difference of $\alpha_{i,j}$ and $\alpha'_{i,j}$ equals the rotation angle

of images if both ith and jth minutiae pairs are genuine. If we define the ground true rotation angle as R_θ, then the condition $|\beta' - R_\theta| <= T_\theta$ should be fulfilled. However, it is not possible to obtain the value of R_θ unless two fingerprints have been correctly aligned already. But because $\Delta\theta$ is also a variable to indicate the rotation angle between two fingerprints, R_θ should be equal to $\Delta\theta_i$ and $\Delta\theta_j$ in theory, if both ith and jth minutiae pairs are genuine minutiae pairs. Therefore, the condition of $|\beta' - R_\theta| <= T_\theta$ could be replaced as $|\beta'_{i,j} - \Delta\theta_i| <= T_\theta$ and $|\beta'_{i,j} - \Delta\theta_j| <= T_\theta$ in practical for the validation of ith and jth minutiae pairs.

Table 5.4: Generated validation table.

Minutiae pair No.		ΔDistance Δd	$\Delta Angle'$ β'	Δ Angle β	Minutiae from Template A	Minutiae from Template B	Validation
1	2	$d_{1,2} - d_{1',2'}$	$\alpha_{1,2} - \alpha_{1',2'}$	$\Delta\theta_1 - \Delta\theta_2$	(x_1, y_1), (x'_1, y'_1)	(x_2, y_2), (x'_2, y'_2)	$V_{1,2}$
$\vdots$	$\vdots$	$\vdots$	$\vdots$	$\vdots$	$\vdots$	$\vdots$	$\vdots$
i	j	$d_{i,j} - d_{i',j'}$	$\alpha_{i,j} - \alpha_{i',j'}$	$\Delta\theta_i - \Delta\theta_j$	(x_i, y_i), (x'_i, y'_i)	(x_j, y_j), (x'_j, y'_j)	$V_{i,j}$
$\vdots$	$\vdots$	$\vdots$	$\vdots$	$\vdots$	$\vdots$	$\vdots$	$\vdots$
$m-1$	m	$d_{m-1,m} - d_{m-1',m'}$	$\alpha_{m-1,m} - \alpha_{m-1',m'}$	$\Delta\theta_{m-1} - \Delta\theta_m$	(x_{m-1}, y_{m-1}), (x'_{m-1}, y'_{m-1})	(x_m, y_m), (x'_m, y'_m)	$V_{m,m-1}$

$$V_{i,j} = \begin{cases} 1 & if\ |\Delta d_{i,j}| <= T_d\ and\ |\beta_{i,j}| <= T_\theta\ and \\ & |\beta'_{i,j} - \Delta\theta_i| <= T_\theta\ and\ |\beta'_{i,j} - \Delta\theta_j| <= T_\theta \\ 0 & else \end{cases} \tag{5.6}$$

Several iterations (let us say I times) of validation processes are performed to obtain the final minutiae pairs. After validation, a new minutiae pair table is generated. This minutiae pair table is used to compute the global similarity score.

5.1.3.2.2 Matching score calculation after minutiae validation

There are two methods that could be used for matching score calculation. One method uses equation 5.2 which is calculated by the percentage of matched minutiae pair numbers compared to the total minutiae number in template A and B. Another alternative calculation method is to consider the Hamming distance as a variable in the matching score calculating process. This matching score method is shown as follows:

$$MS = (1 - \sum_{i=1}^{n_p} v_i/n_p) * n_p^2/(n_1 * n_2) \tag{5.7}$$

where v is Hamming distance value, and n_p is the number of minutiae pairs. n_1 and n_2 are the number of minutiae in template A and B, respectively.

Figure 5.9 shows the experimental results on the FVC2002 DB1a database. In the figure, we can see that using equation 5.7 is much better than using equation 5.2. It is because equation 5.7 takes into the consideration of the additional texture information in calculation rather than using only minutiae number information. Therefore, it makes the matching results more reliable. The experimental results also indicate that using Hamming

distance to calculate the matching score increases the accuracy of a fingerprint recognition system as compared to the traditional matching score calculation method (equation 5.2).

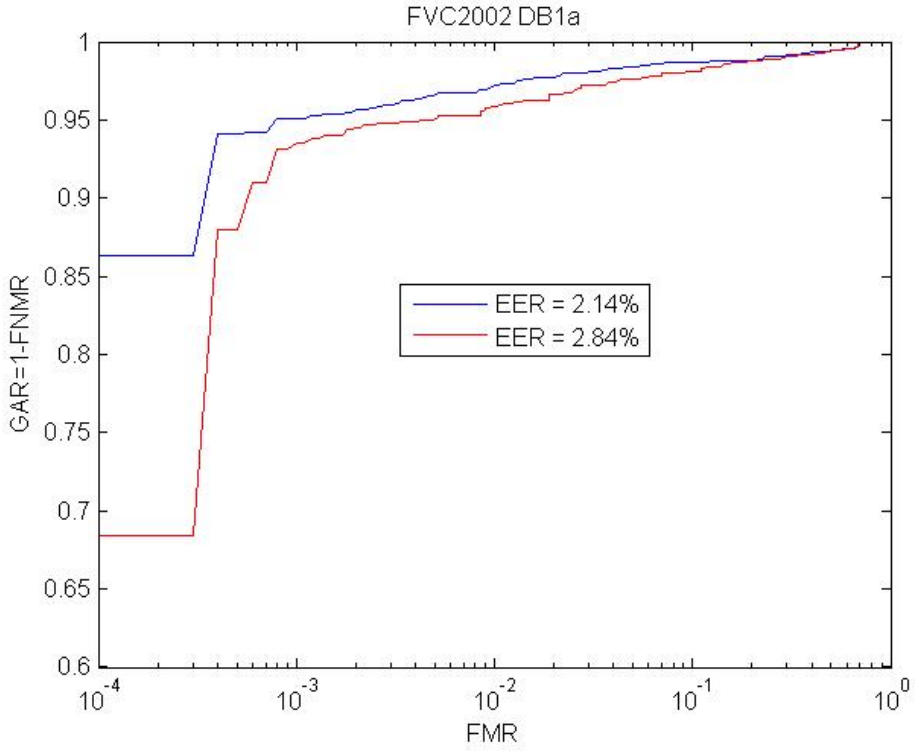

Figure 5.9: The ROC curve of the experimental results of the FVC2002 DB1a database is shown in the figure. The blue curve uses equation 5.7 to calculate the matching scores and the red curve uses equation 5.2. The parameter values are: blocksize for minutiae pairing: 60 x 60; selection of threshold values: $T_d = 15$ pixels and $T_\theta = 15$ degrees.

5.1.4 Use the reliable minutiae pairs for alignment before matching

Another matching score calculation method is to use a reliable pair of minutiae points as a pair of reference points for fingerprint alignment. Then the matching score is calculated based on the alignment. This method is intro-

duced in the following sections.

5.1.4.1 Matching score calculation: based on matched minutiae number

Because the Hamming distance indicates the dissimilarity between two binarized blocks, the lower the HD value is, the higher possibility that a pair of minutiae points is genuine. These minutiae pairs with low HD values may be taken as reference points for alignment.

Alignment based on one minutiae pair can be conducted by setting the minutiae point (x_r, y_r) in the first template as a reference point. Based on this reference point, adequate rotation and shifting are performed to its paired minutiae point (x'_r, y'_r) in the second template to make two points overlapped ($(x'_r, y'_r) \longrightarrow (x_r, y_r)$). Finally, all other minutiae points in the second template are rotated and shifted by the same amount. The equations 5.8 and 5.9 show the shifting and rotating for a minutiae point (x'_i, y'_i) in template B. After alignment, if the differences of distance and angle for two minutiae points are in the range of $[0, T_d]$ and $[0, T_\theta]$, respectively, then these two minutiae are picked up as a pair. Then the equation 5.2 (the traditional matching score calculation method introduced in Section 5.1.3) is used to calculate the matching score.

$$\begin{aligned} x'_i &= x'_i + x_r - x'_r \\ y'_i &= y'_i + y_r - y'_r \end{aligned} \tag{5.8}$$

where (x'_i, y'_i) is a minutiae point in template B, and (x_r, y_r) and (x'_r, y'_r) are a pair of reference points.

$$(x_i', y_i') = [x_i', y_i'] * \begin{bmatrix} cos(\Delta\theta_r) & sin(\Delta\theta_r); \\ -sin(\Delta\theta_r) & cos(\Delta\theta_r) \end{bmatrix} \tag{5.9}$$

where $\Delta\theta_r$ is the rotation angle between two reference points.

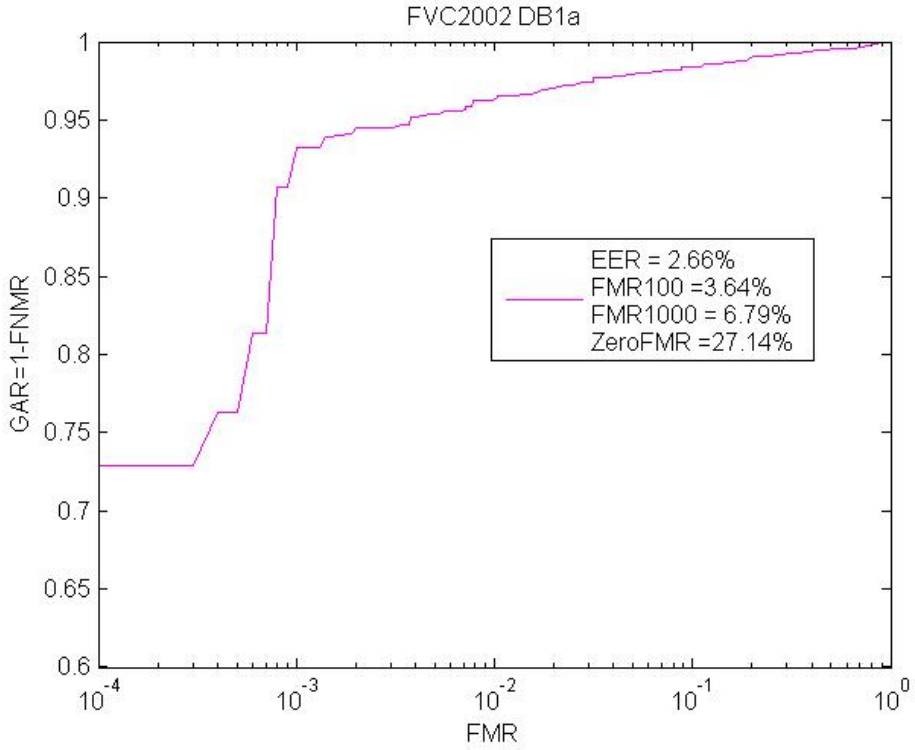

Figure 5.10: FVC2002 DB1a results using the above matching score calculation method ROC curve. This curve shows the result of using the top three minutiae pairs with lowest Hamming distance value for alignment, then the matching score is calculated afterwards using equation 5.2. The parameter values are: blocksize for minutiae pairing: 60 x 60; threshold of distance: $T_d = 15$ pixels and threshold of angle: $T_\theta = 15$ degrees.

Figure 5.10 shows the result of using the top three minutiae pairs with lowest Hamming distance values for alignment. Then the final matching score chooses the highest matching score among three comparisons. The matching score calculation uses the equation 5.2.

5.1.4.2 Matching score calculation: based on matched minutiae number and block similarity

Alternatively, Hamming distance is another way to evaluate the matching similarity. Equation 5.10 shows the calculation of the matching score by using the Hamming distance and paired minutiae numbers. Figure 5.11 shows the ROC curve of FVC2002 DB1a results using the equation 5.7 to calculate the matching scores. Compared to Figure 5.10, the performance of using minutiae blocks is much better than using the traditional matching score calculation method in equation 5.2.

$$MS = (1 - (\sum_{i=1}^{n_p} v_i)/n_p) * n_p^2/(n_1 * n_2) \tag{5.10}$$

where v denotes the Hamming distance value, n_p is the number of paired minutiae, and n_1 and n_2 are the number of minutiae from two enrolled templates respectively.

Figure 5.11 shows the ROC curve of the results of FVC2002 DB1a using the above matching method. The selected parameter values are the same as Figure 5.10. Comparing Figure 5.10 and 5.11, we can see using Hamming distance to calculate the matching score is superior to the method using minutiae numbers for calculation. The EER is improved from 2.66% to 2.05%, which means the overall accuracy is increased. Besides, ZeroFMR is improved from 27.14% to 7.00%. ZeroFMR is a metric to indicate whether a biometric recognition system is suitable for high security applications [SB11]. The decrease of ZeroFMR indicates that using HD for the matching score calculation is more suitable than using the traditional minutiae number based matching score calculation for high security applications.

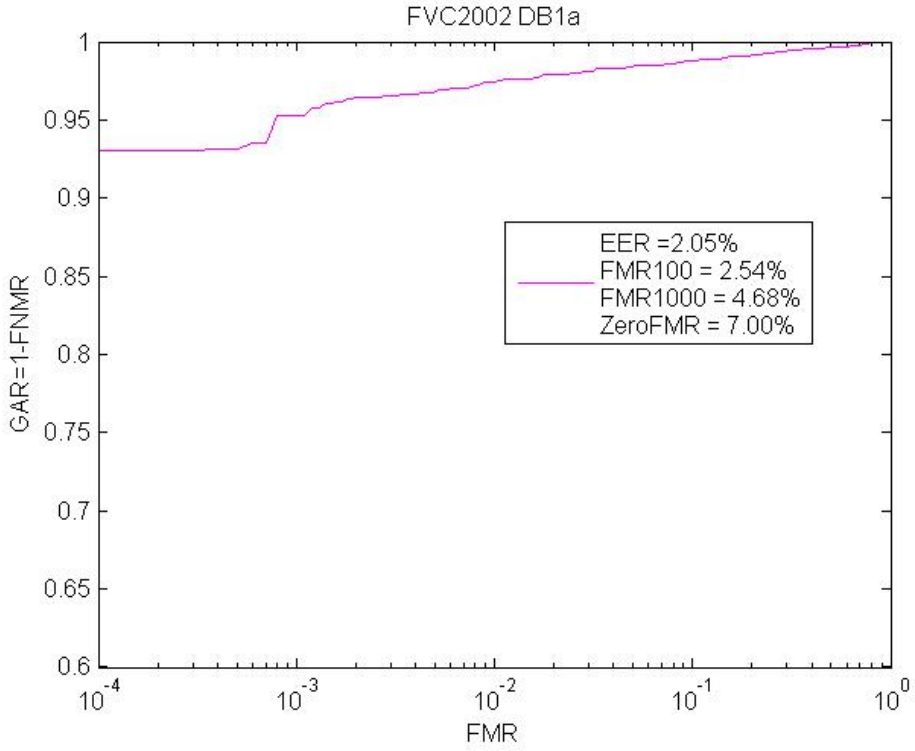

Figure 5.11: The ROC curve of FVC2002 DB1a results using the above matching score calculation method. This curve shows the result of using the top three minutiae pairs with the lowest Hamming distance value for alignment, then the matching score is calculated afterwards. The parameter values are: blocksize for minutiae pairing: 60*60; blocksize for matching: 60*60; threshold of distance: $T_d = 15$ pixels and threshold of angle: $T_\theta = 15$ degrees.

The advantage of choosing the highest matching score as the final matching score is that only one genuine minutiae pair is needed among the N most reliable minutiae pairs to obtain a high matching score for intra-class matching. This method is denoted as M3 for the purpose of comparisons of experimental results.

5.1.4.3 Using average matching score of N times' alignments

The previous global similarity calculation method uses N most reliable minutiae pairs for alignment, then the alignment with the highest matching score is chosen as the final one. This matching method is reasonable, because for a pair of intra-class fingerprint templates, it is highly likely to have one or more genuine minutiae pairs among minutiae pairs with the lowest HD values. For example, Cappelli et al. [CFM10] use the average matching score of the top n (they choose 10) most similar minutiae cylinder pairs as the final matching score.

Alternatively, we try to use the average matching score of each alignment by using the top N most similar minutiae pairs. Figure 5.12 shows the ROC curves of matching results using the average matching score instead of choosing the highest matching score. The EER values are improved in both cases of using equation 5.2 and 5.7 for matching score calculations. The ZeroFMR and FMR1000 of the minutiae pair number based (equation 5.2) method are significantly improved, which are from 27.14% to 6.54% and 6.79% to 4.5 % respectively. In the case of the Hamming distance based method (equation 5.7), though the ZeroFMR and FMR100 is slightly increased, the EER is significantly decreased from 2.05% to 1.76%. This method is denoted as M4 for the purpose of comparisons of experimental results. The difference between M4 and M3 is that M3 only needs one genuine minutiae pair in the N pairs of minutiae used as reference points to obtain a high matching score, but M4 needs the majority of the N pairs of minutiae to be genuine ones to obtain a high matching score. Therefore, M4 eliminates the cases in which some inter-class matching is falsely considered

as matched fingerprints due to the occasionally high matching score by one pair of reference points. Based on the experimental observation, we found that most of these occasional cases happen when both the register template and query template only have a small number of minutiae (e.g. partial fingerprint). Therefore, using the average matching score of N times alignment is more reliable than choosing the highest matching score among N times alignment.

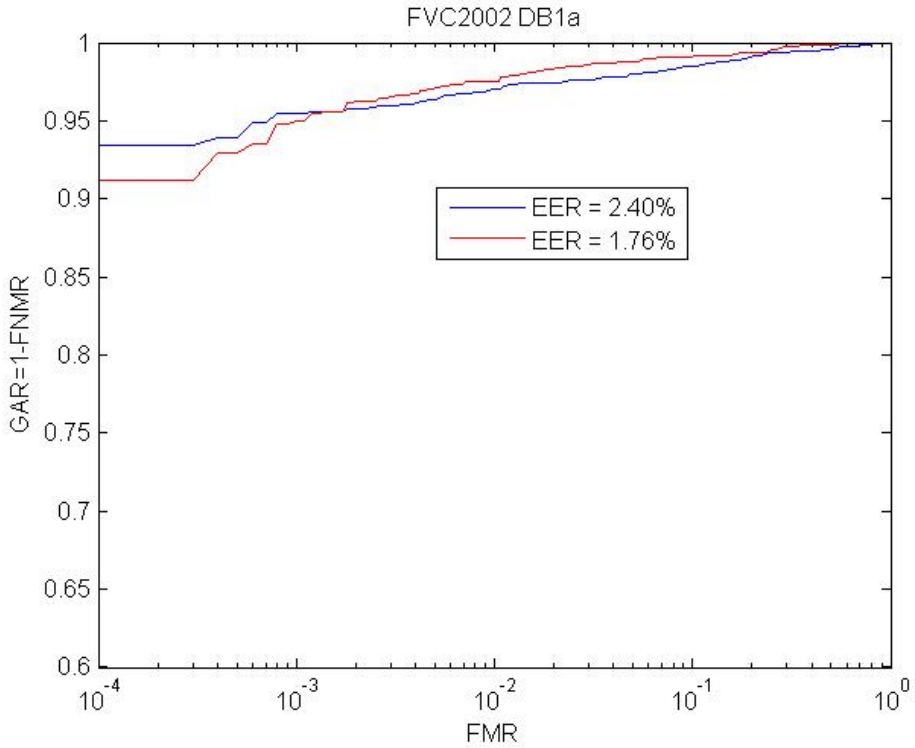

Figure 5.12: Using the average matching score after the alignment using the five (N=5) most reliable minutiae pairs. The blue and red curves use equations 5.2 and 5.7 to calculating the matching score respectively.

In summary, these four global similarity calculation methods are based on the new metric BMB. The accuracy of the fingerprint matching score is highly depended on the reliability of the new metric BMB. The BMB utilizes the texture information surrounding the minutiae points as well as minutiae

information. Thus, more information has been taken into consideration in fingerprint matching compared to other minutiae based (no texture information) and correlation based (no minutiae information) matching methods. Figure 5.13 shows the procedure of the matching process of using BMB for matching. The next section will examine these four global similarity calculation methods by conducting experiments on FVC databases. The experimental results may also indicate the reliability and accuracy of using the new matching metric BMB.

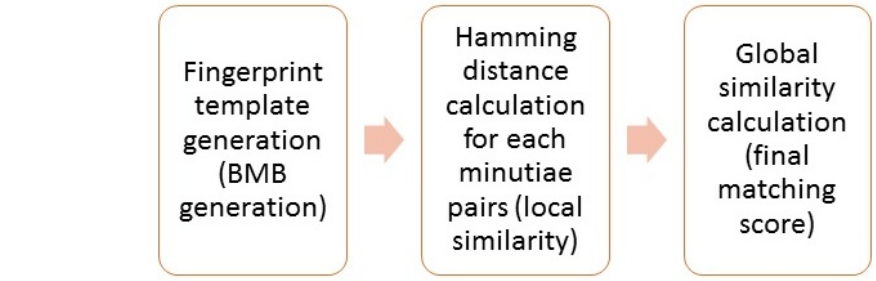

(a)

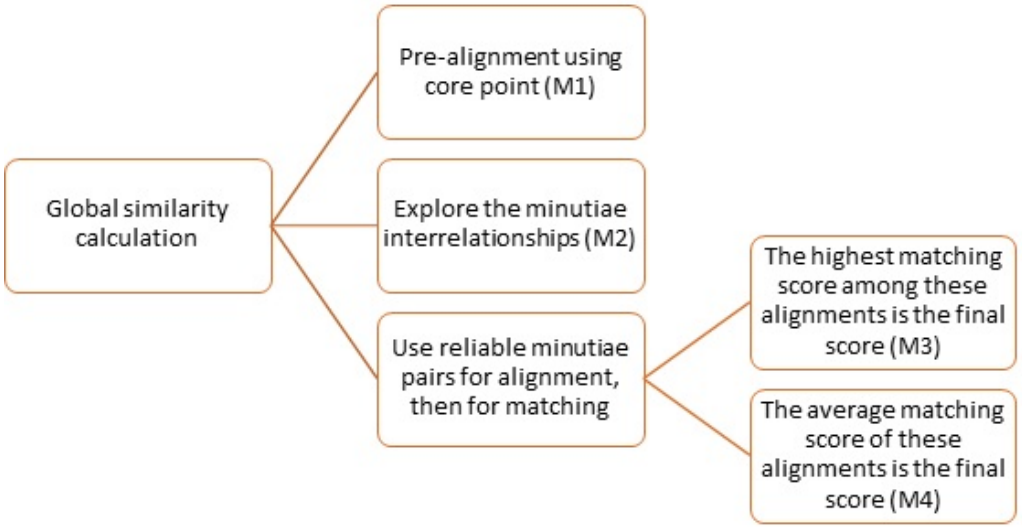

(b)

Figure 5.13: (a), flowchart of the matching process of this method. (b), four global similarity score calculation methods

5.2 Experiments

This section introduces the experiments conducted to evaluate the proposed matching methods. The fingerprint matching system is first designed and implemented. Then the experimental environment and matching protocols are introduced. Subsequently, the optimized parameters' values are selected for this matching method.

5.2.1 Fingerprint matching procedure

A typical fingerprint verification procedure has been introduced in Chapter 1. The matching procedure we designed for experiments has used the algorithms we designed in previous chapters including image pre-processing and core point detection. Besides, it also uses other fingerprint recognition techniques to compose a simple fingerprint verification system, including local ridge orientation and frequency estimation, contextual filtering (Gabor filtering) technique and run-lenth minutiae detection techniques. The following flowchart shows the matching process:

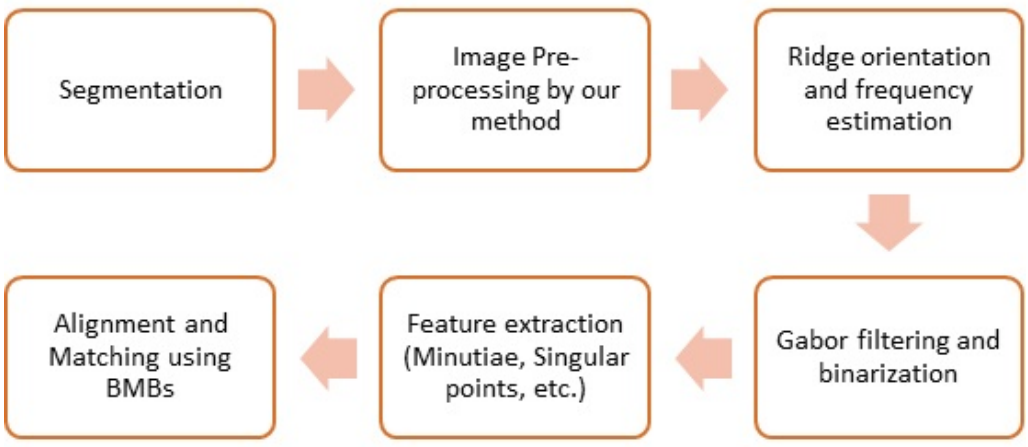

Figure 5.14: The implemented fingerprint matching procedure.

5.2.2 Experimental environment and matching protocols

All the fingerprint recognition techniques are implemented in the Matlab R2013a platform running on a computer with an Intel CPU of core duo 3.33 GHz.

FVC 2002 DB1a, DB2a and FVC2006 DB2a are used to evaluate the designed matching metric. The image acquisition conditions were the same for each database, which are: interleaved acquisition of different fingers to maximize differences in finger placement, no care was taken in assuring a minimum quality of the fingerprints and the sensors were not periodically cleaned. During some sessions, individuals were asked to: a) exaggerate displacement or rotation or, b) dry or moisten their fingers [AFF09]. Therefore, the fingerprint images in these databases contain plenty of variations and noise, which means that they are specially suitable for the evaluations of fingerprint recognition algorithms.

The matching protocol uses the FVC standard. For FVC2002 databases, one database contains 100 groups of fingerprint images. Each group has eight fingerprint impressions from the same finger. There are $C_8^2 * 100 = 2800$ comparisons for intra-class matching. And for inter-class matching, the first image of each group is used for matching. The total number of inter-class matching is $C_{100}^2 = 4950$. Besides the FVC2002 databases, FVC2006 DB2a is also used for experiments. This database contains 140*12 images. Thus the total number of comparisons for intra and inter-class is $C_{12}^2 * 140 = 9240$ and $C_{140}^2 = 9730$ respectively.

5.2.3 Parameter selections

There are four parameters used in our matching methods. Table 5.5 shows the parameter value selections. The selected values are based on the experimental observation and analysis of FVC2002 DB1a.

Table 5.5: Parameter value selections.

Parameters	Value	Descriptions
T_r	60	Threshold of the radius of a minutiae point for the selection of minutiae pairs in the first global similarity calculation method.
T_{HD}	0.35	Threshold of the Hamming distance for the selection of minutiae pairs in the first global similarity calculation method.
T_d	15	Threshold of the difference of spatial distances used in equation 5.6.
T_θ	15	Threshold of the difference directions between any two minutiae points or core point and a minutiae point.
I	5	Times of iterations to validate the minutiae pairs.
N	5	Numbers of minutiae pairs selected for alignment.
s	60	Length of chosen minutiae blocks for minutiae pair generation and matching score calculations. The size of the blocks is s x s.

5.2.3.1 The influence of chosen block size

Because the minutiae blocks are used to evaluate the similarity of minutiae pairs, the size of minutiae blocks is an important factor that affects the global similarities. Thus, we use the FVC2002 DB1a as the experiment database to investigate the influence of the chosen block size. Figure 5.15 shows the experimental results of FVC2002 DB1a using different sizes of blocks. The result shows that using block size of 60 x 60 pixels achieves best EER.

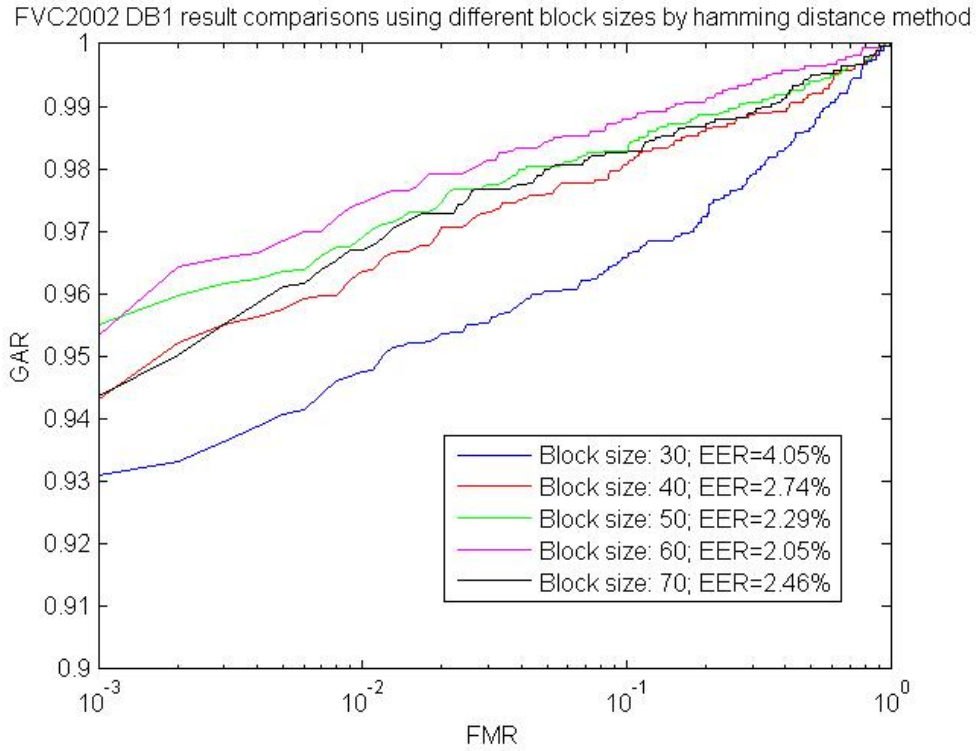

Figure 5.15: The result comparisons using different block sizes for minutiae pair candidate generation using method M3. FVC2002 DB1a database is used for this experiment.

5.2.4 Experimental results and comparisons

We uses FVC2002 DB1a, DB2a and FVC2006 DB2a as the testing databases. EER is the major metric to evaluate the overall performance in this experiment. The experiments include intra-class and inter-class tests. The intra-class test is used to examine the match rate of a pair of fingerprint templates from the same finger. The inter-class test is used to examine the non-match rate of a pair fingerprint templates from different fingers. False non-match rate (FNMR) is a metric to measure the intra-class test (FNMR = 1 - GAR, GAR means Genuine Acceptance rate), while false match rate (FMR) is to measure the inter-class test. Table 5.6 shows the experimental results of our methods as well as other reported matching methods using ROC curves of GAR vs. FMR.

Table 5.6: Comparisons with other reported matching results.

Methods (EER)	FVC2002 DB1a	FVC2002 DB2a	FVC2006 DB2a
Belguechi et al. [BCRAA13]	1.91%	4.56%	-
Benhammadi et al. [BAH+07]	4.27%	2.61%	-
Gao et al. [GYZZ11]	3.5%	3.9%	-
Lumini and Nanni [LN06]	4.2%	3.9%	
Wahby Shalaby and Ahmad [WSOA13]	2.57%	-	-
Choi et al. [CCK11]	1.8%	0.8%	-
Cappelli et al. [CFM10]	-	-	0.15%, 0.73%, 1.04%, 1.21% and 2.98% on the 5 best minutiae extractors from FVC2006
M1:pre-alignment	2.47%	4.23%	2.65%
M2:interrelationships	2.14%	2.49%	3.02%
M3:by eq.5.7	2.05%	2.24%	1.88%
M4:by eq.5.2	2.40%	3.06%	2.89%
M4:by eq.5.7	1.76%	2.13%	1.81%

where M1: Proposed pre-alignment based method; M2: Proposed minutiae block matching method with minutiae pair validation using minutiae interrelationships; M3: Using N minutiae pairs with the lowest Hamming distance for fingerprint alignment before matching. The final matching score selects the highest matching score among the N alignments. The matching calculation uses equation 5.7; M4: Using N minutiae pairs with lowest Hamming distance for fingerprint alignment before matching, the final matching score is the average score of N times alignment.

From Table 5.6, we can see that our methods obtains better experimental result than most of the state-of-the-art matching methods (e.g. [BCRAA13, BAH+07, GYZZ11, LN06]). Feng et. al [FZ11] has reported that the minutiae cylinder code (MCC) method developed by Cappelli et al. [CFM10] is one of the best matching methods so far in their investigation. Cappelli et al. [CFM10] reported that their method achieves 0.15%, 0.73%, 1.04%, 1.21% and 2.98% using the *five best minutiae extractors* in the FVC2006 campaign respectively. Among these five minutiae extractors, four are from commercial developers and one is anonymous developer. Our methods M1, M3 and M4 in the Table obtain 2.65%, 1.88% and 1.81% respectively, which are better than the result using the fifth best extractor from FVC2006 with MCC. Besides, the method M4 using equation 5.7 obtains 1.76% on FVC2002 DB1a which is the best in the table. Figure 5.16, 5.17 and 5.18 shows the results of our methods on FVC2002 DB1a, FVC2002 DB2a and FVC2006 DB2a respectively. From the figures, we can see that M2 which uses minutiae interrelationships are not performed as well as M3 and M4 which uses Hamming distance and top N minutiae pairs' alignment. But it is better than the core based method (M1) and top

N minutiae pairs' alignment without using Hamming distance (M3). Besides, by comparing the experimental results using the equations 5.2 and 5.7 in method M4, we can see that using Hamming distance as a parameter to calculate the matching score obtains better matching results than only using the paired minutiae number percentage as the matching score. The average matching accuracy is improved by 46% when using Hamming distance for the matching score calculation. This is because texture information surrounding minutiae points have contributed to the final matching score calculations. Briefly, the experimental results suggest that the binarized minutiae block is an alternative reliable feature for fingerprint matching.

In the efficiency aspect, the running speed of our methods are on average less than 1, 0.6, 0.5, 0.2 and 0.5 seconds per matching on the MATLAB 2013a platform, respectively, for method M1, M2, M3 by equation 5.7, M4 by equation 5.2 and M4 by equation 5.7. The processing time for template generation and minutiae pair calculation (in Section 5.1.1 and 5.1.2) is on an average less than 0.1 and 0.4 seconds per processing. The fastest method is M3 and M4 using equation 5.2 which does not require Hamming distance comparisons. The second fastest is M3 and M4 using equation 5.7 followed by M2. Because M2 validates the minutiae iteratively by using the minutiae interrelationships, it is not as fast as M3 and M4. The slowest method is using the pre-alignment method, however, this running time contains the alignment and matching stages.

Anyway, the matching accuracy is not only based on the matching algorithms but also on the feature extractors. Good feature extractors normally include a procedure of quality analysis on the extracted features, which has not been implemented in our system. For example, Cappelli et al.'s results

on FVC2006 DB2a vary in different minutiae extractors. Therefore, investigations on reliable feature extractors are necessary in our future work.

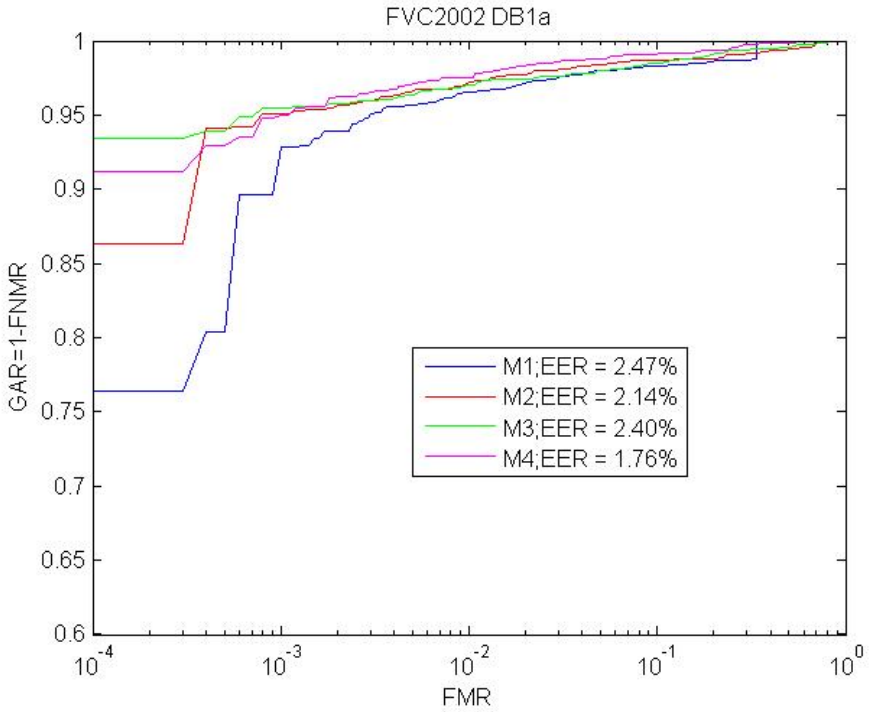

Figure 5.16: Experimental results performed on FVC2002 DB1a database using the above four methods.

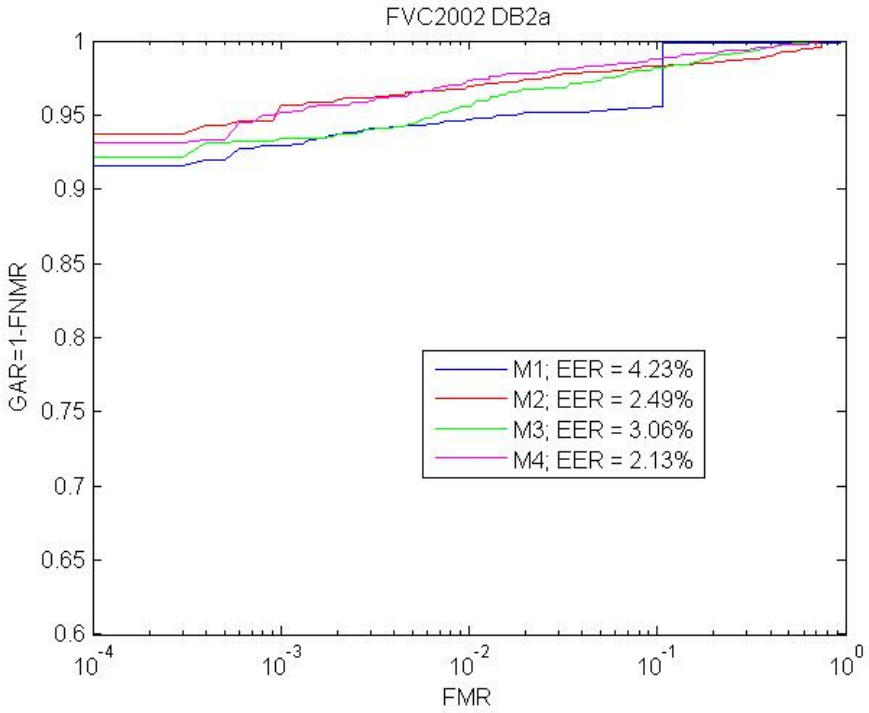

Figure 5.17: Experimental results performed on FVC2002 DB2a database using the above four methods.

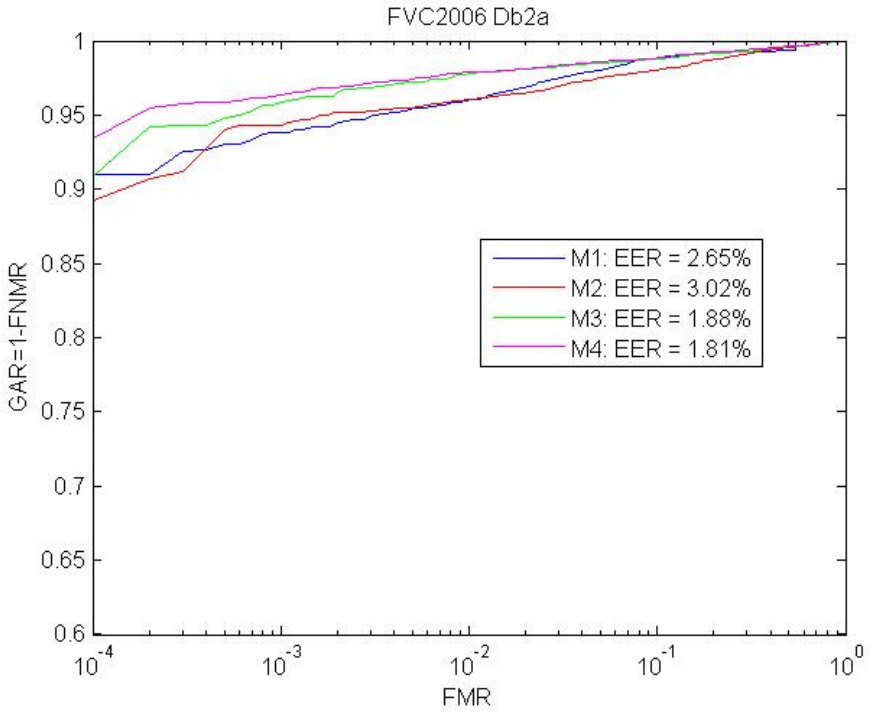

Figure 5.18: Experimental results performed on FVC2006 DB2a database using the above four methods.

5.2.4.1 Analysis of decidability index of using BMB

The decidability index d' is one measure of how well the two distributions (distributions of intra-class and inter-class matching scores) are separated. [Dau04]. The matching errors are caused due to the overlap of the distributions of inter-class and intra-class matching scores. It has been used for performance evaluation for biometric technologies. If their two means are μ_1 and μ_2, and their standard deviations (std) are δ_1 and δ_2, then the decidability index d' is defined as:

$$d' = \frac{|\mu_1 - \mu_2|}{\sqrt{\delta_1^2 + \delta_2^2}} \tag{5.11}$$

The decidability index d' evaluate the how different between intra-class and inter-class matching scores. If the decidability index d' is low, then the distributions of intra-class and inter-class matching scores may close to each other and cause more overlaps. In particular, given a matching score, the decidability index indicates the confidence level that we can determine it belongs to an inter-class comparison or an intra-class comparison. Therefore, it indicates the reliability of the recognition technologies as well.

Very limited research has been done for using decidability index to evaluate the fingerprint recognition techniques, the only research work could be found by the author is Park et al.'s work [PLP03], which uses decidability index to evaluate their matching method. Compared to the Jain et al.'s [JPHP00] method, the decidability index of their matching method is increased from 2.67 to 2.85. In our perception, one major reason that decidability index is not popular in fingerprint recognition is that decidability index is relatively low for fingerprint recognition compared to iris recogni-

tion (the decidability index is in the range of 7 to 14 for iris [Dau04]), and the decidability index may not distinguish among different matching techniques. Besides, the matching accuracy is the major concern in fingerprint recognition, thus improving the matching accuracy is more important to increase the decidability index.

In this work, we use the decidability index to evaluate the reliability of BMB by comparing the obtained decidability index between the matching score calculation methods using HD (equation 5.7) and traditional minutiae based calculation (5.2). Figure 5.19 shows the distributions of matching scores for inter-class and intra-class comparisons for FVC 2002 DB1a using matching method M2 (the ROC curve of the matching results is shown in Figure 5.9). Figure 5.19a shows the matching score distributions using equation 5.2, which is based on the percentage of paired minutiae numbers for matching score calculation. Figure 5.19b shows the matching score distribution using equation 5.7, which incorporates the HD into the final matching score calculation. The decidability index of Figure 5.19a and 5.19b is $d' = 3.13$ and $d' = 4.46$, respectively. We can see that using HD in the final matching score calculation (equation 5.7) obtains much higher decidability index than the traditional matching score calculation method (equation 5.2). Therefore, using HD for matching is a more reliable way than traditional minutiae based matching score calculation, which also indicates that BMB is a reliable metric for fingerprint matching.

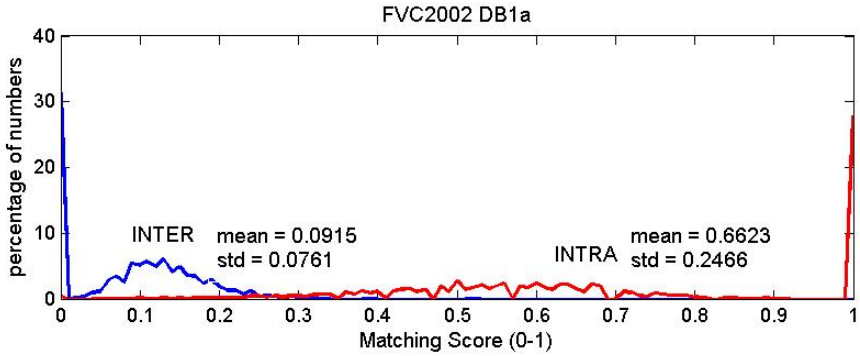

(a) Using equation 5.2 for matching score calculation, which does not use HD.

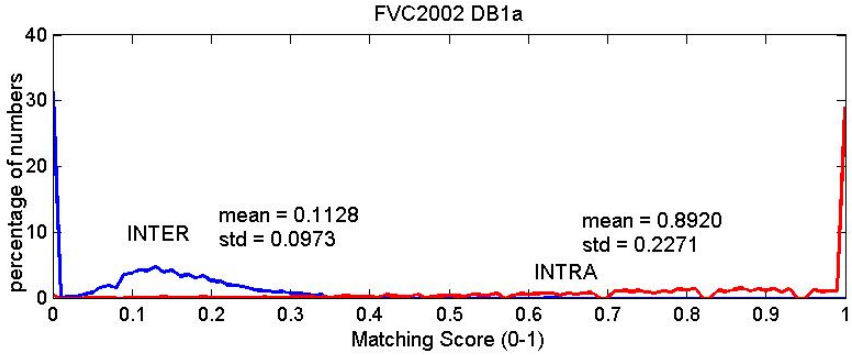

(b) Using equation 5.7 for matching score calculation, which incorporates HD in the matching score calculation.

Figure 5.19: Distribution of matching score of FVC 2002 DB1a dataset using global similarity calculation method M2. The decidability index of (a) and (b) is 3.13 and 4.46. respectively.

In conclusion, the advantages of this matching approach could be summarized as follows:

- The metric BMB not only contains minutiae information (location and direction), but also the texture information. Thus, more information has been taken into consideration in fingerprint matching compared to other minutiae based (no texture information) and correlation based (no minutiae information) matching methods.

- The local similarity calculation of a minutiae pair is straightforward, which is based on the HD value between two BMBs. HD uses XOR operation which is fast and can be performed in one CPU cycle.

- High tolerance to missing and spurious minutiae. In M3 and M4, only one and N genuine minutiae pair are needed to obtain a high matching score, respectively. Besides, spurious minutiae is not probable to obtain low HD values during the comparison of BMBs. Thus, the problem of missing and spurious minutiae is well addressed.

- High tolerance to non-linear distortion. Unlike correlation based methods, only surrounding texture information of minutiae points is used for matching rather than using the texture information of a whole fingerprint. Thus, the tolerance to non-linear distortion of this method is as high as other minutiae based methods, which are much higher than correlation based methods.

- The reliability of BMB is high as shown in the experimental results (the matching results and the decidability index). The matching results are better than most reported matching methods. BMB is able to reduce the possibility that a pair of inter-class fingerprints is falsely matched as a pair of intra-class fingerprints, because the comparisons of BMBs between a pair of inter-class fingerprints could not obtain low HD values as intra-class fingerprints do.

5.3 Conclusions

In this chapter, we have proposed a new matching metric named binarized minutiae block (BMB) for fingerprint matching. Furthermore, four different global similarity calculation methods have been proposed to evaluate this new metric. The first method is based on pre-alignment using core points as reference points and binarized minutiae blocks (denoted as M1). The coarse alignment uses the detected reference points to shift the query fingerprint image. Then a refined alignment stage is performed uses the binarized minutiae blocks. The matching results of this method is better than many other reported methods shown in Table 5.6. The second one (denoted as M2) explores the interrelationships between minutiae points. The third one (denoted as M3) uses the top N minutiae pairs with the lowest Hamming distance for fingerprint alignment. Then N matching scores are calculated using minutiae based calculation equation 5.7. The highest matching score is selected as the final matching score. The last one (denoted as M4) is similar with the third one, but it uses the average matching score of N times of alignments. The results show that all the above methods have achieved decent overall accuracies (EER) comparing to other reported matching methods. The last method obtains the best results compared with the other three methods. The experimental results of M4 show that this method achieves overall matching accuracy of 98.24%, 97.87% and 98.19% on the datasets FVC2002 DB1a, DB2a and FVC2006 DB2a. Besides, our designed fingerprint matching system using M3 and M4 matching methods obtain better results than the system using the fifth best minutiae extractor in the FVC2006 campaign and MCC [CFM10] matching method. The ex-

perimental results also suggest that it is superior than most state-of-the-art matching methods (e.g. methods in [WSOA13, LN06, GYZZ11, WSOA13]) in terms of matching accuracy.

In conclusion, this chapter addresses our third research objective which aims to design a reliable and accurate fingerprint matching method. The next chapter is the conclusion of the whole thesis and possible future work.

Chapter 6

Conclusion

In this thesis, extensive research has been conducted to investigate carious techniques of fingerprint recognition to improve the matching accuracy of a fingerprint recognition system. In particular, the main focus of this research has been in the areas of image pre-processing, singular point detection, fingerprint matching. Experimental results are provided for each designed methods as well as the comparisons with other reported results have been presented. Furthermore, a simple fingerprint recognition system is designed using the developed methods to evaluate the overall matching accuracy. The result shows that our system is superior to most of recent fingerprint recognition systems with respect to overall matching accuracy.

In the following sections, the research contributions and future work are summarized.

6.1 Research Contributions

In this thesis, a remarkable effort has been done to improve the matching accuracy and to design a reliable fingerprint recognition system. The major research contributions are summarized as follows:

- A fingerprint image pre-processing method, which is able to improve the clarity of ridge and valley structures in a fingerprint image. This proposed image pre-processing algorithm is designed based on the contrast stretching and power law transformation techniques, which are able to improve the contrast and brightness of an image, respectively. This method is an alternative choice for fingerprint image normalization. Besides, it is able to improve the image contrast as well as to remove noise and unnecessary information, such as valueless ridges, which often exist on wet/smudged fingerprints. The experimental result shows that the goodness index (GI) is higher when this method is applied than using other image pre-processing methods. The GI value is improved by around 14% than other reported methods. The experimental results also indicate that removing adequate noise in image pre-processing stage enables the subsequent image processing stage (Gabor filtering) to have a better enhancement result, which ultimately improves the performance of feature extraction and matching. This method contributes to the feature extraction part of a fingerprint recognition system.

- A post-processing method for Poincaré Index based singular point detection approach. The singular point detection techniques are useful for fingerprint alignment and classification which are important

components in a fingerprint identification system. This method uses Poincaré Index technique to detect the singular points. In order to address the problem of spurious singular points, singular point validation rules are developed and applied to remove spurious singular points. The genuine detection rate of singular points on FVC 2002 databases is 89.42% which is superior to other Poincaré Index based methods.

- A singular point detection method based on the analysis of fingerprint local ridge orientation field. This method initially separates the local ridge orientation map into four segments according to their orientation values. Then a singular point detection method with designed rules are used to validate and select possible genuine singular points. The result shows that the genuine detection rate of singular points on FVC 2002 databases is 94.05% which is higher than other reported methods. Furthermore, we extended this approach to arch type fingerprints. Thus, it is possible to locate a reference point for an arch fingerprint which can be used for fingerprint alignment or/and fingerprint classification to enhance the speed of fingerprint identification.

- A new matching metric named binarized minutiae blocks (BMB) is proposed for fingerprint matching. This new matching metric a binarized fingerprint image block with a minutiae point in the center. In this method, the binazried minutiae blocks are aligned to make the central minutiae at a fixed direction (make the minutiae angles at 0 degrees in our case). Then the local minutiae similarity is simply generated by comparing the Hamming distances of these minutiae blocks.

Besides, four different global similarity score calculation methods are designed to calculate the final matching score and evaluate this proposed matching metric. The first method uses pre-alignment using SPs as reference points. The second method uses minutiae interrelationships to validate the minutiae pairs, then the matching score is computed by using Hamming distance and number of matched minutiae pairs. The second one explores the interrelationships between minutiae points to validate the minutiae pair candidates. The third one uses the top N minutiae pairs with the lowest Hamming distance for fingerprint alignment. Then the matching score is calculated by selecting the highest matching score among the N times alignments. The last one is similar with third one, but it select the average matching score of N. The results shows that all the above methods achieve high overall accuracies (EER) comparing to other reported methods. The last method obtains the best result comparing the other three methods, which achieves EER of 1.76%, 2.13% and 1.81% on the datasets FVC2002 DB1a, DB2a and FVC2006 DB2a. Besides, our designed fingerprint matching system using the last two matching score calculation methods is able to obtain better results than the system using the fifth best minutiae extractor in FVC2006 campaign with minutiae clinder code (MCC) [CFM10] matching method. As a consequence, the results suggest that using binarized minutiae blocks is an alternative way to obtain accurate and reliable matching results other than correlation based (grey scale texture information), minutiae based and other non-minutiae based methods. The experimental results also indicate that the designed fingerprint matching system is

superior to most of the state-of-the-art fingerprint recognition systems. This new matching metric is contributed to fingerprint matching part of a fingerprint recognition system.

6.2 Future works

Future work includes investigating current fingerprint feature quality analysis techniques in order to improve the feature extraction reliability of our system, template protection, fingerprint authentication system design and implementation. The future work could be summarized as follows:

- Fingerprint feature quality analysis. Fingerprint quality analysis is able to remove unreliable features (e.g. minutiae, ridges etc.). The feature extractor implemented in our matching system is not as good as other state-of-the-art methods especially on the contextual filtering and minutiae extractor parts. Implementing new techniques may improve the overall performance of this fingerprint matching system.

- Fingerprint template protection. This is an important aspect in a fingerprint recognition system which is used to prevent compromises of fingerprint templates. Choosing and/or designing suitable template protection techniques for our designed fingerprint templates are necessary.

- Fingerprint authentication system design and implementation. We have implemented the core parts of a fingerprint authentication system. However, there are still some work should be done such as design of the authentication protocols and database protection techniques.

- Automated latent fingerprint recognition. Latent fingerprint recognition is a new area in fingerprint recognition. Latent fingerprints refer to the fingerprints that are not visible immediately by the naked eye, like the fingerprints left in a crime scene. There are a large amount of non-relevant information and noise in latent fingerprints, which make the automated latent fingerprint recognition extremely difficult. Designing reliable latent fingerprint recognition techniques is a challenge which needs to be addressed in the future.

In conclusion, this research has developed several fingerprint recognition techniques to improve the overall matching accuracy of a fingerprint recognition system. The designed fingerprint matching system achieves superior performance compared to most of the state-of-the-art fingerprint matching systems. However, there are some future work remained in order to further improve the overall matching accuracy of a fingerprint verification system including the implementation of the state-of-the-art feature extraction techniques and designing of fingerprint template protection techniques.

Appendices

Appendix A

Some Samples of Fingerprint Images in FVC databases

This appendix lists some samples of fingerprint images of different levels of quality from FVC databases. During the fingerprint capturing stage, individuals were asked to: a) exaggerate displacement or rotation or, b) dry or moisten their fingers [AFF09]. Therefore, the fingerprint images in FVC databases contain plenty of variations and noise, which means that they are specially suitable for the evaluations of fingerprint recognition algorithms.

(a) (b)

(c) (d)

Figure A.1: Samples of good quality fingerprint images

(a) (b)

(c) (d)

Figure A.2: Samples of poor quality fingerprint images

Bibliography

[AB12] Ali Ismail Awad and Kensuke Baba. Singular point detection for efficient fingerprint classification. *International Journal of New Computer Architectures & their Applications*, 2(1):1–7, 2012.

[ADB85] Carlo Arcelli and Gabriella Sanniti Di Baja. A width-independent fast thinning algorithm. *IEEE Trans. Pattern Anal. Mach. Intell.*, 7(4):463–474, April 1985.

[AFF09] Fernando Alonso-Fernandez and Julian Fierrez. Fingerprint databases and evaluation. In StanZ. Li and Anil Jain, editors, *Encyclopedia of Biometrics*, pages 452–458. Springer US, 2009.

[AG14] Ahmed Abbood Alaa and Sulong Ghazali. Fingerprint classification techniques: A review. *International Journal of Computer Science*, 11(1):111–122, January 2014.

[AM09] F. Ahmad and D. Mohamad. A review on fingerprint classification techniques. In *2009 International Conference onComputer Technology and Development, ICCTD '09*, volume 2, pages 411–415, Nov 2009.

[Ast07] Paul Astrom. The study of ancient fingerprints. *Journal of Ancient Fingerprints*, 1(1):2–3, 2007.

[BAH+07] F. Benhammadi, M. N. Amirouche, H. Hentous, K. Bey Beghdad, and M. Aissani. Fingerprint matching from minutiae texture maps. *Pattern Recogn.*, 40(1):189–197, January 2007.

[Bar13] Jeffery G. Barnes. *Fingerprint Source Book*. CreateSpace Independent Publishing Platform, 1st edition, 2013.

[BB11] S. Bodo and T.M. Buzug. Fingerprint segmentation and quality map using a combined frequency model. In *2011 IEEE Instrumentation and Measurement Technology Conference (I2MTC),*, pages 1–5, 2011.

[BCRAA13] R. Belguechi, E. Cherrier, C. Rosenberger, and S. Ait-Aoudia. Operational bio-hash to preserve privacy of fingerprint minutiae templates. *IET Biometrics*, 2(2):76–84, June 2013.

[BD06] Christopher D. Brown and Herbert T. Davis. Receiver operating characteristics curves and related decision measures: A tutorial. *Chemometrics and Intelligent Laboratory Systems*, 80(1):24 – 38, 2006.

[BDNB06] Arijit Bishnu, Sandip Das, Subhas C. Nandy, and Bhargab B. Bhattacharya. Simple algorithms for partial point set pattern matching under rigid motion. *Pattern Recogn.*, 39(9):1662–1671, September 2006.

[BG02] Asker M. Bazen and Sabih H. Gerez. Systematic methods for the computation of the directional fields and singular points of fingerprints. *IEEE Trans. Pattern Anal. Mach. Intell.*, 24(7):905–919, July 2002.

[BL10] Nandita Bhattacharjee and Chien Eao Lee. Fingerprint image processing and fuzzy vault implementation. *J. Mob. Multimed.*, 6(4):314–338, December 2010.

[BLE09] Jin Bo, Ying Yu Long, and Chen Dan Er. A novel fingerprint singular point detection algorithm. In *Proceedings of the 3rd WSEAS international conference on Computer engineering and applications*, CEA'09, pages 97–100, 2009.

[Bra97] Andrew P. Bradley. The use of the area under the {ROC} curve in the evaluation of machine learning algorithms. *Pattern Recognition*, 30(7):1145 – 1159, 1997.

[CCK11] Heeseung Choi, Kyoungtaek Choi, and Jaihie Kim. Fingerprint matching incorporating ridge features with minutiae. *Information Forensics and Security, IEEE Transactions on*, 6(2):338–345, June 2011.

[CDE09] CDEFFS. Data format for the interchange of extended fingerprint and palmprint features, working draft version 0.4. Accessed on June, 2014 `http://fingerprint.nist.gov/STANDARD/cdeffs/Docs/CDEFFS_DraftStd_v04_2009-06-12.pdf`, June 2009.

[CDJ05] Yi Chen, Sarat C. Dass, and Anil K. Jain. Fingerprint quality indices for predicting authentication performance. In *Proceedings of the 5th international conference on Audio- and Video-Based Biometric Person Authentication*, AVBPA'05, pages 160–170, 2005.

[CEMM00] R. Cappelli, A. Erol, D. Maio, and D. Maltoni. Synthetic fingerprint-image generation. In *Proceedings of the 15th International Conference on Pattern Recognition*, pages 471–474, 2000.

[CFM10] R. Cappelli, M. Ferrara, and D. Maltoni. Minutia cylinder-code: A new representation and matching technique for fingerprint recognition. *IEEE Transactions on Pattern Analysis and Machine Intelligence*, 32(12):2128–2141, Dec 2010.

[CLMM99] R. Cappelli, A. Lumini, D. Maio, and D. Maltoni. Fingerprint classification by directional image partitioning. *IEEE Transactions on Pattern Analysis and Machine Intelligence*, 21(5):402–421, 1999.

[CMM+06] Raffaele Cappelli, Dario Maio, Davide Maltoni, James L. Wayman, and Anil K. Jain. Performance evaluation of fingerprint verification systems. *IEEE Trans. Pattern Anal. Mach. Intell.*, 28(1):3–18, 2006.

[CMMS09] Guo Cao, Yuan Mei, Zhihong Mao, and Quan-Sen Sun. Fingerprint matching using local alignment based on multiple

pairs of reference minutiae. *Journal of Electronic Imaging*, 18(4):043002–7, 2009.

[CR05] S. Chikkerur and N. Ratha. Impact of singular point detection on fingerprint matching performance. In *Fourth IEEE Workshop on Automatic Identification Advanced Technologies*, pages 207–212, Oct 2005.

[CTCY04] Xinjian Chen, Jie Tian, Jiangang Cheng, and Xin Yang. Segmentation of fingerprint images using linear classifier. *EURASIP J. Appl. Signal Process.*, 2004:480–494, January 2004.

[Dau04] J. Daugman. How iris recognition works. *Circuits and Systems for Video Technology, IEEE Transactions on*, 14(1):21–30, Jan 2004.

[DNA14] How much does paternity test cost. `http://www.homednadirect.com.au/dna-news/how-much-does-paternity-test-cost.html`, accessed on May, 2014.

[FDJ12] H. Fleyeh, E. Davami, and D. Jomaa. Segmentation of fingerprint images based on bi-level processing using fuzzy rules. In *2012 Annual Meeting of the North American Fuzzy Information Processing Society (NAFIPS)*, pages 1–6, Aug 2012.

[FFCS06] Yansong Feng, Jufu Feng, Xiaoguang Chen, and Zhen Song. A novel fingerprint matching scheme based on local structure

compatibility. In *18th International Conference on Pattern Recognition (ICPR2006)*, volume 4, pages 374–377, 2006.

[FLW00] Kuo Chin Fan, Cheng Wen Liu, and Yuan Kai Wang. A randomized approach with geometric constraints to fingerprint verification. *Pattern Recognition*, 33(11):1793 – 1803, 2000.

[FOTG07] Julian Fierrezaguilar, Javier Ortegagarcia, Doroteo Torretoledano, and Joaquin Gonzalezrodriguez. Biosec baseline corpus: A multimodal biometric database. *Pattern Recognition*, 40(4):1389–1392, 2007.

[FZ11] Jianjiang Feng and Jie Zhou. A performance evaluation of fingerprint minutia descriptors. In *2011 International Conference on Hand-Based Biometrics (ICHB)*, pages 1–6, Nov 2011.

[GAKD00] S. Greenberg, M. Aladjem, D. Kogan, and I. Dimitrov. Fingerprint image enhancement using filtering techniques. In *Proceedings of the 15th International Conference on Pattern Recognition*, volume 3, pages 322–325, 2000.

[Got12a] C. Gottschlich. Curved-region-based ridge frequency estimation and curved gabor filters for fingerprint image enhancement. *IEEE Transactions onImage Processing*, 21(4):2220–2227, April 2012.

[Got12b] Carsten Gottschlich. Curved gabor filters for fingerprint image enhancement. *IEEE Transactions on Image Processing*, 21(4):2220–2227, 2012.

[GS12] C. Gottschlich and C. B. Schonlieb. Oriented diffusion filtering for enhancing low-quality fingerprint images. *IET Biometrics*, 1(2):105–113, June 2012.

[GW01] Rafael C. Gonzalez and Richard E. Woods. *Digital Image Processing*. Addison-Wesley Longman Publishing Co., Inc., Boston, MA, USA, 2nd edition, 2001.

[GYZZ11] Zhifan Gao, Xinge You, Long Zhou, and Wu Zeng. A novel matching technique for fingerprint recognition by graphical structures. In *2011 International Conference on Wavelet Analysis and Pattern Recognition (ICWAPR)*, pages 77–82, 2011.

[GZY06] Jinwei Gu, Jie Zhou, and Chunyu Yang. Fingerprint recognition by combining global structure and local cues. *IEEE Transactions on Image Processing*, 15(7):1952–1964, July 2006.

[HAD06] Feng Hao, Ross Anderson, and John Daugman. Combining crypto with biometrics effectively. *IEEE Trans. Comput.*, 55(9):1081–1088, September 2006.

[Ham50] R. W. Hamming. Error Detecting and Error Correcting Codes. *Bell System Techincal Journal*, 29(2):147–160, 1950.

[HB12] Jianchun He and Jinjun Bao. Normalization of fingerprint image using the local feature. In *2012 International Conference on Computer Science Service System (CSSS)*, pages 1643–1646, Aug 2012.

[HM90] Andrew K. Hrechak and James A. McHugh. Automated fingerprint recognition using structural matching. *Pattern Recognition*, 23(8):893 – 904, 1990.

[HWJ98] L. Hong, Yifei Wan, and A. Jain. Fingerprint image enhancement: algorithm and performance evaluation. *IEEE Transactions on Pattern Analysis and Machine Intelligence*, 20(8):777–789, 1998.

[HYZ+10] Chunfeng Hu, Jianping Yin, En Zhu, Hui Chen, and Yong Li. A composite fingerprint segmentation based on log-gabor filter and orientation reliability. In *17th IEEE International Conference on Image Processing (ICIP)*, pages 3097–3100, 2010.

[Jai11] Anil K. Jain. Automatic fingerprint matching using extended feature set. Accessed on June, 2014: `https://www.ncjrs.gov/pdffiles1/nij/grants/235577.pdf`, 2011.

[JCD06] A. Jain, Yi Chen, and M. Demirkus. Pores and ridges: Fingerprint matching using level 3 features. In *18th International Conference on Pattern Recognition (ICPR 2006)*, volume 4, pages 477–480, 2006.

[JCD07] Anil K. Jain, Yi Chen, and Meltem Demirkus. Pores and ridges: High-resolution fingerprint matching using level 3 features. *IEEE Transactions on Pattern Analysis and Machine Intelligence*, 29(1):15–27, 2007.

[JPHP00] A. K. Jain, S. Prabhakar, L. Hong, and S. Pankanti. Filterbank-based fingerprint matching. *Trans. Img. Proc.*, 9(5):846–859, May 2000.

[JPLK06] Wonchurl Jang, Deoksoo Park, Dongjae Lee, and Sung-jae Kim. Fingerprint image enhancement based on a half gabor filter. In *Proceedings of the 2006 international conference on Advances in Biometrics*, ICB'06, pages 258–264, Berlin, Heidelberg, 2006. Springer-Verlag.

[JRL97] Anil K. Jain, Nalini K. Ratha, and Sridhar Lakshmanan. Object detection using gabor filters. *Pattern Recognition*, 30:295–309, 1997.

[JRP04] Anil K. Jain, Arun Ross, and Salil Prabhakar. An introduction to biometric recognition. *IEEE Trans. on Circuits and Systems for Video Technology*, 14:4–20, 2004.

[JY00] Xudong Jiang and Wei-Yun Yau. Fingerprint minutiae matching based on the local and global structures. In *Proceedings of the 15th International Conference on Pattern Recognition*, volume 2, pages 1038–1041, 2000.

[JY08] Luping Ji and Zhang Yi. Fingerprint orientation field estimation using ridge projection. *Pattern Recognition*, 41(5):1491 – 1503, 2008.

[KAN08] D.K. Karna, S. Agarwal, and Shankar Nikam. Normalized cross-correlation based fingerprint matching. In *Fifth Inter-*

national Conference on Computer Graphics, Imaging and Visualisation, pages 229–232, Aug 2008.

[KCH12] Ravinder Kumar, Pravin Chandra, and M. Hanmandlu. Fingerprint singular point detection using orientation field reliability. *Advanced Materials Research*, 403:4499–4506, 2012.

[KJ96] Kalle Karu and Anil K. Jain. Fingerprint classification. *Pattern Recognition*, 29(3):389–404, 1996.

[KP02] Byung-Gyu Kim and Dong-Jo Park. Adaptive image normalisation based on block processing for enhancement of fingerprint image. *Electronics Letters*, 38(14):696–698, 2002.

[KT84] Masahiro Kawagoe and Akio Tojo. Fingerprint pattern classification. *Pattern Recogn.*, 17(3):295–303, June 1984.

[KV00] Z.M. Kovacs-Vajna. A fingerprint verification system based on triangular matching and dynamic time warping. *IEEE Transactions on Pattern Analysis and Machine Intelligence*, 22(11):1266–1276, Nov 2000.

[KW87] Michael Kass and Andrew Witkin. Analyzing oriented patterns. *Computer Vision, Graphics, and Image Processing*, 37(3):362 – 385, 1987.

[LB09] Chien Eao Lee and Nandita Bhattacharjee. Fingerprint image processing and minutiae extraction for fuzzy vault. In *Proceedings of the 7th International Conference on Advances*

in Mobile Computing and Multimedia, MoMM '09, pages 36–43, New York, NY, USA, 2009.

[LCG+11] Chongjin Liu, Jia Cao, Xin Gao, Xiang Fu, and Jufu Feng. A novel fingerprint matching algorithm using minutiae phase difference feature. In *Image Processing (ICIP), 2011 18th IEEE International Conference on*, pages 3201–3204, Sept 2011.

[LELJSM07] Almudena Lindoso, Luis Entrena, Judith Liu Jimenez, and Enrique San Millan. Correlation-based fingerprint matching with orientation field alignment. In Seong-Whan Lee and StanZ. Li, editors, *Advances in Biometrics*, volume 4642 of *Lecture Notes in Computer Science*, pages 713–721. Springer Berlin Heidelberg, 2007.

[Ley04] John Leyden. FBI apology for madrid bomb fingerprint fiasco-'substandard' digital prints led to oregon lawyer. accessed on June, 2014: `http://www.theregister.co.uk/2004/05/26/fbi_madrid_blunder/`, May 2004.

[LL03] K. Lee Lerner and Brenda Wilmoth Lerner. *Encyclopedia of Espionage, Intelligence, and Security.* 2003.

[LML13] Yue Li, M. Mandal, and Cheng Lu. Singular point detection based on orientation filed regularization and poincaré index in fingerprint images. In *2013 IEEE International Conference on Acoustics, Speech and Signal Processing (ICASSP)*, pages 1439–1443, May 2013.

[LN06] Alessandra Lumini and Loris Nanni. Two-class fingerprint matcher. *Pattern Recognition*, 39(4):714 – 716, 2006.

[LTG07] Jiang Li, S. Tulyakov, and V. Govindaraju. Verifying fingerprint match by local correlation methods. In *the First IEEE International Conference on Biometrics: Theory, Applications, and Systems*, pages 1–5, Sept 2007.

[LXL04] Chaoqiang Liu, Tao Xia, and Hui Li. A hierarchical hough transform for fingerprint matching. In David Zhang and AnilK. Jain, editors, *Biometric Authentication*, volume 3072 of *Lecture Notes in Computer Science*, pages 373–379. Springer Berlin Heidelberg, 2004.

[LYC+10] Peng Li, Xin Yang, Kai Cao, Xunqiang Tao, Ruifang Wang, and Jie Tian. An alignment-free fingerprint cryptosystem based on fuzzy vault scheme. *Journal of Network and Computer Applications*, 33(3):207 – 220, 2010.

[Mal04] Davide Maltoni. Generation of synthetic fingerprint image databases. In Nalini Ratha and Ruud Bolle, editors, *Automatic Fingerprint Recognition Systems*, pages 361–384. Springer New York, 2004.

[MC89] B.M. Mehtre and B. Chatterjee. Segmentation of fingerprint images a composite method. *Pattern Recognition*, 22(4):381 – 385, 1989.

[MM97] D. Maio and D. Maltoni. Direct gray-scale minutiae detection in fingerprints. *IEEE Transactions on Pattern Analysis and Machine Intelligence*, 19(1):27–40, 1997.

[MMC+02] D. Maio, D. Maltoni, R. Cappelli, J.L. Wayman, and A. K. Jain. Fvc2002: Second fingerprint verification competition. In *In Proceedings of 16th International Conference on Pattern Recognition (ICPR2002), Quebec City*, pages 811–814, 2002.

[MMC+04] Dario Maio, Davide Maltoni, Raffaele Cappelli, JimL. Wayman, and AnilK. Jain. Fvc2004: Third fingerprint verification competition. *Lecture Notes in Computer Science*, 3072:1–7, 2004.

[MMJP09] Davide Maltoni, Dario Maio, Anil K. Jain, and Sail Parbhakar. *Handbook of fingerprint recognition*. Springer, New York, 2009.

[MMKC87] B. M. Mehtre, N. N. Murthy, S. Kapoor, and B. Chatterjee. Segmentation of fingerprint images using the directional image. *Pattern Recogn.*, 20(4):429–435, July 1987.

[MMNM11] Ishmael S. Msiza, Mmamolatelo E. Mathekga, Fulufhelo V. Nelwamondo, and Tshilidzi Marwala. Fingerprint segmentation: An investigation of various techniques and a parameter study of a variance-based method. *International Journal of Innovative Computing, Information and Control*, 7(9):5313 – 5326, 2011.

[NB05] Kenneth Nilsson and Josef Bigun. Registration of fingerprints by complex filtering and by 1d projections of orientation images. In *Proceedings of the 5th International Conference on Audio- and Video-Based Biometric Person Authentication*, AVBPA'05, pages 171–183, Berlin, Heidelberg, 2005. Springer-Verlag.

[OR04] Choonsuk Oh and Young Kee Ryu. Study on the center of rotation method based on minimum spanning tree matching algorithm for fingerprint recognition. *Optical Engineering*, 43(4):822–829, 2004.

[OWT+08] T. Ohtsuka, D. Watanabe, D. Tomizawa, Y. Hasegawa, and H. Aoki. Reliable detection of core and delta in fingerprints by using singular candidate method. In *2008 IEEE Computer Society Conference on Computer Vision and Pattern Recognition Workshops*, pages 1–6, June 2008.

[PLP03] Chul-Hyun Park, Joon-Jae Lee, and Kil-Houm Park. Fingerprint matching based on directional image feature in polar coordinate system. In Nicolai Petkov and MichelA. Westenberg, editors, *Computer Analysis of Images and Patterns*, volume 2756 of *Lecture Notes in Computer Science*, pages 293–300. Springer Berlin Heidelberg, 2003.

[PPJ03] Salil Prabhakar, Sharath Pankanti, and Anil K. Jain. Biometric recognition: Security and privacy concerns. *IEEE Security and Privacy*, 1(2):33–42, March 2003.

[RB00] Nalini Is. Ratha and Ruud M. Bolle. Robust fingerprint authentication using local structure similarity. In *In Workshop on applications of Computer Vision*, pages 29–34, 2000.

[RCJ95] Nalini K. Ratha, Shaoyun Chen, and Anil K. Jain. Adaptive flow orientation-based feature extraction in fingerprint images. *Pattern Recognition*, 28(11):1657 – 1672, 1995.

[RHZ76] Azriel Rosenfeld, Robert A. Hummel, and S.W. Zucker. Scene labeling by relaxation operations. *IEEE Transactions on Systems, Man and Cybernetics*, 6(6):420–433, June 1976.

[SB11] Willian Stalls and Lawrie Browns. *Computer Security: Principles and Practice, Chapter 3, User Authentication:92-97.* 2 edition, Prentice Hall, 2011.

[SF06] Henry Schuster and Terry Frieden. Lawyer wrongly arrested in bombings: 'we lived in 1984'. accessed on June, 2014: `http://edition.cnn.com/2006/LAW/11/29/mayfield.suit/index.html?eref=rss_law`, Nov 2006.

[SG06] Zhixin Shi and V. Govindaraju. Fingerprint image enhancement based on skin profile approximation. In *the 18th International Conference on Pattern Recognition*, volume 3, pages 714–717, 2006.

[SHC03] Jung-Hwan Shin, Hui-Yeoun Hwang, and Sung Chien. Minutiae extraction from fingerprint images using run-length code. In Ning Zhong, ZbigniewW. Ra, Shusaku Tsumoto, and Einoshin Suzuki, editors, *Foundations of Intelligent Systems*,

volume 2871 of *Lecture Notes in Computer Science*, pages 577–584. Springer Berlin Heidelberg, 2003.

[SHC06] Jung-Hwan Shin, Hui-Yeoun Hwang, and Sung-Il Chien. Detecting fingerprint minutiae by run length encoding scheme. *Pattern Recognition*, 39(6):1140 – 1154, 2006.

[SHFD07] Weiguo Sheng, G. Howells, Michael Fairhurst, and F. Deravi. A memetic fingerprint matching algorithm. *IEEE Transactions on Information Forensics and Security*, 2(3):402–412, 2007.

[SM93] B.G. Sherlock and D.M. Monro. A model for interpreting fingerprint topology. *Pattern Recognition*, 26(7):1047 – 1055, 1993.

[Smi97] Steven W. Smith. *The Scientist & Engineer's Guide to Digital Signal Processing*. California Technical Pub, 1997.

[SMM94] B. G. Sherlock, D.M. Monro, and K. Millard. Fingerprint enhancement by directional fourier filtering. *IEE Proceedings: Vision, Image and Signal Processing*, 141(2):87–94, Apr,1994.

[Sta12] Australian Bureau Statistics. Personal fraud costs australians $1.4 billion. Accessed on June, 2014: `http://www.abs.gov.au/ausstats/abs@.nsf/latestProducts/4528.0Media%20Release12010-2011/`, April 2012.

[TB03] Xuejun Tan and Bir Bhanu. A robust two step approach for fingerprint identification. *Pattern Recognition Letters*, 24(13):2127 – 2134, 2003.

[TYC+10] Xunqiang Tao, Xin Yang, Kai Cao, Ruifang Wang, Peng Li, and Jie Tian. Estimation of fingerprint orientation field by weighted 2d fourier expansion model. In *the 20th International Conference on Pattern Recognition*, pages 1253–1256, Aug 2010.

[WBGS10] Li Wang, Nandita Bhattacharjee, Gopal Gupta, and Bala Srinivasan. Adaptive approach to fingerprint image enhancement. In *Proceedings of the 8th International Conference on Advances in Mobile Computing and Multimedia*, MoMM '10, pages 42–49, New York, NY, USA, 2010. ACM.

[WBS11] Li Wang, Nandita Bhattacharjee, and Bala Srinivasan. A novel technique for singular point detection based on poincaré index. In *Proceedings of the 9th International Conference on Advances in Mobile Computing and Multimedia*, MoMM '11, pages 12–18, New York, NY, USA, 2011. ACM.

[WBS12a] Li Wang, N. Bhattacharjee, and B. Srinivasan. Fingerprint reference point detection based on local ridge orientation patterns of fingerprints. In *Neural Networks (IJCNN), The 2012 International Joint Conference on*, pages 1–8, June 2012.

[WBS12b] Li Wang, Nandita Bhattacharjee, and Bala Srinivasan. A method for fingerprint alignment and matching. In *Proceed-*

ings of the 10th International Conference on Advances in Mobile Computing and Multimedia, MoMM '12, pages 297–301, New York, NY, USA, 2012. ACM.

[WCT98] A. Wahab, S. H. Chin, and E.C. Tan. Novel approach to automated fingerprint recognition. *IEE Proceedings: Vision, Image and Signal Processing*, 145(3):160–166, 1998.

[WH12] Song Wang and Jiankun Hu. Alignment-free cancelable fingerprint template design: A densely infinite-to-one mapping (ditom) approach. *Pattern Recognition*, 45(12):4129 – 4137, 2012.

[WHP07] Yi Wang, Jiankun Hu, and Damien Phillips. A fingerprint orientation model based on 2d fourier expansion (fomfe) and its application to singular-point detection and fingerprint indexing. *IEEE Trans. Pattern Anal. Mach. Intell.*, 29(4):573–585, April 2007.

[Wik14a] Wikipedia. Biometrics. accessed on June, 2014: `http://en.wikipedia.org/wiki/Biometrics`, 2014.

[Wik14b] Wikipedia. Fingerprint recognition. `http://en.wikipedia.org/wiki/Fingerprint_recognition`, accessed on: June, 2014.

[WLHF08] Wei Wang, Jianwei Li, Feifei Huang, and Hailiang Feng. Design and implementation of log-gabor filter in fingerprint image enhancement. *Pattern Recogn. Lett.*, 29(3):301–308, February 2008.

[WLN07] Xuchu Wang, Jianwei Li, and Yanmin Niu. Definition and extraction of stable points from fingerprint images. *Pattern Recognition*, 40(6):1804 – 1815, 2007.

[WSG04] Chaohong Wu, Zhixin Shi, and Venu Govindaraju. Fingerprint image enhancement method using directional median filter, in biometric technology for human identification. In *Proceedings of the SPIE*, 2004.

[WSOA13] M. A. Wahby Shalaby and M. Omair Ahmad. A multilevel structural technique for fingerprint representation and matching. *Signal Process.*, 93(1):56–69, January 2013.

[WYY11] Dawei Weng, Yilong Yin, and Dong Yang. Singular points detection based on multi-resolution in fingerprint images. *Neurocomputing*, 74(17):3376 – 3388, 2011.

[XZWG12] Zhe Xue, Tong Zhao, Min Wu, and Tiande Guo. A novel segmentation algorithm of fingerprint images based on mean shift. In De-Shuang Huang, Phalguni Gupta, Xiang Zhang, and Prashan Premaratne, editors, *Emerging Intelligent Computing Technology and Applications*, volume 304 of *Communications in Computer and Information Science*, pages 203–211. Springer Berlin Heidelberg, 2012.

[YA06] Neil Yager and Adnan Amin. Dynamic registration selection for fingerprint verification. *Pattern Recognition*, 39(11):2141 – 2148, 2006.

[YZYY10] Gongping Yang, Guang-Tong Zhou, Yilong Yin, and Xiukun Yang. K-means based fingerprint segmentation with sensor interoperability. *EURASIP J. Adv. Signal Process*, 2010(54):1–12, February 2010.

[ZGLR01] D. Simon Zorita, J. Ortega Garcia, S. Cruz Llanas, and J. Gonzalez Rodriguez. Minutiae extraction scheme for fingerprint recognition systems. In *2001 International Conference on Image Processing*, volume 3, pages 254–257, 2001.

[ZGZ07] Jie Zhou, Jinwei Gu, and David Zhang. Singular points analysis in fingerprints based on topological structure and orientation field. In *Proceedings of the 2007 international conference on Advances in Biometrics*, ICB'07, pages 261–270, Berlin, Heidelberg, 2007. Springer-Verlag.

[ZT07] Feng Zhao and Xiaoou Tang. Preprocessing and postprocessing for skeleton-based fingerprint minutiae extraction. *Pattern Recognition*, 40(4):1270 – 1281, 2007.

[ZWZ06] Xiaolong Zheng, Yangsheng Wang, and Xuying Zhao. A detection algorithm of singular points in fingerprint images combining curvature and orientation field. *Lecture Notes in Control and Information Sciences*, 345:593–599, 2006.

[ZWZ07] Xiaolong Zheng, Yangsheng Wang, and Xuying Zhao. A robust matching method for distorted fingerprints. In *IEEE International Conference on Image Processing*, volume 2, pages 377–380, Sept 2007.

[ZYHZ05] En Zhu, Jianping Yin, Chunfeng Hu, and Guomin Zhang. Quality estimation of fingerprint image based on neural network. In Lipo Wang, Ke Chen, and YewSoon Ong, editors, *Advances in Natural Computation*, volume 3611 of *Lecture Notes in Computer Science*, pages 65–70. Springer Berlin Heidelberg, 2005.

[ZYHZ06] En Zhu, Jianping Yin, Chunfeng Hu, and Guomin Zhang. A systematic method for fingerprint ridge orientation estimation and image segmentation. *Pattern Recognition*, 39(8):1452 – 1472, 2006.

[ZYZ05] En Zhu, Jianping Yin, and Guomin Zhang. Fingerprint matching based on global alignment of multiple reference minutiae. *Pattern Recognition*, 38(10):1685 – 1694, 2005.

[ZZYJ13] Weizhou Zhao, Hui Zhang, Baozhen Yang, and Huili Jing. Fingerprint segmentation based on pixel feature and fuzzy theory. *The International Journal of Computer Science and Applications*, 2:569–572, May 2013.

[ZZZL09] Qijun Zhao, Lei Zhang, David Zhang, and Nan Luo. Direct pore matching for fingerprint recognition. In *Proceedings of the 3rd International Conference on Advances in Biometrics*, ICB '09, pages 597–606, Berlin, Heidelberg, 2009. Springer-Verlag.

[ZZZL10] Qijun Zhao, David Zhang, Lei Zhang, and Nan Luo. High resolution partial fingerprint alignment using pore-valley descriptors. *Pattern Recogn.*, 43(3):1050–1061, March 2010.